EnergyChem 4 (2022) 100079

Contents lists available at ScienceDirect

EnergyChem

journal homepage: www.sciencedirect.com/journal/energychem

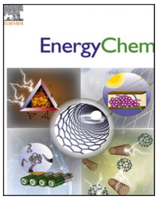

Advanced porous organic polymer membranes: Design, fabrication, and energy-saving applications

Yanpei Song, Changjia Zhu, Shengqian Ma [*]

Department of Chemistry, University of North Texas, 1508W Mulberry St, Denton, TX 76201, United States of America

ARTICLE INFO

Keywords:
Porous organic polymers
Energy-saving membrane applications
Gas separation
Liquid separation

ABSTRACT

Membrane separation technology is of great research interest in industry owing to its unparalleled merits such as high selectivity with unsuppressed permeability, reduced carbon footprint, small capital investment, and low energy consumption in comparison to traditional separation techniques. In the last few decades, polyamide membranes dominate the membrane industry until the porous organic polymers (POPs) get a ticket into the area of membrane separation. POPs bearing rich pore architectures and feasible functionalization are ready for fabricating novel membranes for rapid and precise molecular sieving. Here, a background overview of separation technology is provided, followed by a brief introduction of various POP-based membranes and the fabrication approaches of these membranes. Then, recent advancements of POP-bases membranes in energy-saving applications including gas separation and liquid separation are highlighted together with discussions about membrane design and generation involved. Finally, a concise conclusion with our perspective and challenges remaining for the future development of POP-based membranes are outlined.

1. Introduction

Separation technology, as one of the most primitive skills held in hands by human beings, has driven social development in a very profound way for ages [1]. Thanks to this skill, our ancestors were able to refine and extract copper from the unexploited minimal ores and make tools for production from bronze, ushering in an age of humans working with metals for the first time. Besides, the extraction of medicine from natural herbs was another remarkable progress in the utilization of the separation technology in ancient agricultural society, saving the lives of countless people. As its definition, separation is the process of distinguishing required components from a mixture containing two or more distinct substances and obtaining the enriched one or more constituents from the mixture. In the modern industrial manufacturing, a significative separation is generally considered to completely divide a mix, whether it be in solid, liquid, or gas, into pure constituents via physical, chemical, or physicochemical methods depending on the differences of components of the mixture in chemical or physical properties, such as chemical affinity and reactivity, molecular structure, melting and boiling points, solubility, density, mass, etc. Not only has separation technology widely applied in industry, but it is also commonly seen in daily lives. For instance, the extraction of coffee is the act of pouring hot water over the coffee grounds to dissolve soluble compounds out of coffee and separate the liquid from the mixture of undrinkable coffee grains by filter paper. During this process, the amount of water used, the brewing time, and the temperature of the water would determine the flavor of coffee, namely, these factors would influence the leaching of chemical constituents from the coffee [2]. The separation of coffee extract from the coffee grounds herein is a physical process via a simple filtration of liquid from a heterogeneous mixture mixed with solid. Besides, the methods such as precipitation, evaporation, centrifugation, and sublimation, which are employed to separate desired products from the heterogeneous mixtures are also summarized as physical separations, in which no chemical reaction is observed [3,4]. However, these separation methods normally cannot be implemented on a mass basis, which is hindered by large equipment and space requirements, costly initial investment, and huge off-site disposal of residuals after the separation [5]. Therefore, tremendous efforts have made to establish the large-scale separation from homogeneous mixtures. Notice, however, the physical separation from heterogeneous mixtures is also important and irreplaceable in some particular applications. For example, centrifugation is widely used in diagnostic laboratories for blood and urine tests [6,7], and also in the enrichment of uranium-235 from natural uranium which is the major fuel source for nuclear power plants [8].

---

[*] Corresponding author.
E-mail address: Shengqian.Ma@unt.edu (S. Ma).

https://doi.org/10.1016/j.enchem.2022.100079

Still and all, the separation of target components from homogeneous mixtures is favored in the modern industry, and we will focus on our discussion on such separation technology as follow [9–14].

The purification of constituents from the chemical mixtures via a simple and effective separation is critical in industry, and it is calculated that nearly half of industrial energy is used by this process [15,16]. Thus, developing a method that could separate industrial feedstocks and products efficiently and economically might be the potential solution to reduce energy consumption and greenhouse gas emission; and newer separation using solid media is gradually taking place of the high-cost traditional separation technology [17–30]. For example, thermal separation as a typical separation technology is deprecated gradually, because it requires a cooling and heating process and consumes a lot of energy [31]. One of the most promising technologies for advanced separation is membrane technology which has been widely applied to the separation of chemical mixtures nowadays. In the late 1960s, the first commercial breakthrough of a membrane-based separation system was successfully made by Loeb and Sourirajan [32], and the asymmetric reverse osmosis (RO) membrane developed by them was used for large-scale water desalination since then water purification by RO membrane had come into reality. One decade later, Monsanto realized H_2 separation by commercial membrane for the first time, indicative of the arrival of a new era of commercialized gas separation in industry [33]. Membranes with a uniform surface can be functionalized as thin barriers with selective cognization for specific chemical components that allow certain chemical species to permeate and separate from the mixtures. As a forward-looking technology [34], membrane separation owns the merits, such as high energy efficiency and gentle environmental footprint, making it the key enterprise towards a sustainable energy future. Over the past few decades, the optimization of membranes was processed in both structure construction and space functionalization; [35,36] and currently, various intelligent membranes have been successfully developed for gas and liquid separation [37–43]. For the accomplishment of effective separation of certain chemical constitution from the homogeneous mixture, the tunable nanochannels constructed from the nano and micro voids in membranes play very crucial roles, otherwise, the dense thin film without any cavities might stop or slow down the chemical permeation. Based on this principle, there are diverse porous materials that could be chosen to construct porous membranes, such as metal-organic frameworks (MOFs) [44–47], covalent organic frameworks (COFs) [48–51], and amorphous porous organic polymers (POPs) [52–60]. These framework materials with micropores are built up from the small building blocks via the linkage of various bonds. Particularly, COFs are classified as a branch of POPs with crystalline structures [61–65], which have much more ordered and uniform nanostructures as compared to amorphous POPs. In addition, both COFs and POPs are synthesized from organic monomers and connected via covalent bonds, while the organic ligands of MOFs are linked through the coordination bonds between metal nodes and organic units. Thus, MOFs are a class of typical organic-inorganic hybrid porous materials, distinguishing them from POPs. In this review, we look at the recent development of POPs and will briefly discuss the MOF-based membranes when in need in the following content.

Porous organic polymers are an emerging class of porous materials constructed by lightweight elements, such as H, B, C, N, O, and Si, the microporosity of such materials gives them rigid pore architectures and opportunities for pore engineering. Besides, POPs normally connected and extended by strong and irreversible bonds have higher thermal and chemical stability than organic-inorganic hybrid porous materials [65–70]. Therefore, POPs have demonstrated promising potential in a range of applications due to their permanent porosity and ease of functionalization, which includes, but are not limited to, gas storage and separation [71–74], heterogeneous catalysis [75–83], chemical sensing [84–89], energy conversion and storage [90–95], drug delivery [96–100], and environmental remediation [101–106]. Although covalent organic frameworks are a part of POPs, they are mostly formed by reversible covalent bonds, allowing reversible condensation between monomers, and this fact, then, results in their crystalline structures from molecular levels with highly ordered pore shapes and sizes. Another type of crystalline porous material with tailored porosity, MOFs, has been widely reported and employed in the fabrication of membranes, showing superior molecular sieving capacity as compared to traditional polymer membranes. However, the disadvantages of MOF-based membrane are also apparent, several challenging problems of this type of membranes, such as weak interaction with substrate support, low structural/chemical stability in a humid environment, harsh fabrication conditions of the large-area membrane, and short operating lifetime, must be addressed constructively before the large-scale utilization of MOF-based membrane in the real industrial process [107–110]. Other than improving the MOF-based membrane performance and optimizing its growing process, another option is using much more stable and scalable POPs to prepare advanced membranes for effective chemical separation, especially in liquids. Apart from crystalline POPs, the study of various amorphous POPs, such as conjugated microporous polymers (CMPs) [111–114], hypercrosslinked polymers (HCPs) [115–119], polymers of intrinsic microporosity (PIMs) [120–123], porous aromatic frameworks (PAFs) [124–126], and porous organic cages (POCs) [127–132], are also developed rapidly, stimulating significant cutting-edge research of such area in the past decades (Scheme 1).

A mass of recent research on POP-based membranes is focusing on gas separation and chemical separation from liquids. In contrast to conventional materials for synthetic membranes, POP-based membranes with continuous microporous frameworks in structure can be designed and functionalized more conveniently according to the behavior study of chemical transportation in pore environment, overcoming the long-term existing problem of trade-off between permeability and selectivity of membranes: (1) rich porous structure and higher specific surface area combined with short transport distance promise the high permeability in these membranes; [48,49] (2) the microporosity existing in POPs is well matched with the kinetic diameters of gas and liquid molecules, closing the deal of achieving size-selective separations in the membranes; [52,53] (3) massive building blocks and various synthesis reactions can be selected to produce versatile porous organic polymers, affording a huge reserve of precursors to choose from for the fabrication of POP-base membranes; [54,57] (4) microenvironments of the pore can be nicely tuned via covalent or noncovalent modifications [133,134], amplifying the capacity of chemical recognition and facilitating the transport of permeated species; (5) rigid polymeric frameworks connecting by strong bonds provide the resulting membranes with robust chemical, mechanical, and thermal stability, and thus improving their durability, even under complex operational conditions [55,59]. Given the rapid evolution of POP-based membranes and their ever-extended applications, herein, we provide a comprehensive overview of the development of advanced porous organic polymer membranes. Subsequently, the fabrications and modifications of POP-based membranes, such as membrane preparation methods, pore architecture engineering, and task-specific functionalization will be discussed in detail, followed by a particular summary of the energy-saving applications of POP-based membranes. Finally, a concise conclusion, current challenges, and our outlook toward advanced POP-based membranes will be outlined, as well, hoping to provide some useful guidelines for the future design and fabrication of POP-based membranes, and then satisfy the needs of advanced applications in industrial processes.

2. POP-based membranes: chemistry and fabrication

A membrane is generally regarded as a thin barrier or spacer layer which could allow the selective transportation of analytes from a gas/liquid mixture at different diffusion rates driven by an external force, enabling the successful retention of the analytes that are repelled chemically or physically by membranes. Based on this concept, membranes could cover a wide range of applications including gas separation, water treatment and purification, oil/water separation, pervaporation, and fuel-cell technology. Specifically, the physical pore size in the matrix material determines the degree of selectivity of a membrane, which can be classified as nanofiltration (NF), ultrafiltration (UF), and microfiltration (MF), thus, pore size control is the first key property to think about while designing a task-specific membrane separation system. In addition, hydrophilicity/hydrophobicity is another crucial property that can influence the performance of the resulting POP-based membrane in various separations significantly. What's more, in some cutting-edge areas such as desalination and ion nanofiltration, the surface charge of the membrane is playing a key role; and the electrostatic interactions between the free-moving ions and contact surface determine the permeability of the neutral solvent as the result of the rejection of solutes. Usually, membranes will be directly exposed to various harsh environments at work, meaning the stability of the membrane should be evaluated overall before the employ of such membrane in the real-world application. To sum up, it is crucial to consciously choose suitable POPs for membrane separation compared to other applications. In this section, the key properties of POP-based membranes would be summarized in detail combined with the principle of selecting suitable POPs for the membrane fabrication.

2.1. Key properties of POP-based membranes

2.1.1. Pore structure

The porosity of the matrix material has a direct bearing on the membrane permeability due to the size exclusion, especially in POP-based membranes. The pore size of the POPs selected as the membrane basement would affect the pore size contribution of POP-based membranes either directly or indirectly, determining the membrane permeability and application afterward. On the other hand, the pore structure of POPs would also influence the membrane permeability to a certain extent. For example, the micropores have ordered 3D structures will be preferential for separation applications, because the well-organized pores with infinite extension in all directions will provide a short transport distance and plenty of transport pathways for the permeation of analytes, and the 3D structure also affords more opportunities for target molecules to diffuse into the pores and then go through the membrane more easily with the equal possibility in each direction, thus achieving higher chemical permeances as compared to the POP-based membrane with 2D pores. Most POPs possess 3D micropores, but only COFs among these porous organic polymers are connected and extended with well-constructed basic units, forming uniform pore geometry. Besides, the regular stack of pores in COFs forms aligned 1D nanochannels which support the smooth transport of molecules or ions along the 1D nanochannels. By contrast, the rest of the POPs are amorphous with irregular micropore shapes, so they usually have various pore geometries in structure and wider pore distribution, which afford them owning lower transport resistance and better permeances.

For most of POPs, they have plenty of micropore space, and the corresponding membranes fabricated by POPs are usually filled with micropores. This fact meets the requirement of the dimensions of UF and NF membranes that are widely applied in some separation-related applications, such as desalination [135], water purification [136], pervaporation [137], and oil/water separation [138]. However, as it branched out into detailed requirements for UF membranes (2 – *ca.* 100 nm) [139] and NF membranes (0.5 – *ca.* 2 nm) [140], the average pore size of POPs which is suitable for the UF membrane would not qualify for NF membrane applications such as desalination, thus, the selection of POPs for membrane fabrication should be individually targeted. Fortunately, we have vast stores of reported POPs with a wide range of pore sizes, and we can screen and choose the most suitable POPs for the task-specific membrane fabrication from this huge POPs reservoir. Besides, the pore size of the POP-based membranes could be also nicely tuned at the design stage via the manipulation of the length and shape of the organic building blocks, and subsequently, the pore structure will be influenced by these basic units. Especially for COFs construction, the pore size can be greatly changed if the length of linear links is increased or reduced. Additionally, the dimensions of the pore in COF can also be transformed when applying building blocks with different geometries in the COF synthesis (Fig. 1). For example, 1,3,5-triformylphloroglucinol (Tp) as the trigonal planar linker combined with a linear link such as 2, 2′-bipyridine-5,5′-diamine (Bpy) could be condensed as a 2D COF with extended hexagonal pores [141–142]. However, a 3D COF can be obtained if the trigonal planar linkers are replaced by tetrahedral organic nodes, such as COF-300 which was synthesized from tetra-(4-anilyl) methane and terephthaldehyde (PDA) [143].

Apart from manipulating the structure of linkers, the pore size of POPs can also be adjusted by the attachment of side groups to the pore walls, either attaching the side groups to the monomers before the condensation [144,145] or repainting the voids after the formation of the network via post-synthetic modification [146–148]. This method has been widely used in the functionalization of MOFs and COFs to endow them with different functions in the same sort of material. A prominent work of the pore attachment modification of COF-based membrane was conducted by Wang and co-workers [149], they designed a series of linear monomers with various alkoxy side chains and placed them into the skeleton of COFs which were constructed by 1, 3,5-tris(4-aminophenyl)benzene (TAPB) and linear links to afford analogous COFs with different pore sizes and moisture resistance. In this study, the pore sizes of the TAPB-TPOC$_x$-COF ($x = 1$, 4, and 6) were calculated as 3.2, 2.6, and 2.4 nm along with the increment of length of alkoxy side chains. What's more, the representative cumulative pore volume changed more significantly, showing the values like 0.863, 0.507, 0.107 cm^3 g^{-1} for TAPB-TPOC$_1$-COF, TAPB-TPOC$_4$-COF, and TAPB-TPOC$_6$-COF, respectively. The above example indicates that the subtle modification of alkoxy chains of the monomers will result in a significant blocking effect, having a striking influence on the pore size control of the porous networks and subsequently affecting the chemical permeation in membranes. Post-synthetic modification is another useful toolbox to tailor the pore environment in porous materials, which was originally proposed by Hoskins and Robson in 1990 [150], and then applied to the functionalization of MOFs by Wang and Cohen in 2007 [151]. Subsequently, the feasibility of post-synthetic modification in porous materials was approved by the successful implementation of such method in CMPs [152,153], PAFs [154], and COFs [155–157]. The pioneering work of applying post-synthetic modification to functionalize COFs via covalent bond formation was carried out by Jiang and co-workers [158]. They first designed the linear monomers with the azide groups attached, which were later condensed with hexahydroxytriphenylene (HHTP) to afford an azide-functionalized COF with an identical hexagonal skeleton to that of COF-5. The azide units in the resulting COFs can be clicked with various alkynes for pre-designable functionalization, not only would it change the pore size of COFs through the attachment of groups with different lengths and shapes, but it also introduces various functions to the COFs, offering them great potential in a variety of applications (Fig. 2). Soon after, the same group extended the click chemistry in COFs and successfully altered the original COFs as a platform for multipurpose including chiral organocatalysts and CO$_2$ adsorbents [159]. The above facts suggest that the modification of pore walls in porous organic materials can be obtained by either bottom-up strategy or post-synthetic modification of the resulting networks, which can serve as the guideline for the pore control of POP-based membranes, as well.

2.1.2. Hydrophilicity/hydrophobicity

In some membrane separation applications such as oil/water separation and organic pervaporation, the pore hydrophilicity/hydrophobicity of the POPs is of vital importance, thus, the adjustment of such property of POPs is the key point of optimizing the aqueous and solvent-based separation performance of POP-based membranes [160]. A

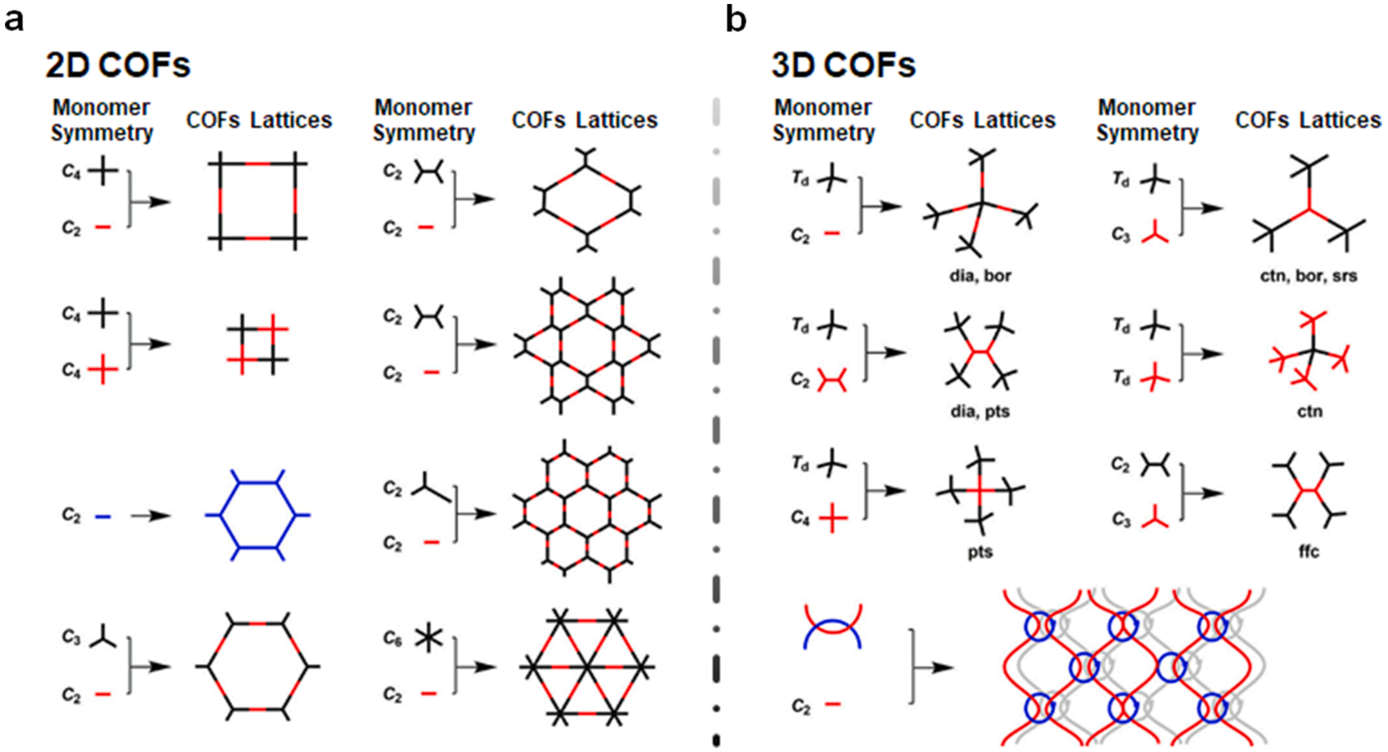

Fig. 1. Types of building blocks for the design of 2D and 3D COFs with various topological diagrams. Reproduced with permission [185]. Copyright 2020, American Chemical Society.

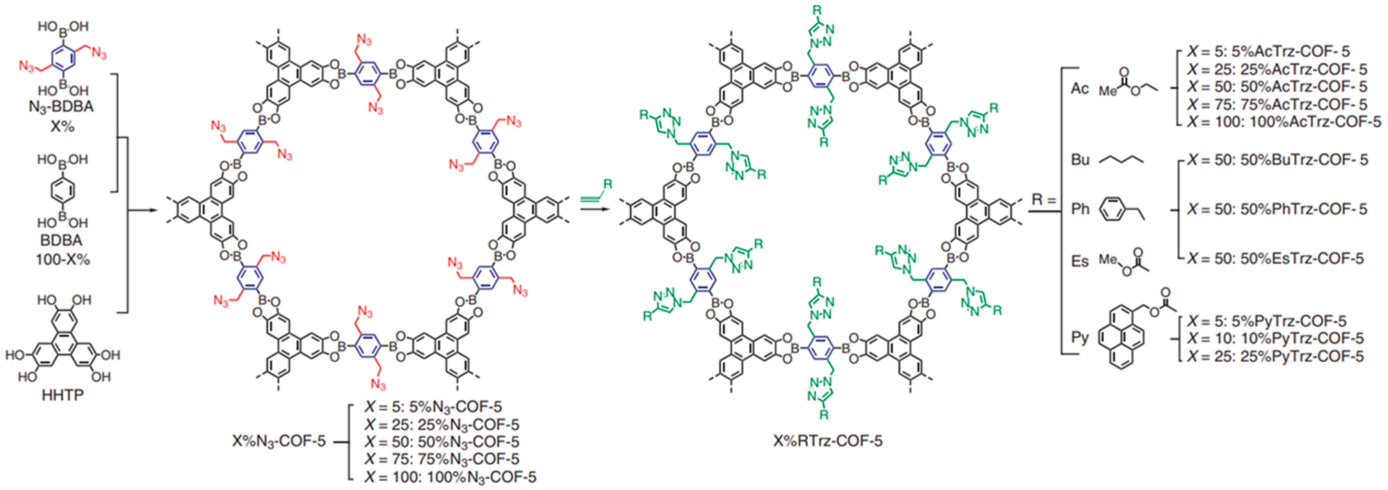

Fig. 2. Synthesis of COFs with azide-integrated walls and their capabilities for post-synthetic modification. Reproduced with permission [158]. Copyright 2011, Springer Nature.

membrane bearing hydrophilicity means that it enables the favored diffusion of water molecules through the micropores in the membrane and retains the organic solvent on the membrane surface [161]. Therefore, to obtain successful separation of water from the mixture of aqueous and organic solvent in a POP-based membrane, the coating of the contact surface with hydrophilicity is of the essence, meaning that the tailoring of POPs with hydrophilic pores is necessary. To introduce the pore hydrophilicity in POPs, there is a basic approach that is all set up for the employ according to the design and synthesis of POPs [162], that is the attachment of the building blocks with hydrophilic functional groups such as hydroxyl groups or polar functional groups (amines and alkoxy groups) that can also enhance the pore hydrophilicity. These functional groups can be introduced to POPs via *de novo* synthesis of the monomers or post-synthetic attachment to the pore walls via covalent bonds. Besides, the introduction of open metal sites in the matrix material is another scalable way to improve its hydrophilicity, but mostly in MOFs rather than in POPs [163]. Hydrophobicity of the POPs could also be tuned following the above methods by the introduction of hydrophobic functional groups such as fluorine-containing chains [164,165]. Our group reported the first example of imparting superhydrophobicity on COFs by grafting 1H,1H,2H,2H-perfluorodecanethiol chains onto a vinyl-functionalized COF via a thiol-ene click reaction (Fig. 3a) [166]. The resulting COF-VF demonstrated superhydrophobic behavior with the maintenance of the microporosity and crystallinity of the parent COF-V. We integrated COF-VF with various substrates such as melamine foam, paper, and magnetic liquid, to test its superhydrophobicity. In the

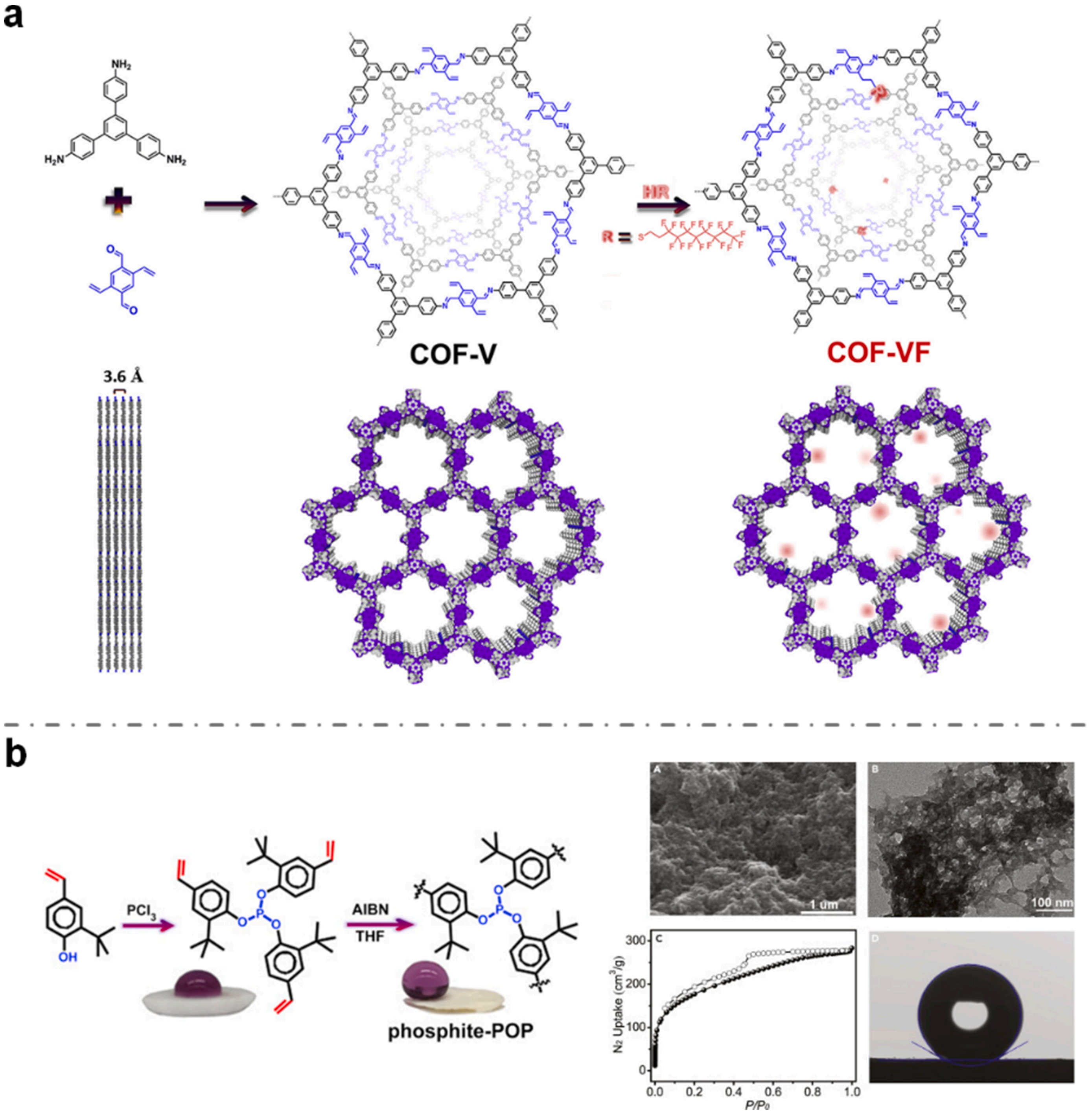

Fig. 3. (a) Schematic illustration of imparting superhydrophobicity on COF-V. Reproduced with permission [166]. Copyright 2018, Elsevier. (b) Synthetic route of Phosphite-POP and corresponding characterization. Reproduced with permission [167]. Copyright 2016, Elsevier.

oil-sorption experiments, the COF-VF@foam exhibited outstanding removal ability of organic solvents from its mixture of water together with excellent recyclability with a great sorption capacity retention after ten cycles of sorption, suggesting that COF-VF decorated by fluorine-containing chains would have great potential in the separation applications such as aqueous/organic solvents separation. Furthermore, it also indicates that grafting hydrophobic functional groups to POPs to obtain hydrophobicity is feasible as well as POP-based membranes. Besides, the hierarchically porous structures in porous polymers could also enhance their hydrophobicity, which has been completely proven in our previous study of superhydrophobic porous frameworks [167]. In this report, we synthesized a phosphite-POP with hierarchical porosity, which was confirmed by scanning electron microscopy (SEM) and nitrogen sorption isotherms at 77 K (Fig. 3b). The superhydrophobicity of phosphite-POP was characterized by the contact angle of a water droplet on its surface, which was as high as 152°. Generally speaking, if the contact angle is higher than 90°, the water molecules will be repulsed by the surface of the material and not allowed to pass through the membrane pores even though the pore size of the membrane is much larger than the kinetic diameter of water molecules.

2.1.3. Surface charge

Given the great potential of advanced POP-membranes in some cutting-edge research areas such as desalination and ion nanofiltration, the surface charge of the membrane including charge type and charge density is becoming an important property. While the membrane is applied in these applications, the effect of physical size sieving and electrostatic interactions (namely, the Donnan effect) would cooperate and contribute to the rejection of unfavored solutes. When the membrane processes the same charge with the solutes, the rejection between the membrane surface and contact solutes will be amplified significantly combined with better antifouling properties. Therefore, it is a considerable factor in the design and fabrication of novel membranes. To confer the POP-based membranes with charge as expected, there are two universal methods for us to select, one is to nicely design and synthesize the linking monomers, and the other is to graft specific charged sits to the membrane via covalent or noncovalent bonds after it is produced. For the ionic POPs synthesis, the design starting from the linking monomers is also called the bottom-up method, which requires us to carefully choose ionic precursors according to the concrete requirements for the particular application. Some monomers with charges have been widely used for the construction of ionic COFs (iCOFs) and ionic POPs, for example, ethidium bromide (EB) (3,8-diamino-5-ethyl-6-phenylphenanthridinium bromide), the commercially available cationic dye commonly used in the DNA areas, was first reported for the construction of iCOFs by Zhang and Li in 2016 [168]. After they got the pristine charged COF with Br^-, the counterions were subsequently changed to be F, Cl, and I via ion exchange processes, hence changing the pore environment of EB-COFs. Some other ionic monomers, such as triaminoguanidinium chloride (TG_{Cl}) [169,170], 2,5-diaminobenzene-1,4-disulfonic acid (DABDA) [171,172], 5,6-bis(4-formylbenzyl)-1,3-dimethyl-benzimidazolium bromide (BFBIm) [173], 3,8-diamino-5-[3-(diethylmethylammonio)propyl]-6phenylphenanthridinium diiodide (PI) [174], and 2,5-diaminobenzenesulfonic acid ($Pa\text{-}SO_3H$) [175], were designed and applied to the synthesis of iCOFs and iCOF-based membranes. In 2018, the first example of positively charged COF-based membranes was stressed by Li and Ma [176], and Li-Oakey [177] introduced the first negatively charged COF-based membranes almost at the same time (Fig. 4). These two initial works inspired the development of the charged COF-based membranes, and a mass of iCOFs has been used for the fabrication of membranes afterward. Additionally, the surface charge of the amorphous POP-based membranes can also be introduced and modified handily by careful selection of coupling reactions or special design of monomers. Zhu and co-workers picked up 4-pyridinylboronic acid and cyanuric chloride as the building blocks to synthesize the ionic PAF via *in situ* quaternarization of pyridine in the resulting framework [178]. And then Ag^+ ions were settled down in the

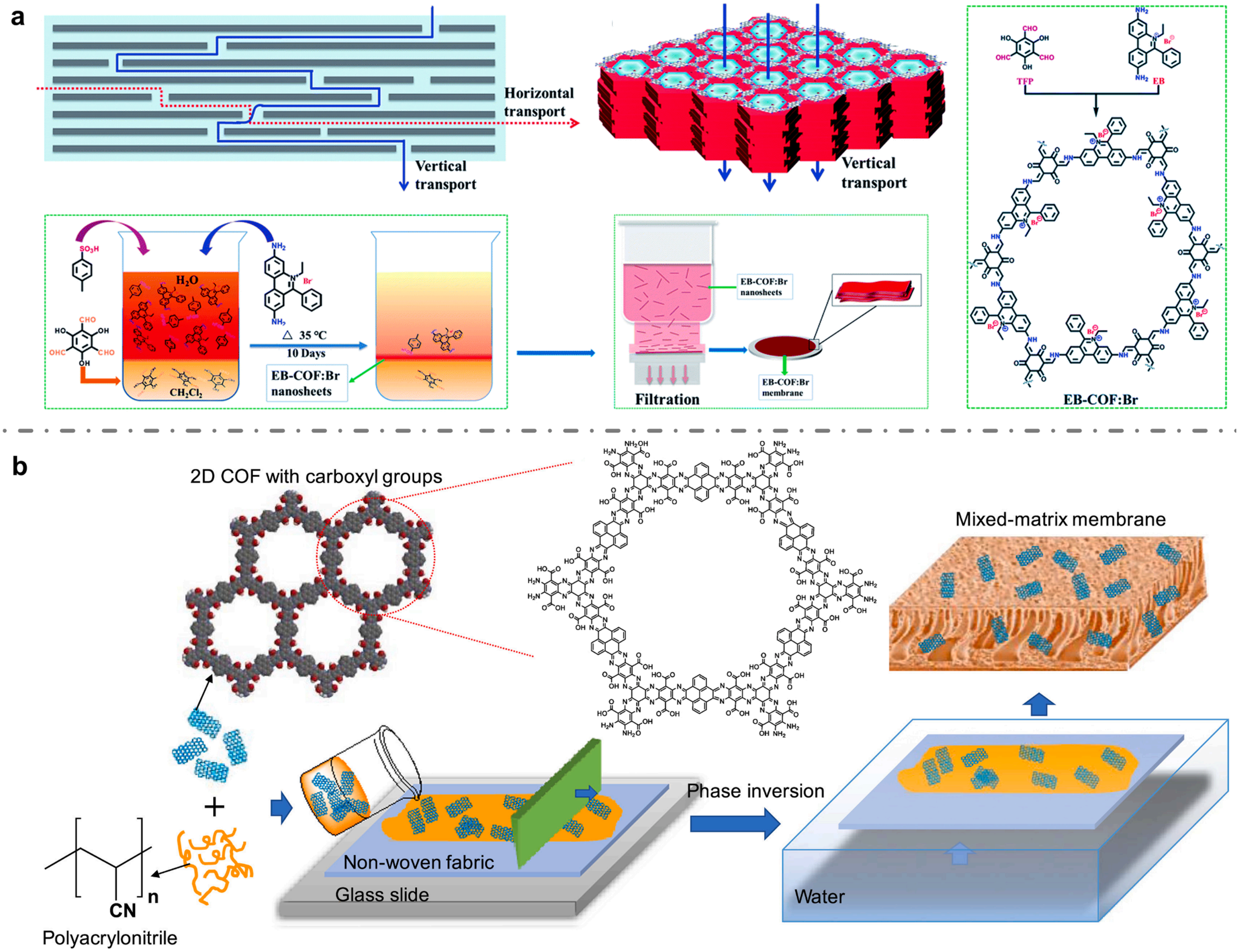

Fig. 4. (a) Schematic representation of the interfacial crystallization process used to synthesize the EB-COF:Br nanosheets. Reproduced with permission [176]. Copyright 2018, Royal Society of Chemistry. (b) Schematic illustration for the fabrication of mixed-matrix ultrafiltration membrane of 2D COF and PAN. Reproduced with permission [177]. Copyright 2019, Elsevier.

cavity of synthesized PAF-50 after contacting with the Cl^- ions inside. Finally, the powder AgCl-PAF-50 was mixed with poly(methyl methacrylate) (PMMA) to produce mixed-matrix membrane (MMM) and used for antibacterial coatings in accordance with requirements. Lai et al also contributed a lot in the field of POP-based membranes and reported an example of ionic CMP-based membrane very recently [179]. The soft ionic CMP monomer they used was constituted of an electroactive carbazole moiety and a long alkyl chain with an ionic end group; and the generated ionic CMP-based membrane revealed superior performance for the fast and selective ion transport thanks to its flexible ionic centers. Beyond designing charged POP-based membranes via bottom-up synthesis, the subsequent introduction of charged sites to the synthesized network is another widely adopted method for charging the POP-based membranes. Sun and co-workers report a 3D COF-based membrane encapsulated with charged dye molecules, and various dye molecules were immobilized in the robust 3D COF membrane, COF-300 [180]. The resulting membranes processing excellent permselectivity and low membrane resistance demonstrated great potential for harvesting salinity gradient energy. This strategy was also used to place ionic sites in soluble PIM-based membranes. Zhang and co-workers prepared the uniform solution containing PIM and ionic liquid first, and casted the target membrane from the solution [181]. In this way, the PIM membrane could be charged conveniently and effectively.

2.1.4. *Stability*

The stability of the POP-based membranes in harsh conditions is vital for long-term operation. Although the crystalline POPs, COFs, have many advantages in the pore engineering and functionalization as compared to amorphous POPs, such as CMPs, PAFs, HCPs, and PIMs. The stability of COFs, however, is usually lower than that of the rest of POPs due to their weak and reversible connecting bonds of organic monomers. To obtain the ordered pore structures, the reversibility of the connecting bonds is crucial, offering sufficient space for the self-healing of unordered units. Though most of the resulting COFs own rigid structures and the stability of the framework is greatly enhanced by the extended conjugated networks, those amorphous POPs constructed by stronger and irreversible covalent bonds are more able to sustain structure stability. Nowadays, some ultrastable COFs which were linked by stronger covalent bonds, even irreversible bonds, have been reported, joining the family of COFs (Fig. 5) [182–186]. The development of these ultrastable COFs greatly supports the COF-based membranes to participate in more toilsome membrane separations. However, the study of ultrastable COF-based membranes is still in its infancy, calling for more attention and effort. From the foregoing, the selection of POPs for the membrane fabrication should be in line with the specific working conditions, and we should achieve a balance between the performance and stability of the membrane. As we know it, the well-organized pore structures in MOFs and COFs offer them great opportunities for superior molecule sieving, however, the order of those crystalline porous materials would be receded even destroyed after long-time exposure to the complex working environment, thereby degrading their performance. Therefore, the amorphous POP-based membranes with uncontrollable pore structures but higher stability such as PAFs, CMPs, and HCPs are still playing crucial and critical roles in practical separation applications, even though we have seemingly fancier COFs with better performance as an alternative. For instance, if a membrane must be placed in the extremely acidic or basic surroundings, its stability would be the first principle to consider instead of its performance in terms of economics. We will discuss different POP-based membranes in the following content and the criterion of how to choose suitable POPs as the matrix material for the membrane fabrication.

2.2. *Choices of porous organic polymers*

2.2.1. *COF-based membrane*

Covalent organic frameworks, as one of the most popular porous crystalline materials after zeolites and MOFs, demonstrated their superior performance over conventional polymer materials after their first introduction to the world [187]. The skeleton of COFs which is supported by lightweight elements is full of porosity and accessible surface area, offering enough chemical space for the pore engineering and functionalization [188,189]. Inspired by these merits, COFs come under the spotlight, emerging as ideal candidates for a variety of applications including gas storage/separation, catalysis, drug delivery, sensors, environmental remediation, and energy storage and conversion [190]. The first two 2D COFs were reported by Yaghi in 2005, which were connected by reversible boroxine and boronate ester. However, the pioneer COFs constructed by such covalent bonds were very sensitive to acid, base, and even water. The poor chemical stability of these COFs impeded the application of such beautiful porous crystalline frameworks until the first 3D COFs linked by imine bonds were introduced by the same group in 2009 [191]. The crystalline imine-linked COFs have stronger connections and more rigid structures than the boroxine/boronate ester-linked COFs, demonstrating excellent resistance to acid, base, water, and various organic solvents. Thus, the research of COFs applications reached a new development stage, giving the opportunity to handle the COFs in a state other than solid, such as membrane applications. To obtain an imine-linked COF membrane, some scalable fabrication strategies including *in situ* casting or growth and interface-assisted synthesis have been well studied and widely applied. Additionally, a bunch of reversible covalent organic bonds other than imine bonds to synthesize powder COFs, such as triazine, hydrazone, imide, olefin, ether, and oxazole [192], were subsequently employed to produce COF-based membranes using the mentioned fabrication

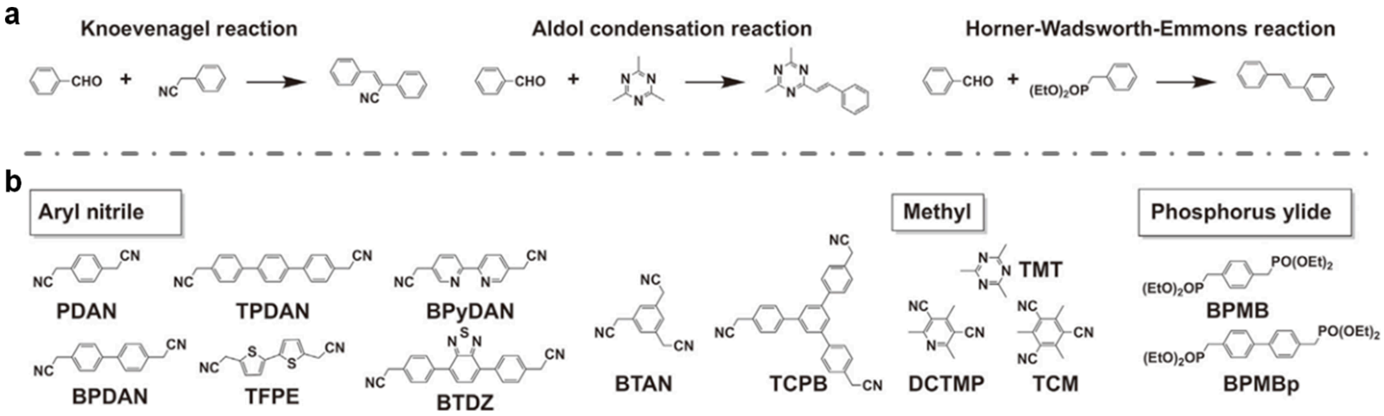

Fig. 5. (a) Reactions and (b) building blocks for the synthesis of sp^2 carbon covalent organic frameworks (COFs). Reproduced with permission [182]. Copyright 2021, Elsevier.

methods. On the other side, the research on the crystalline structures of COFs has also been advanced greatly from the atomic level to the bulk scale. The first single-crystal evidence of 3D COFs was obtained by Yaghi and co-workers in 2013 [193], and the single-crystal structure of COF-300 was determined by single-crystal 3D electron diffraction using the rotation electron diffraction (RED) method. The breakthrough of growing single crystals of COFs was reported by Yaghi, Wang, and Sun in 2018 [194]. It was the first report of the general approach using aniline as a modulator to grow high-quality single-crystal 3D COFs that were large enough for single-crystal x-ray diffraction (SXRD). Subsequently, several groups also developed novel methods for growing single crystals of 2D COFs. Wei [195] and Zhao [196] successfully obtained the large-scale single crystals of rod-like and rhombus plate-like 2D COFs, respectively (Fig. 6).

A variety of synthetic approaches for COF preparation has been developed over the past years. Thereinto, solvothermal synthesis is the most popular method for obtaining COFs where a sealed vessel with deoxygenation is required, and the type and ratio of solvents should be carefully selected in line with the solubility of monomers. Additionally, the reaction time and temperature, type of catalyst, and quantity of solvent and catalyst are all important to offer an ideal COF with uniform pore size, large surface area, and high crystalline. The 3D COF reported with the largest surface area was given in solvothermal synthesis, and a calculated Brunauer–Emmett–Teller (BET) surface area of 4210 $m^2\ g^{-1}$ was achieved [197]. Furthermore, ionothermal synthesis is another communally used method for preparing COFs, especially covalent triazine frameworks (CTFs) which is a branch of the COFs linked by triazine. In 2008, Thomas et al. firstly got a crystalline triazine framework via the cyclotrimerization of 1,4-dicyanobenzene in molten $ZnCl_2$ under 400 °C, named CTF-1 [198]. In this reaction, $ZnCl_2$ plays a crucial role in the successful polymerization of CTFs, which not only serves as the reaction catalyst but also as the solvent. CTF-1 bearing sheet-like structure with hexagonal pores and excellent chemical and thermal stability together with a high BET surface area of 791 $m^2\ g^{-1}$ is of great potential for separation applications in complex working conditions. However, the synthetic process for most of CTFs is very harsh, and amorphous CTFs would be obtained as a rule. Thus, fabricating a membrane based on CTFs should be well-designed and avoid fussy reaction conditions. Usually, the CTF-based membranes are firstly blended with other matrix polymers and produced via traditional membrane fabrication methods then. As for other methods for the fabrication of the COF-based membranes, further discussion will be given in detail in the next section.

2.2.2. CMP-based membrane

The most significant characteristics of CMPs are their permanent and rigid microporosity and extended π-conjugated networks, which make them unique as compared to other porous organic polymers. Though CMPs are a class of typical amorphous POPs, they are much more well-organized with regular 3D pore structures. The microporous structures of CMPs can be adjusted and functionalized easily through the design of linker and grafting of required functional groups, being similar to the pore engineering of COFs. Thus, CMPs were used for the gas storage when they were reported for the first time by Cooper and co-workers, just as other pioneer porous materials [199]. The strong chemical or physical affinity of the pore walls to the gas molecules in CMPs was further employed as the molecular sieving for gas separation. Being different from other POPs, the extended π-conjugated skeleton existing in CMPs endows them with the capacity to apply in the fields, such as photocatalysis, light emittance, chemical sensing, and energy storage [200]. Besides, Cooper et al. reported the first soluble CMP networks in 2012 by the means of grafting tert-butyl-functionalized groups to the

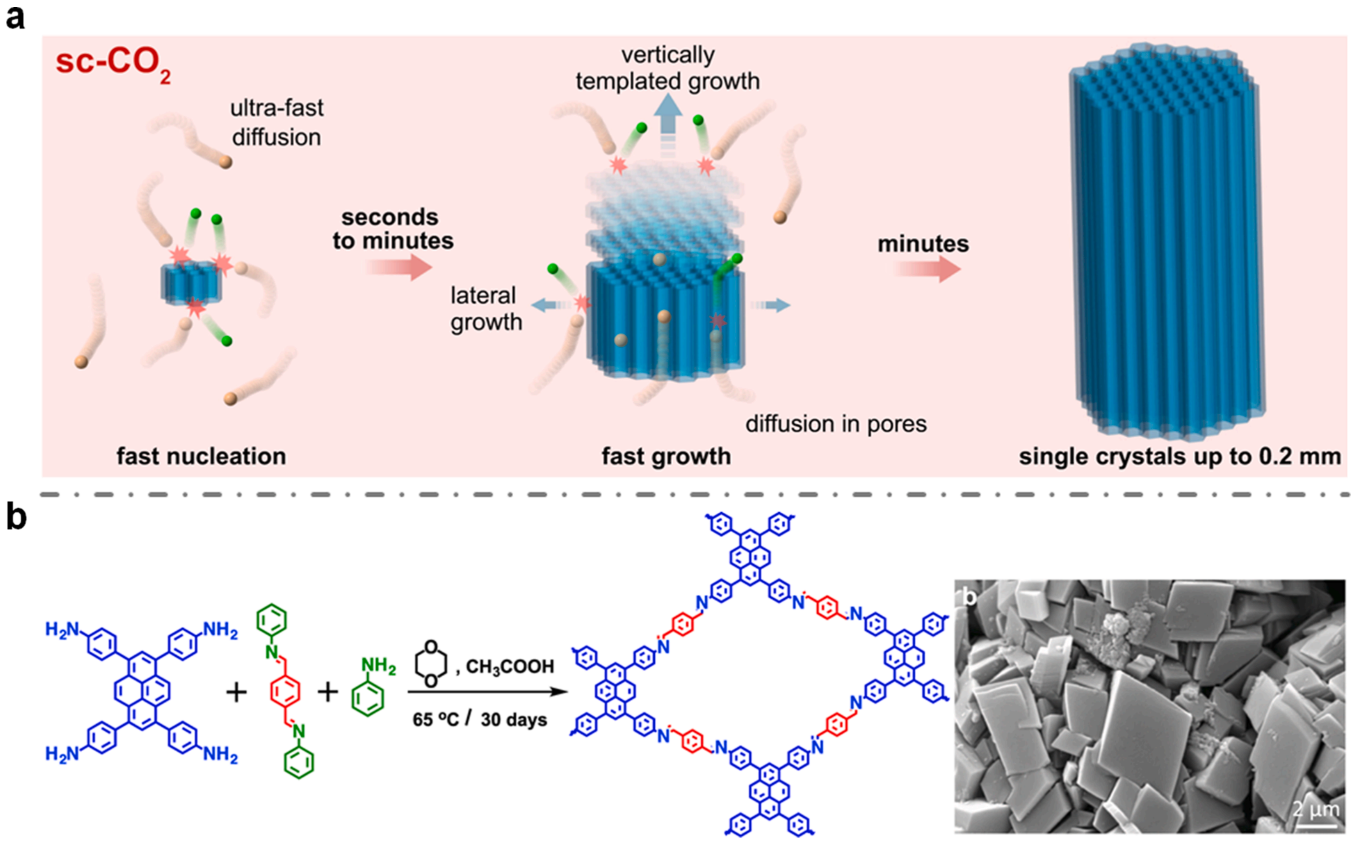

Fig. 6. (a) Schematic illustration of the single-crystal polymerization of 2D COFs in supercritical CO_2 (sc-CO_2). Reproduced with permission [195]. Copyright 2021, Springer Nature. (b) Schematic illustration of the growth of 2D COF single crystals via template polymerization. Reproduced with permission [196]. Copyright 2022, Springer Nature.

skeleton to offer a hyperbranched CMP network (Fig. 7) [201]. This soluble CMP network could be dispersed and dissolved in the solvent and then the CMP-based membrane could be cast from the solution. Soon after, Patra [202] and Hu [203] et al. developed another two soluble CMP networks based on this approach, respectively, and obtained two new CMP-based membranes from the CMP solutions. However, the major of CMPs is usually synthesized in powder form and insoluble in any common solvent, and only a few examples of the soluble CMPs are reported, demonstrating that the *in suit* casting of CMP-based membranes from the CMP solution is limited by the recent synthetic strategy and novel technological methods are required to fabricate CMP-membranes.

The functionalization of CMPs in their linkers and skeletons can be manipulated at the molecular level, giving them great potential in applications except for gas storage and separation. Combined with the intrinsic property of extended π-conjugation in structure, CMPs usually could serve as a bifunctional platform for advanced application [111]. Varying from other POPs, the π-conjugation of the CMPs can be easily and greatly altered via the subtle modification of connecting bond types and monomer linkers. Take the synthetic reactions of CMPs construction as an example, several well-known reactions, such as Sonogashira–Hagihara reaction, Yamamoto reaction, Friedel–Crafts reaction, Suzuki cross–coupling reaction, Heck reaction, phenazine ring fusion reaction, cyclotrimerization reaction, and oxidative coupling reaction, have been employed to connect the building blocks of the CMPs [204]. COFs could also be considered as a special type of CMPs with crystalline structures, although the connecting bonds of imine-linked COFs synthesized via Schiff-base reaction have less π-conjugation than that of the typical CMPs, the regular basic units joined together widely extend the π-conjugation of COFs, the trade-off between π-conjugation and ordered structures enable the COFs working in some π-conjugation-favored applications, as well. As we're aware, there are two principles for material functionalization to introduce the required group sites to the CMPs. One is to synthesize the building blocks with well-designed active sites and then the functional sites can be carried to the skeleton during the construction of the CMPs. The other way would be much easier than *de novo* synthesis of the monomers, that is post-synthetic modifications for the resultant backbone in CMPs. There is a mass of methods to graft the needed functional groups to the networks with the help of diverse chemical reactions. Usually, the extra introduction of the functional groups would take place of the pore space and then shrink the pore volume, thus reducing the pore size and lowering the surface area. Therefore, considering carefully for the CMPs selection for the fabrication of molecular sieving membranes according to the kinetic diameter of the chemical molecules is significant.

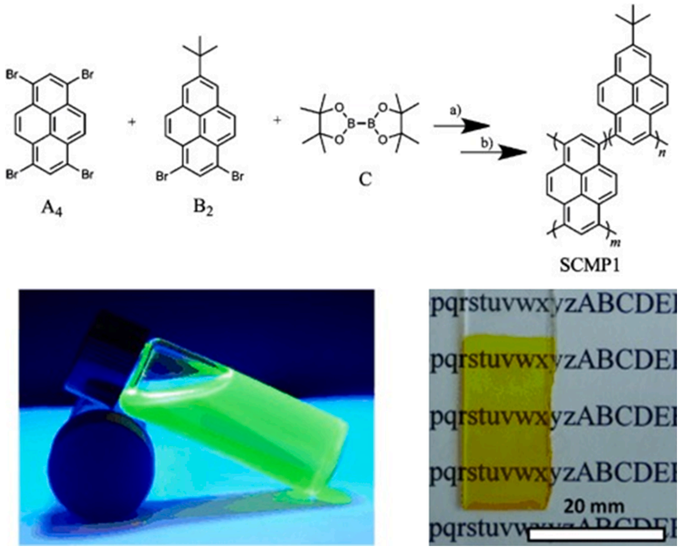

Fig. 7. Schematic representation of the synthesis of soluble CMP networks. Reproduced with permission [201]. Copyright 2012, John Wiley and Sons.

2.2.3. *PIM-based membrane*

As mentioned above, the rare soluble CMPs are superexcellent matrix materials to cast defect-free membranes from solutions. Thus, as a kind of soluble organic polymers with microporosity, polymers of intrinsic microporosity (PIMs) are the ideal candidate for membrane fabrications [205,206]. The microporosity of PIMs originates from the inefficient packing of the polymer chains due to the stiff and distorted backbone structures. Meanwhile, the rigid polymer structures existing in PIMs can stop the free bond rotation and chain motion, thus maintaining the microcavities of PIMs. In contrast to other POPs, the origin of the porosity in PIMs is much more intuitive than that of COFs or CMPs without the formation of permanent pores. For COFs or CMPs, the framework is supported by the continuous pore structures, the pore structure of PIMs, however, is the result of the contortion of the polymer chains. Thus, such a unique mechanism of porosity formation offers vast choices of organic monomers and reaction conditions for the successful synthesis of soluble PIMs, which are ideal candidates for membrane processability. Most PIM-based membranes can be directly processed from a PIM solution via a simple casting or surface coating [207]. To date, various soluble PIMs have been reported and applied in the membrane sieving, such as gas separation. The first example of dioxane-linked PIM and the correlative membrane was reported by McKeown and co-workers in 2004 [208], and subsequently a lot of attention of the design and synthesis of functional PIMs and PIM-based membranes was received. In this work, the resulting linear PIM-1 was synthesized by the non-network polycondensation of 3,3,3′,3′-tetra-methyl-1,1″-spirobisindane-5,5′,6,6′-tetrol and 2,3,5,6-tetrafluorophthalonitrile, all monomers of which are commercially available. The porosity of PIM-1 was measured by an N_2 adsorption/desorption isotherm, giving a high BET surface area of 860 m^2 g^{-1}. Besides, PIM-1 could be directly dissolved in polar aprotic solvents such as tetrahydrofuran (THF), which allowed the easy fabrication of membrane by evaporating solvent, affording the self-supported PIM-1 membrane (Fig. 8) [209]. The porosity of the glassy membrane was also measured, giving a lower BET surface area of 620 m^2 g^{-1}. The PIM-1 membrane was applied to the pervaporative removal of phenol from an aqueous solution, exhibiting competitive permeation behavior with that of other commercial membranes. Later, McKeown et al. replaced the relatively flexible spirobisindane (SBI) component of PIM-1 with more rigid spirobifluorene (SBF) to synthesize PIMs with greater shape persistence, and a PIM-based membrane with high gas permeability and enhanced selectivity was successfully obtained for the challenging gas separation, such as O_2/N_2, CO_2/CH_4, CO_2/N_2, and H_2/N_2 [210]. Apart from replacing the flexible portions in PIMs, this group also designed a new synthetic strategy to prepare the rigid PIM, applying two new monomers with bridged bicyclic rings to the PIM synthesis. They designed and synthesized two rigid units, called 2,6(7)-diamino-9,10-dimethylethanoanthracene and 5,5′,(6),(6′)-diamino-3,3,3′,3′-tetramethyl-1,1′-spirobisindane, to process the polymerization reaction, yielding two novel PIMs with the similar structures like PIM-1, named as PIM-EA-TB, and PIM-SBI-TB, respectively [211]. These much more rigid PIMs were also used for fabricating microporous membranes which were mounted for the multiple gas separation. The PIM-based membranes can also be prepared by supporting the thin film of PIMs, forming composite membranes. Livingston and co-workers reported a novel method to transport ultrathin PIM-1(35 nm thick) which was obtained from a spin coating of PIM-1 chloroform solution on a glass substrate to polyacrylonitrile (PAN) UF or alumina supports [212]. The resulting composite membrane exhibited excellent performance in organic solvent nanofiltration, rejecting hexaphenylbenzene (HPB) about 90% in heptane.

The functionalization of PIMs can be easily processed via the

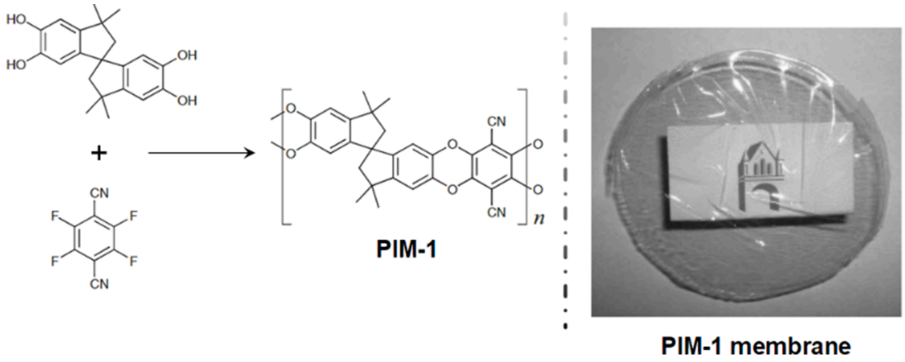

Fig. 8. Schematic illustration of the synthesis of PIM-1 and corresponding membrane cast from the PIM-1 solution. Reproduced with permission [209]. Copyright 2012, John Wiley and Sons.

conversation of nitrile groups of PIMs, which can be chemically replaced by other functional groups including amine [213], tetrazole [214], carboxyl [215], thioamide [216], and amidoxime [217]. The diversity of the function groups grafting in PIMs endows them with the capacity for versatile membrane applications. Smith et al. synthesized a family of functionalized PIM-1 via the tailor of nitrile moiety for better gas sorption [218]. Firstly, the pristine PIM-1 was treated with borane dimethyl sulfide complex to afford PIM-NH_2, the −CN groups of which were converted to $-NH_2$. Then, the resulting insoluble PIM-NH_2 was further reacted with di-tert-butyl decarbonate in a solid-state to afford PIM-*t*-BOC. In comparison with the parent PIM-1, PIM-NH_2 demonstrated improved CO_2 sorption performance due to a strong affinity between the $-NH_2$ group and CO_2. In 2008, McKeown and Budd utilized the formation of polyimide to connect the ladder-like units to yield the so-called PIM-polymides (PIM-PI) [219]. These microporous polymers bearing high surface area and adjustable pore size together with rigid polymer backbone promised that the corresponding porous membranes could be cast from these PIM-PIs with good performance of gas permeation. To date, the three types of polymerization reactions mentioned above were widely used for the construction of PIMs, offering PIMs with three major linkages including dibenzodioxin, Tröger's base (TB), and imide [123,220]. In addition to the change of linking bonds of PIMs to adjust their pore size and pore shape, the variation of the topology of the building blocks is another effective method to manipulate the microporosity of the resulting PIMs. Pinnau et al. designed two triptycene-based monomers with rigid 3D structures for PIM polymerization [221]. The resulting PIMs, called TPIM-1 and TPIM-2, were substituted with isopropyl/propyl at 9,10-bridgeheads, respectively, all exhibiting high separation performance for H_2/N_2, H_2/CH_4, and O_2/N_2 gas pairs, which indicated the importance of the topology of monomers in the pore size control for selective gas permeation. Later, based on this knowledge, McKeown et al. developed a 2D ribbon-shaped polymer, PIM-TMN-Trip, bearing inefficient packing of 2D chains, which demonstrated ultrapermeability for gasses [222]. The monomer, TMN-Trip was firstly synthesized and then reacted with tetrafluoroterephthalonitrile to offer PIM-TMN-Trip which owned a high BET surface area of 1050 m^2 g^{-1}. The physical characterization and gas permeability tests of PIM-TMN-Trip indicated that the disrupted packing of 2D chains would enhance intrinsic microporosity and polymer ultrapermeability. The last but not least, the polymerization of organic units via the connection of ether bonds is also applied in the ultrastable COFs construction. Fang [223] and Yaghi [224] reported an example of dioxin-linked COFs synthesized by the condensation of 2,3,6,7,10,11-hexahydroxytriphenylene (HHTP) and tetrafluorophthalonitrile (TFPN) independently. The resulting dioxin-linked crystalline polymers processing permanent and robust pore structure has ultrahigh chemical and thermal stability combined with high surface area. Besides, the existence of nitrile groups in the skeleton which are ready for the conversation to other functional groups can be reacted with a variety of chemicals to offer the COF with a wide range of applications. For example, after the treatment with hydroxylamine, the −CN groups can be completely replaced by amidoxime functionalized substitutions, offering the COF with the capacity for uranium sequestration.

2.2.4. HCP-based membrane

As early as the 1970s, hypercrosslinked polymers were successfully synthesized by Davankov and Tsyurupa [225]. HCPs represent one of the earliest examples of organic porous materials, and after decades of development, HCPs are still playing vital roles in gas adsorption and separation. In comparison with conventional crosslinked polystyrene, HCPs bearing highly crosslinked and compactly packed polymer chains have much more robust pore structures, thus forming permanent microporosity with a higher surface area. The significant feature of HCPs as compared to the other POPs with rigid porosity is the feasible synthesis for large-scale production. Most of the monomers used for the polymerization of HCPs are commercially available and easy to be modified. Besides, the synthesis conditions of such polymers are more moderate than that of other POPs. The overwhelming majority of HCPs are crosslinked via Friedel-Crafts alkylation, but the formation of extended HCP networks can be divided into three major techniques including direct polymerization of monomers, post-crosslinking of polystyrene-based unites, and external crosslinking [226]. At first, Davankov and Tsyurupa obtained the hypercrosslinked polystyrene via the crosslinking of dissolved linear or lightly crosslinked precursor in a thermodynamically compatible solvent. The solvent would occupy the swollen space between the polymer chains and then catalysts (Lewis acids, such as $SnCl_4$, $FeCl_3$) would be introduced to generate crosslinks between chains and halogen-containing compounds to immobilize the voids. After removing the solvent in vacuum, the occupied space by the solvent would be maintained and formed micropores. Thus, a hypercrosslinked polystyrene network is synthesized with a rigid structure and robust pore. This method, however, is limited by the restricted accessible liner precursors. Alternatively, one-step crosslinking of well-designed monomers for HCPs synthesis is much favored. The small bischloromethyl monomers such as dichloroxylene (DCX) and 4,4′-bis(chloromethyl)-1,1′-biphenyl (BCMBP) were used to synthesize novel HCPs via the self-condensation, which was reported by Cooper and co-worker, and the resulting HCP owning a high BET surface area of 1904 m^2 g^{-1} was unitized for hydrogen storage [227]. What's more, Tan et al. developed a low-cost versatile approach to connect rigid aromatic building blocks including benzene, biphenyl, 1,3,5-triphenylbenzene, methylbenzene, chlorobenzene, and phenol via a novel method called "knitting" strategy [228,229]. With the action of $FeCl_3$ as the catalyst, the benzene rings could be crosslinked by the formaldehyde dimethyl acetal as the bridge. Inspired by this success, a massive of HCPs via the direct crosslink of aromatic monomers under mild synthesis conditions have been reported, widely extending the family of HCPs. Due to the wide selection of aromatic monomers, the pore structure of HCPs can be further controlled as required through the rational design of basic building blocks with specific geometry and functionality, affording the resulting HCPs with diverse applications, such as metal ions sorption and isolation from the water, which is a popular research area for the study of HCP applications.

Just as other POP-based membranes, the initial application discovered for HCP-based membranes is the gas separation by taking advantage of the nanoscale channels existing in the membranes. Dai and coworkers reported a polymeric molecular sieve membrane via an *in situ* crosslinking strategy to construct hierarchical and tailorable porosity in the HCP-based membrane [230]. They immersed polystyrene (PS) membrane as the substrate support in the 1,2-dichloroethane solution of formaldehyde dimethylacetal (FDA) as the cross-linker and $FeCl_3$ as the catalyst; and the system was heated to 80 °C for 24 h without disturbing (Fig. 9). Then, the resulting wet membrane was washed with acetone, hydrochloric acid, and pure water in sequence to remove any unreacted chemical components, and dried at 60 °C under vacuum for 24 h to afford the final nanoporous membrane. Gas permeability measurements were performed after the membrane was mounted in a test chamber afterward, finding that the resultant porous polymeric membrane processed particularly high CO_2 permeability and CO_2/N_2 selectivity. Additionally, they also declared that the CO_2 permeabilities of the membranes were in line with their enhanced hierarchical porosity and higher surface areas. HCP-based membranes are also widely employed in ion separation, such as nanofiltration. Zhang et al. introduced a series of composite membranes assembled by PAN and the HCP thin film [231]. The novel NF membranes functionalized by a hypercrosslinked polyamide barrier layer exhibited high efficiency for Na^+/Mg^{2+} selective separation with considerable permeate flux.

2.2.5. PAF-based membrane

Porous aromatic frameworks are a type of special porous framework which is directly linked by the carbon–carbon-bonds from aromatic-based building blocks. Thus, most of PAFs are constructed via covalent coupling reactions between monomers, such as Yamamoto reaction, which is also the first coupling reaction used for the formation of PAFs. In 2009, Zhu et al. reported the targeted synthesis of a porous solid with a rigid pore structure and ultrahigh surface area of 5600 $m^2\ g^{-1}$, named PAF-1 [232]. The resulting polymer was polycondensated by tetrakis (4-bromophenyl)methane with the existence of bis(cyclooctadiene) nickel(0) ($Ni(COD)_2$) as the catalyst, forming a diamond-liked framework. After that, numerous PAFs with different coupling bonds and various framework topologies are artificially created. PAF-2 was designed immediately after the first introduction of PAF-1 which was synthesized based on the triangular triazine ring fusing of tetrakis (4-cyanophenyl)methane, the coupling reaction of which is the same for CTFs construction [233]. The surface area of PAF-2, however, was much smaller than that of PAF-1, only being 891 $m^2\ g^{-1}$. From this, we can find the selection of coupling reactions for PAF synthesis would influence the resulting surface area of PAFs even though the basic building blocks share the same geometry and similar molecular size. Later, more reactions, such as oxidative Eglinton reaction, nucleophilic substitution reaction, Suzuki–Miyaura coupling reaction, Sonogashira–Hagihara reaction, Scholl reaction, Friedal–Crafts reaction, and imidization reaction, are applied to self- or copolymerization of building blocks to yield PAFs (Fig. 10) [125]. The monomers with diverse geometries are designed on purpose to form the aromatic frameworks with various topologies, and the decorated tetraphenylmethane blocks are the most preferred monomers yet.

PAFs consisting of 2D/3D rigid periodic aromatic frameworks are supported by the robust aromatic skeletons, featured ultrastable porosity together with high surface areas and chemical and thermal stability, which offer PAFs the great resistance under harsh chemical treatments. Thus, the post-synthetic modification of resulting PAFs to afford them specific functions is scalable. Our group synthesized a series of modified PAF-1 which were obtained by easy treating the pristine PAF-1 with various chemical reactants. We first functionalized PAF-1 with the acid group, such as $–SO_3H$, to introduce the catalytic site in the PAF-1 skeleton for the polymerization of furfuryl alcohol (FA) [234]. Then, the H^+ was ion-exchanged by Ag^+ to afford a metal-doped framework, named as PAF-1-SO_3Ag. The successful doping of Ag^+ allowed the introduction of π-complexation with the carbon–carbon double bonds of olefin molecules to PAF-1, and the modified PAF-1-SO_3Ag was used for the selective adsorption of ethylene over ethane, indicating that PAF-1-SO_3Ag had the capacity to separate ethane from the mixture of ethylene and ethane. PAF-1 can also be functionalized as

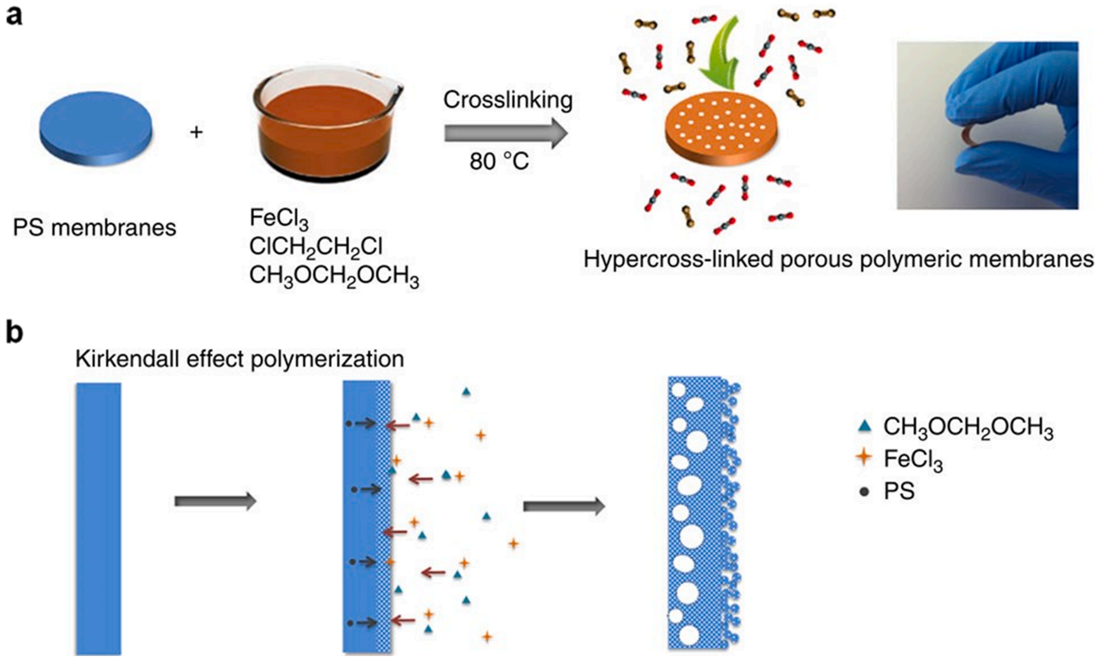

Fig. 9. Schematic illustration of (a) the preparation procedure for the porous polymeric membranes and (b) the non-equilibrium diffusion at the interface in membrane by Kirkendall effect polymerization. Reproduced with permission [230]. Copyright 2014, Springer Nature.

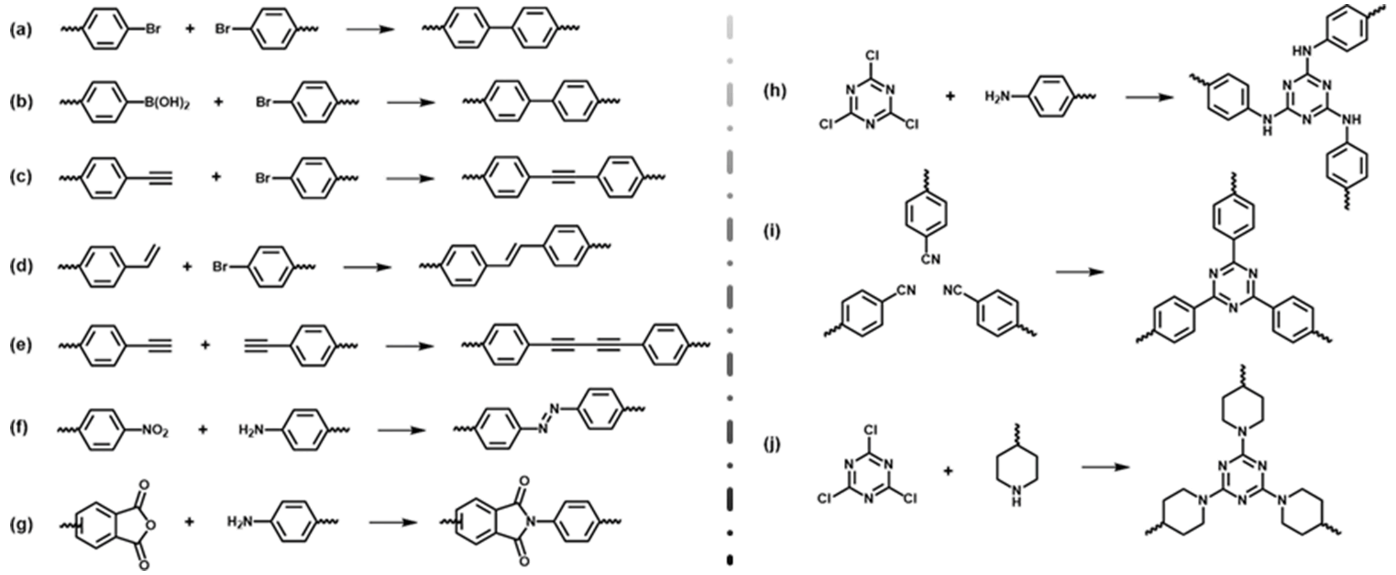

Fig. 10. Schematic representation of commonly used coupling reactions for the synthesis of porous frameworks. Reproduced with permission [125]. Copyright 2020, American Chemical Society.

a metal ions adsorption platform by grafting various groups with a strong affinity to specific ions. Depending on the accessible chloromethylation of PAF-1, we successfully introduced –SH group [235], –CH$_2$N$^+$(CH$_3$)$_3$X$^-$ (OH$^-$, Cl$^-$) group [236,237], –CH$_2$AO group [238], and –NH(CH$_2$)$_2$AO group [239] to the backbone of PAF-1 for task-specific adsorption of metal ions, such as Hg$^+$, AuCl$_4^-$ and Au(CN)$_2^-$, ReO$_4^-$, and UO$_2^{2+}$.

By contrast to COFs, the powder PAFs are commonly synthesized by irreversible reactions and the formation process was under kinetic control. This fact hinders the production of PAFs in another state of solid, such as membranes. Usually, to obtain a PAF-based membrane, it is necessary to combine it with other polymeric supports to afford MMMs, which is also a general technology to produce CMP containing MMMs. Zhu et al. mechanically mixed the PAF-56P particles and glassy polysulfone (PSF) in N-Methyl-2-pyrrolidone (NMP) to obtain a homogeneous suspension [240]. Then the PAF-56P/PSF solution was spun to cast the MMMs through the dry jet-wet method. The gas separation performance of the PAF-56P/PSF membrane was evaluated in a sealed membrane chamber, demonstrating selective permeance for CO$_2$ when a binary CO$_2$/N$_2$ gas mixture passed through the membrane. Recently, PAF-based membranes could also be obtained via *in situ* grow on the modified surface, and the same group successfully grown the iPAF-5 on a reactive surface to obtain a continuous PAF membrane [241], which demonstrated great potential for gas separation.

2.2.6. POC-based membrane

Porous organic cages are a type of unique porous materials without permanent porosity and infinite networks or framework. Each porous organic cage stands for a single molecular, and the porosity of such material is built from discrete organic cage molecules. In contrast to other crystalline porous materials whose porosity originates from the intrinsic pores, such as MOFs and COFs, the porosity of the POCs is extrinsic and is constituted between neighboring molecules. Broadly defined, some chemicals including macrocycles and cage-like compounds, such as cyclodextrin, polyhedral oligomeric silsesquioxanes (POSS), and Noria, are also regarded as organic cage molecules [242]. These molecules have been known for some time and studied, however, the concept of POCs was established until Cooper et al. stressed the first synthetic organic cage molecules which were synthesized via the Schiff base formation of aldehyde and amine groups [243]. After that, the discovery of such unique porous materials has been carried out rapidly, not only in the synthetic strategies but also in the applications development. A distinguishing feature of this type of artificial organic cage molecules is that they are discrete organic molecules and bear good solubility in a variety of organic solvents relative to COFs and CMPs [244]. This characteristic feature of POCs allows them to be suitable for solution-processable techniques, such as free-standing membranes or thin films fabrication. POC-based membranes can be simply produced by the self-assembly of resulting organic cage molecules during the controlled evaporation of the solvent. Additionally, POC-based membranes can also be built up from the interfacial polymerization (PI) of organic cage molecules, which is also used commonly for the free-standing COF-based membrane fabrication nowadays. Cooper's group reported the first casting of continuous and defect-free POC-based thin films via a solution-processing method without the addition of other support polymers (Fig. 11) [245]. The synthesized POCs including CC3, CC13, ASPOC, RCC3, and FT-RCC3 were firstly dissolved in chloroform or solvent pair (methanol/dichloromethane) to obtain a homogenous POC solution, and then thin films were fabricated via spin-coating the cage solution and drying on different substrates to prepare microporous films. The defect-free thin films with a designed film thickness can be formed using the technique of spin-coating, which is facile, adjustable, and reproducible. Moreover, the alteration of substrates offers the POC-based thin films the capacity for versatile applications. But being different from the self-assembly of COFs, organic cage molecules existing in POC membranes are packed together by *van der Waals* forces or hydrogen bonds, which are weaker than other intermolecular forces, such as covalent, ionic, or coordinative bonds. Therefore, mixing POCs with polymeric matrix or other POPs such as PIMs is also widely reported to support functionalized POCs in the membranes. As for the preparation of POC-based membranes, an interesting example of the *in situ* growth of free-standing membranes needs to be stressed. Chung et al. introduced a strategy of the interfacial polymerization between cyclodextrin (CD) and trimesoyl chloride (TMC) to prepare the porous membrane [246]. The resulting membrane processes a novel property, that is, the pores formed during the connection of CDs with the TMCs as the bridges are hydrophilic while the pore surface inside the cavities of CDs is hydrophobic. Thus, this membrane demonstrated high performances in both nonpolar and polar solvents, widely extending its applications. Accordingly, POSS- and Noria-based POC membranes were also fabricated by applying a similar synthetic strategy [242,247].

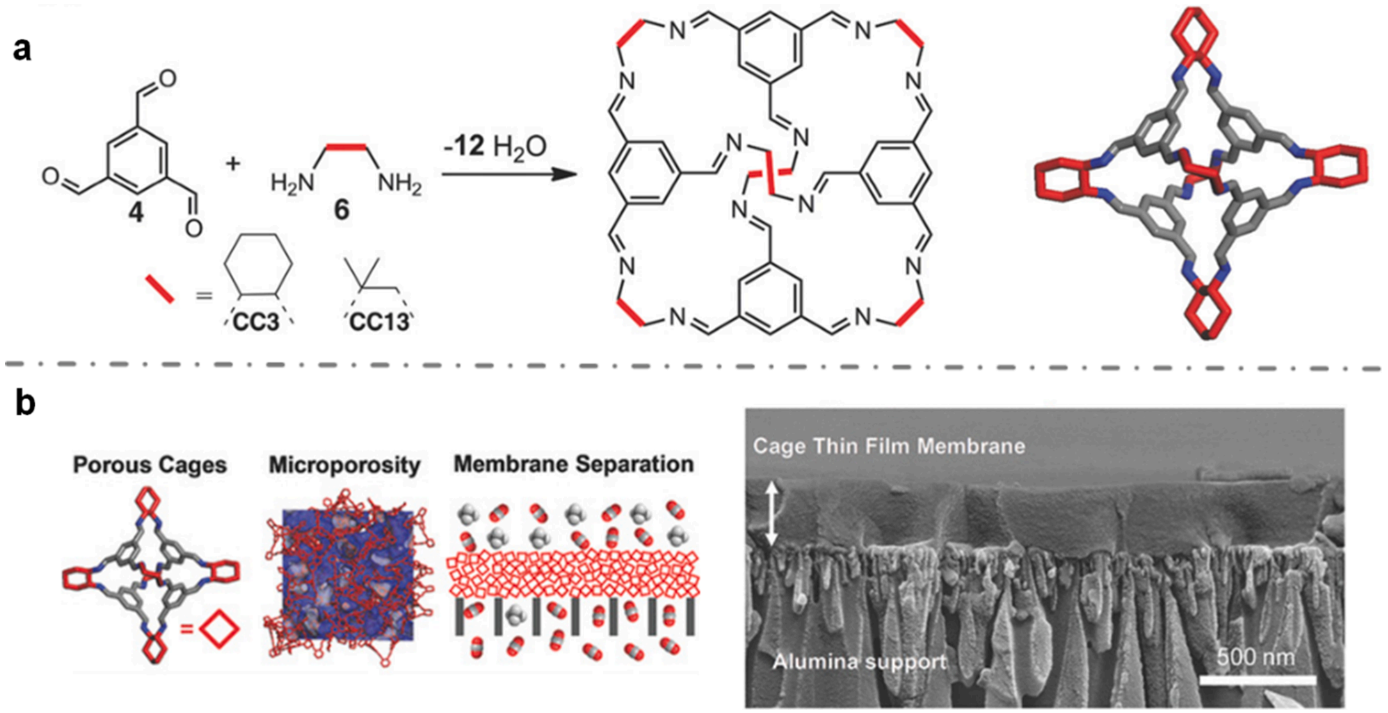

Fig. 11. (a) Schematic illustration of the synthesis of POCs. (b) Schematic illustration of the fabrication of POC-based membrane. Reproduced with permission [245]. Copyright 2016, John Wiley and Sons.

2.3. *Fabrication of POP-based membranes*

Over years of development of conventional polymeric and advanced POP-based membranes, several widely used methods for membrane fabrication have been well-known and studied, such as *in situ* casting or growth, interface-assisted synthesis, blending, and layer-by-layer stacking (Scheme 2). Soluble POPs including PIMs, POCs, and rare CMPs, can be directly dissolved in organic solvents, forming homogenous polymer solutions. Then the spin-coating technology will be provided to cast thin films or membranes from the solution with tailored thickness. Those membranes obtained by this method usually have defect-free surfaces and uniform thickness. However, COFs, HCPs, and most of CMPs are usually insoluble in any common solvent after being yielded in the state of solid. Thus, delicate methods for manipulating solid-state POPs to another state of solid (thin film or membrane) are urgently required. In the following content, both bottom-up strategy and top-down strategy for casting POP-based membranes will be discussed and evaluated in detail.

2.3.1. *In situ casting or growth*

Various POPs in the state of solid powder have been commonly used for molecular sorption benefiting from their controlled pore structure and versatile pore environment. However, the bulk porous materials required a laborious regeneration process each time after the accomplishment of the adsorption. Besides, massive well-designed POPs should be used to fill the chromatographic column to obtain good separation performance. Membrane technology, distinguishing from powder separation, depends on the thin barrier to allow the selective transportation of analytes from the mixture and reject unfavored analytes to permeate into the porous membrane. Thus, for preparing the membrane, only very few matrix materials are needed to form the thin film and the set-up membrane usually has a long-life cycle with high efficiency. For POP-based membrane synthesis, the preferential method of fabrication is *in situ* growth of the thin film or membrane. Using this method, a membrane with a continuous POP surface can be obtained successfully with high permselectivity which is rare in the blending membranes, enabling the membrane to fully take advantage of the pore structures of POPs for membrane separation. It follows that synthesizing continuous POP-based membranes by this strategy is in great demand for better separation performance. In terms of *in situ* approach for membrane fabrication, it can be divided into two specific strategies: (1) *in situ* casting of membrane from solution; (2) *in situ* growth of an ultrathin POP film on the modified support. The first strategy is limited by the physical property of POPs, such as solubility. Only a few types of POPs, such as soluble PIMs and POCs, would be suitable for this method to obtain a continuous defect-free porous membrane. For example, Jansen et al. obtained the POC and PIM composite membrane employing *in situ* crystallization of POC molecules from a homogeneous solution prepared by CC3 and PIM-1, then generated the membrane *in situ* via the solution casting method [248].

For most insoluble POPs, such as COFs, the *in situ* growth of an ultrathin COF film would be a promising way to fabricate the continuous membrane with a defect-free surface. The first example of growing COF thin film on the surface of porous substrates was stressed by Lu and Ge in 2014 [249]. They functionalized the porous α-Al_2O_3 ceramic support with 3-aminopropytriethoxysilane (APTES) and 4-formylphenylboronic acid (FPBA) in sequence to offer accessible boronic acid units for the formation of COF-5. Then, the modified α-Al_2O_3 ceramic support was immersed into the solution containing 1,4-benzenediboronic acid (BDBA) and 2,3,6,7,10,11-hexahydroxytriphenylene (HHTP) to grow uniform particles of COF-5 seeding from the boronic acid units attached on the support surface. The closely associated particle formed continuous membranes, however, the surface of this COF-5 based membrane was irregular and the interspace between COF particles was ubiquitous. Technically, it couldn't be referred to as the *in situ* growth of COF film. The year was 2017 and Banerjee et al. creatively added aromatic diamine to the aqueous solution of *p*-toluene sulfonic acid (PTSA) to form an organic salt firstly, then Tp was mixed with the salt under vigorous shaking to get the dough (Fig. 12) [250]. Later, the suspension was knife-cast on a clean glass plate and dried at 60–120 °C for 12–72 h. Finally, the synthesized COF-membrane was peeled off from the glass plate and washed with distilled water and acetone to remove any residue

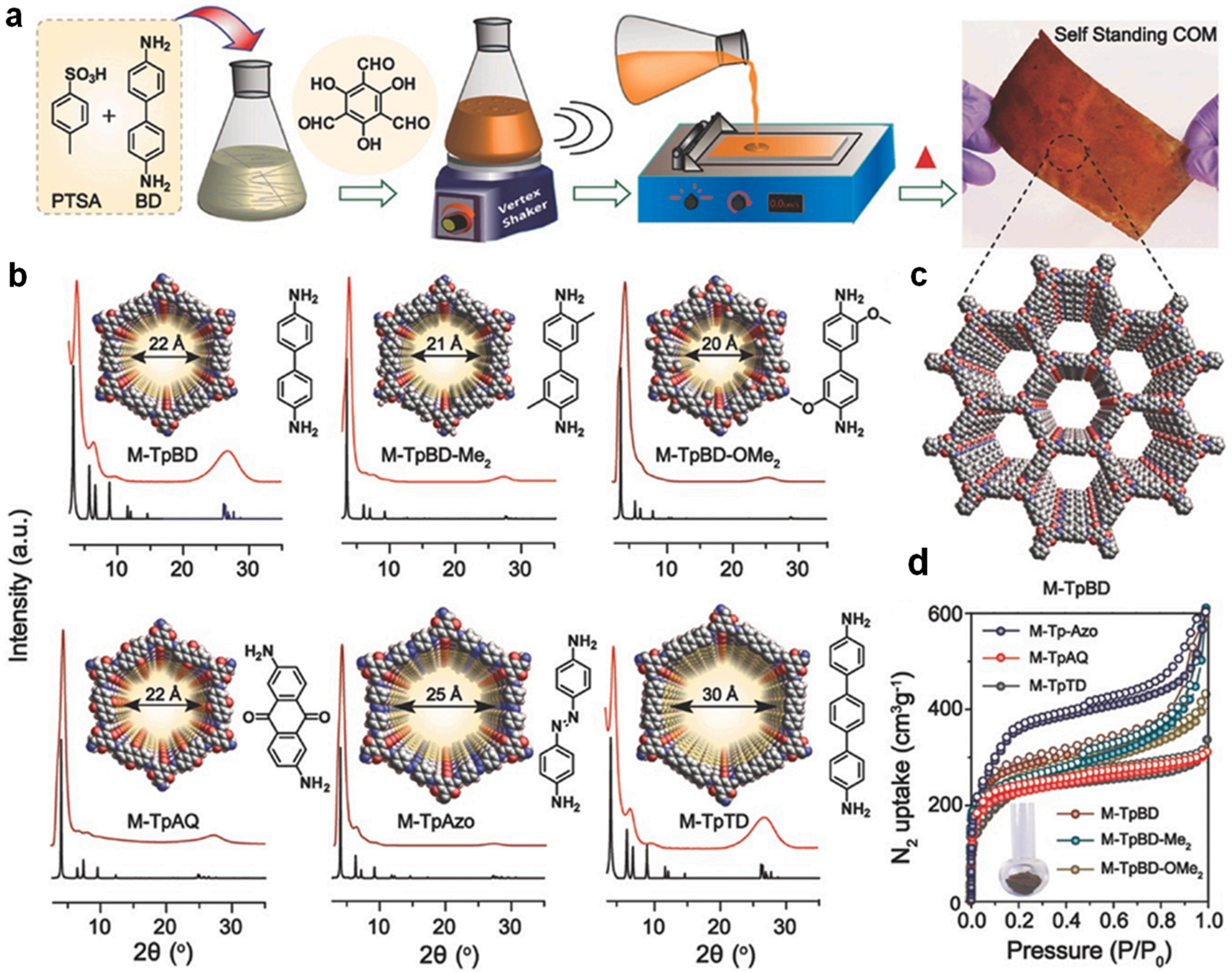

Fig. 12. (a) Schematic representation of the COMs (M-TpBD) fabrication. (b) Comparison of the experimental PXRD patterns of COMs with that derived from simulated eclipsed stacking models. (c) Space-filling packing model of M-TpBD hexagonal framework. (d) Comparison of N_2-adsorption isotherms of all six COMs presented in this work. Reproduced with permission [250]. Copyright 2016, John Wiley and Sons.

including PTSA, unreacted reagents, and monomer fragments. Significantly, the thickness of these COF-based membranes can be nicely controlled by adjusting the interval between the knife and the supporting glass plate. Thus, a series of M-TpBD of thickness ranging from ~200–700 μm were generated by this means. In contrast to the COF-5 membrane mentioned above, the M-TpBD membrane had a continuous surface without defects and cracks from the aggregation of layered COF nanosheets, which was verified by the SEM images. The NF performance of synthesized membranes was evaluated for the permeation toward acetone and acetonitrile afterward. The results demonstrated that the acetonitrile flux provided by M-TpTD was 2.5 times magnitude higher than that by current reported NF membranes made by polyamides with a similar solute rejection (~99%). Inspired by this success, this strategy was further employed to generate TpBD(Me)$_2$, TpAzo, and TpBpy based proton exchange membranes by slightly optimizing the casting of the precursor of COF membranes on a mold rather than a glass plate [251]. Soon after, Caro et al. developed a COF-COF bilayer membrane with a layered-stacking structure that bears an interlaced pore network to pile molecular sieves in order with larger and smaller holes, thus giving the novel membrane with excellent sieving selectivity for gas separations [252]. The dual-amino-Al_2O_3 disk was chosen in this report to support the COF-COF bilayer membrane and then was immersed in the solution containing 1,3,5-triformylbenzene (TFB), *p*-phenylenediamine (PA), and hydrazine hydrate to synthesize the target membrane. The container was left at room temperature for 72 h for the formation of COF-LZU1 which was produced from the polycondensation of TFB and PA followed by the heat process to form ACOF-1 on the surface of COF-LZU1. Finally, COF-LZU1–ACOF-1 composite membrane supported on a porous Al_2O_3 disk was washed with dioxane and ethanol to get rid of the residual unreacted reactants retaining in the pores of synthesized COFs. The novel COF-COF membrane exhibited higher permselectivity for binary gas mixtures, such as H_2/CO_2, H_2/N_2, and H_2/CH_4 than that of the individual COF-LZU1 and ACOF-1 membranes owing to the interlacing of various pore networks, and the overall performance surpassing the Robeson upper bounds. Additionally, the composite membrane with MOF-in-COF structure was also reported by Caro and co-workers [253]. They took advantage of the porosity of COFs to install Co^{2+} on the pore walls, then 2-methylimidazole was introduced into the Co^{2+} loaded COF membrane to synthesize ZIF-67 inside the 1D channels of TpPa-1 to form hierarchical pore structures. The resulting MOF-in-COF membrane supported by α-Al_2O_3 substrate was then mounted with a homemade apparatus for gas-separation measurement and the N_2 was used as the sweep gas. The results demonstrated that this hierarchical porous membrane could selectively sieve H_2 from a binary gas mixture, such as H_2/CO_2, H_2/CH_4, H_2/C_3H_6, and H_2/C_3H_8, which was mixed with gasses bearing distinct kinetic diameters.

The COF-based membrane supported by a polymeric matrix features the great potential for liquid separation such as nanofiltration. Jiang et al. reported a bottom-up strategy to coat the ultrathin sulfonated imine-linked COF layer (SCOF) on the PAN support [254]. The matrix PAN support was loaded by ultrathin polydopamine layer at first which served as a medium to offer accessible nucleation sites for COF formation. Then, the support was placed in the solution prepared by Tp and Pa-SO_3H at room temperature for 72 h to afford the formation of SCOF followed completely wash with 1,4-dioxane, ethanol, and DI water to get SCOF/PDA/PAN membrane. The filtration performance of the resulting composite membrane was evaluated for dye rejection in an aqueous solution using a dead-end stirred cell filtration device under the stable pressure which originated from compressed nitrogen gas. The results indicated that the SCOF layer in the composite membrane acted as a selective barrier which only allowed the permeation of pure water and rejected the entrance of dye molecules to the channels in the membrane.

PAF-based freestanding membranes can also be generated via the *in situ* casting from the solution, which was reported by Zhu and coworkers [255]. They first modified the PAF skeleton with flexible monomers 1, 3, 5-tri(4-cyanophenoxy)-benzene which contained ether groups to enhance the structural flexibility, and after, the target PAF could be synthesized from the polycondensation of 1,3,5-tri(4-cyanophenoxy)-benzene as the building blocks by using a super acid of trifluoromethanesulfonic acid (CF_3SO_3H) as the catalyst according to the previous work reported by Dai et al. [256]. And they modified this process specifically to generate the PAF-based membrane via this one-step acid-catalyzed reaction. After the addition of CF_3SO_3H to 1, 3, 5-tri(4-cyanophenoxy)-benzene and the mixture was stirred at −5 °C under argon for 2 h, followed by pouring the solution onto a glass plate. The polymerization of PAF-97 would be finished after heating the liquid at 100 °C for half an hour, then the transparent and free-standing PAF-97 membrane was obtained. Cooper et al. proposed a soluble CMP by a two-sept type Suzuki-catalyzed aryl-aryl coupling copolymerization and then cast freestanding membrane based on the synthesized SCMP [201]. The dichloromethane solution dissolved SCMP was tiled on a glass plate, followed by slow evaporation of the solvent. Finally, the transparent and yellow SCMP film could be peeled from the glass plate. Tang and co-workers developed a surface-initiated polymerization strategy through C–C coupling reactions to generate CMP-based membranes *in situ* [257]. 1,3,5-triethynylbenzene (1,3,5-TEB) with three different dibromobenzenes, 1,4-dibromobenzene, 1,3-dibromobenzene and 1, 2-dibromobenzene, respectively, together with as-grafted silica wafers were added into the solution mixture of toluene and triethylamine containing tetrakis(triphenylphosphine)palladium and CuI as the catalysts to perform the fabrication of CMP-based membranes at 100 °C. The bromobenzene groups grafted on the surface of silica wafers acted as the seed of membrane growth. Then the synthesized CMP was protected by a thin layer of PMMA via typical spin-coat processing.

2.3.2. Interface-assisted synthesis

The research of interfacial polymerization has been studied in depth and this technology is the most commercial approach for the synthesis of thin-film composite (TFC) membranes with polyamide or polyester separating layers. This method allows the large-area generation of thin continuous films with the defect-free surface, especially being capable for advanced COF-based membrane production [258]. A pioneering work of generating continuous COF-based membranes by interfacial polymerization was proposed in 2017. Banerjee et al. utilized a liquid-liquid interface as a synthetic template under ambient conditions for COF thin film preparation [259]. During this process, the control over the rate of the Schiff base reaction is of great importance to form a crystalline COF rather than amorphous polymers. As we all know, the self-healing of amorphous structures into ordered structures is a thermodynamic process, thus requiring enough time to complete it. In this work, a salt-mediated technique to form amine-*p*-toluene sulfonic acid (PTSA) salt dissolved in the aqueous phase was used to react with the aldehyde in the organic phase, rather than using free amine directly. The H bonding within the as-prepared PTSA-amine salt effectively retards the diffusion rate, thus slowing down the diffusion of precursors through the interface. Finally, the nucleation of target COF can be thermodynamically controlled by a lower rate of the Schiff base reaction. Beyond that, they extended this strategy of using PTSA to react with the monomer with amine groups before the crystallization to various COFs, generating a series of 2D COF thin films with different pore sizes at room temperature [260]. Recently, the field of fabricating 3D COF membranes is rising rapidly. Jiang et al. reported their work on the synthesis of COF-300 membrane via the interfacial polymerization method (Fig. 13a) [261]. The typical monomer for constructing 3D COFs, tetrakis(4-aminophenyl) methane was chosen as the building blocks, and *p*-phthalaldehyde as the bridge was used to connect tetraphenylmethane units. The amine monomer solution was prepared in the acetic acid aqueous solution and transformed into the beaker. Then, the mesitylene solution dissolved aldehyde monomer was added carefully on the top of the amine monomer solution, forming an aqueous/organic solvent interface. Afterward, the beaker would be sealed and placed into the oven under 65 °C without any disturbance. After 24 h later, the COF thin film was formed at the liquid interface and then taken out, followed by the wash with N, N-Dimethylformamide and 1,4-dioxane. They treated the synthesized COF thin film with etidronic acid as proton carriers to afford it with proton conduction capacity, evaluating by a two-point-probe method.

More recently, a new approach using $Sc(OTf)_3$ (Lewis acid catalyst) as a catalyst for Schiff base reaction is proposed to form COF-base freestanding membranes through interfacial polymerization. Dichtel et al. was the first group to use $Sc(OTf)_3$ to synthesize imine-linked COFs and then employed this catalyst in the production of imine-linked COF membranes [262]. In their report, they presented a novel method to synthesize the COF thin films via liquid-liquid interfacial polymerization (Fig. 13b) [263]. They dissolved TAPB together with PDA in a 1,4-dioxane/mesitylene solution to obtain homogenous solutions, and the resulting solution was layered on the top of the aqueous solution of $Sc(OTf)_3$. After three days of polymerization, the freestanding membrane was grown on the interface and transformed out from the container. Then, they modified the reactions by shorting the reaction time to get a thin film of TAPB-PDA COF and transferred it onto the surface of a silicon wafer or a carbon grid to get substrate-supported membranes.

Generating the polyamide film at the liquid/air interface is another established method, and wildly used for the fabrication of continuous COF thin films recently. Lai et al. first utilized this strategy to synthesize an ultrathin COF film which was constructed from the polycondensation of Tp and 9,9-dihexylfluorene-2,7-diamine (DHF) through the Langmuir–Blodgett (LB) method [264]. DHF and TFP were respectively dissolved in toluene to prepare the stock solutions. Then, DHF and TFP solutions are well mixed and slowly spread on the water surface which was filled in the LB trough in advance. The surface layer was compressed after the evaporation of toluene, followed by the addition of trifluoroacetic acid dropwise into the solution to start the polymerization. When the reaction is completed, a continuous TFP-DHF ultrathin film with a thickness of 3 nm is grown at the water-air interface. They also introduced two methods to transfer the synthesized COF films on the support surface, named as Langmuir–Blodgett (vertical) method and the Langmuir–Schaefer (horizontal) method, respectively. Subsequently, the same groups modified this method by using $Sc(OTf)_3$ as the catalyst instead of trifluoroacetic acid to prepare 2D COF membranes with different pore sizes by controlling the alkyl chains attached in monomers [265].

Transferring the fragile COF thin films to the specific support to improve the mechanical strength of membranes to meet the requirements for real-world separation applications is tricky. To solve this

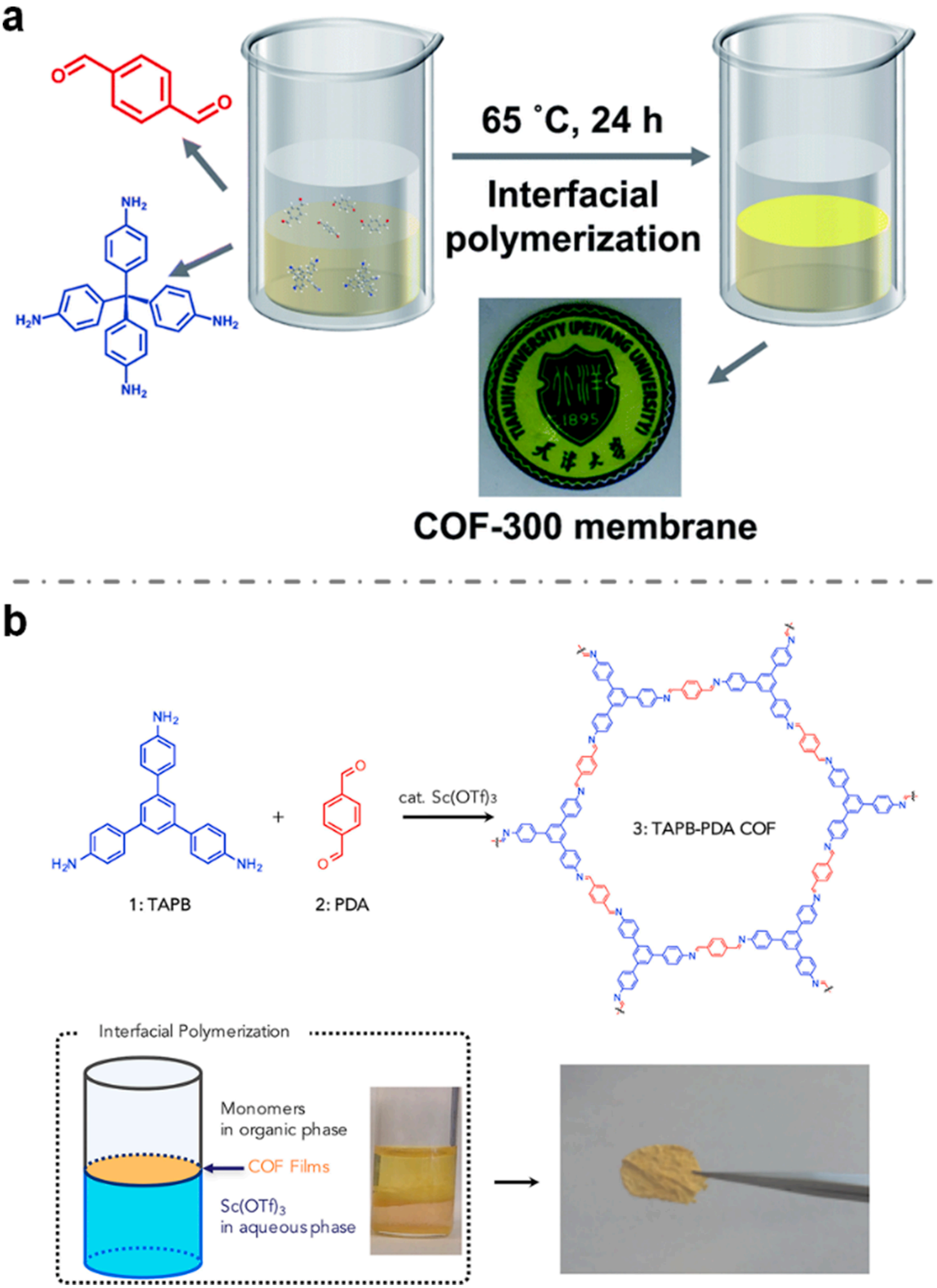

Fig. 13. (a) Schematic illustration of the fabrication of the COF-300 membrane via interfacial polymerization. Reproduced with permission [262]. Copyright 2021, Royal Society of Chemistry. (b) Interfacial polymerization of TAPB-PDA COF using *Sc*(OTf)$_3$ as the catalyst. Reproduced with permission [263]. Copyright 2018, Elsevier.

problem, the porous substrate was placed at the liquid-liquid interface, forming a liquid-solid-liquid interface for the ready formation of COF-based membranes. Sun and our group have reported several COF-based membranes which were prepared via this method [266–271]. Taking the COF-EB_xBD_y/PAN membranes as an example, we used a multivariate (MTV) strategy to readily manipulate the charge density of synthesized membranes in one COF. A series of membranes of COF-EB_xBD_y constructed by the addition of various ratios of EB and benzidine (BD) were directly formed on the surface of an asymmetric PAN ultrafiltration membrane via the liquid-solid-liquid interface polymerization [266]. The PAN support was vertically mounted in the connection of two chambers of the homemade diffusion cell. Afterward, the aqueous solution of EB and BD with different rations and *p*-toluenesulfonic acid was poured into one of the chambers. On the other side, a CH_2Cl_2 solution dissolved Tp was introduced. The diffusion cell was sealed and kept at 30 °C without disturbing for four days. The resulting composite membrane can be easily taken out from the diffusion cell and be ready for separation test after the wash with methanol and air-dry. Additionally, Wang et al. proposed a similar method to synthesize COF and polysulfone (PSF) composite membrane [272]. In their report, the PSF support was fixed on a membrane holder firstly, and PA aqueous solution was dropped to the PSF substrate to load PA inside the substrate. After the Pa-saturated substrate was obtained, Tp hexane solution was gently poured onto the surface. The interface polymerization of the COF, TpPa, would happen during draining off the hexane solution. The color of the membrane surface changed immediately along with the permeance of Tp solution, indicating the rapid formation of COF on the surface of the PSF substrate. Then the wet membrane was heated to 60 °C for 5 min to improve the adherence between TpPa and substrate. In this process, the aqueous solution filled in the support voids, PSF substrate, and organic solution above the support surface formed a micro liquid-solid-liquid interface. Subsequently, the same group further developed the liquid-liquid interface polymerization for COF membranes, some novel methods, such as unidirectional diffusion synthesis [273], secondary growth [274], and pressure-modulated synthesis [275] have been well studied to generate advanced COF/porous substrate composite membranes for dye removal and desalination.

2.3.3. *Blending*

The blending (or mixing) of POPs with the polymer solution to cast a composite membrane is a straightforward and cost-effective method, which is suitable for all types of POPs either soluble or insoluble. It has been widely used to fabricate conventional polymetric membranes, and currently, these traditional membranes by blending (or mixing) with a certain ratio of functional POPs during the forming process might be given with a superior separation performance compared with the pristine membrane. One of the most used COFs in the wedding with polymers to cast porous membranes is SNM-1, which is a type of 3D COF with rich imine groups constructed by Melamine and PDA. Jiang et al. was the first group to propose this COF for the fabrication of MMMs [276]. Sodium alginate (SA) and PIM-1 were added to the suspension of SNM-1 particles, respectively, to cohere SNM-1 and from uniform membranes after the evaporation of solvents. The resulting MMMs with hydrophilicity, permanent microporosity, stable structure, and ordered nanochannels exhibited improved permeability with stable long-time running. Additionally, COF-LZU1 incorporated into poly(vinylamine) (PVAm) [277,278], NUS-2/NUS-3 blended with poly(ether imide) (Ultem) or polybenzimidazole (PBI) [279], ACOF filled in polyimide Matrimid® 5218 [280], TpPa-1 dispersed in polyether-*block*-amide (PEBA) [281], were also developed to cast MMMs via the induced phase inversion when the support coated with blending being immersed in water to form a membrane. To avoid the hydrolysis of COFs when being treated in water for a long time, Xu and co-workers selected TpPa-2 as the nanofiller to prepare MMMs and used the synthesized membrane for water purification (Fig. 14) [282]. With the slight modification of the aldehyde monomer with the attachment of methyl groups, the synthesized TpPa-2 sharing a similar topology and pore structure with TpPa-1 exhibited exceptional resistance to hydrolysis and high chemical stability in a wide range of pH. TpPa-2 particles were further blended with PSF and PEG400 to obtain a homogeneous casting solution with vigorous stirring. The solution was then cast onto a glass plate carefully by a casting knife. Finally, the MMMs would be produced via non-solvent induced phase inversion by immersing the coating glass plate in deionized water. The pure water permeability of the resulting membrane was tested by using a homemade cross-flow UF setup, suggesting enhanced nanofiltration capacity as compared to a pure PSF membrane. In addition, the hydrolytic and chemical stabilities of TpPa-2 which was produced via microwave synthesis were also evaluated via immersion test in organic solvent (n-hexane) and aqueous solution including deionized water, natural seawater, NaOH solution, and HCl solution. Zhao et al. reported two powder COFs, NUS-9, and NUS-10, which were functionalized by sulfonic acid groups in their frameworks [171]. The synthesized sulfonated COFs were blended with nonconductive polymer support to generate a series of MMMs with proton conductivity up to 1.58×10^{-2} S cm^{-1}. In this work, polyvinylidene fluoride (PVDF) was used to disperse the COF particles and the

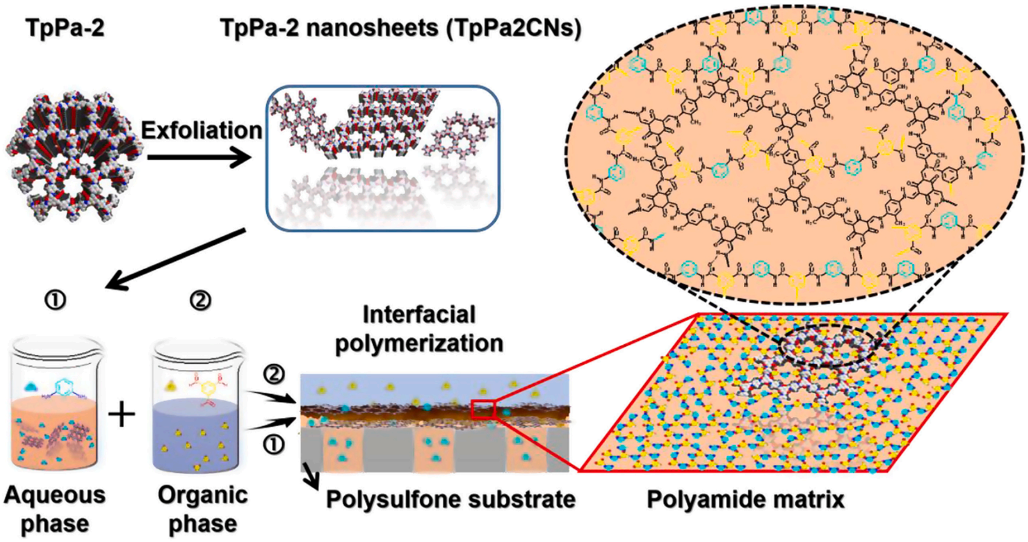

Fig. 14. Schematic illustration of fabrication and structure of TpPa2CNs/PA membranes. Reproduced with permission [282]. Copyright 2020, Elsevier.

composite membranes were prepared through solution casting. With the increased loading of sulfonated COF in the MMMs, the performance of proton conductivity of MMMs has improved accordingly, suggesting that the sulfonated nanovoids in MMMs stemmed from COF particles contributed to the formation of nanochannels for proton transformation. However, further increase of COFs in MMMs was limited by the brittleness of obtained MMMs. Thus, the rational blending of COFs and polymer support with an optimized ratio is crucial to obtain robust and stable MMMs with optimal performance.

PIMs, a typical class of glassy polymers, are considered as the ideal matrix to incorporate with other functional fillers to produce MMMs. Pure PIM-based membranes are vulnerable to physical aging, the blending strategy to cast PIMs-based MMMs would be an effective technique to prevent or slow down the physical aging of PIMs, improving the performance of such membranes in separation applications. Very recently, Hill and Freeman incorporated PAF-1 to PIM-1 membrane to enhance the gas separation performance [283]. PIM-1 polymer was first dissolved into anhydrous chloroform and the pre-prepared PAF-1 nanoparticles then were added to the PIM-1 solution with complete stirring. Afterward, the thin MMM could be fabricated by the spin coating method. HCP can also be used as the nanofiller to mix with PIM polymer solutions to form thin-film nanocomposite (TFN) membranes with enhanced organic solvent nanofiltration. Cooper and co-workers described the formation of MMMs from the blending of PIM-1 and HCP-Polystyrene via an emulsion polymerization process [284]. With the addition of the prepared submicron-sized HCP particles to PIM-1, they could obtain an HCP suspension with a homogeneous distribution of particles. The suspension was later cast on a glass or Teflon mold to prepare the MMMs which processed fewer surface defects and cracks due to the good dispersion of smaller HCP particles in PIM-1 as compared to the previous MMMs fabricated with the mixing of PIM and larger HCP particles. What's more, the preparation of MMMs by blending PIM polymer with POCs was also given with a slight modification of the method discussed above [285,286].

2.3.4. Layer-by-layer stacking

Most of 2D COFs bearing planar nanosheets or monolayers can be exfoliated for the fabrication of membranes via a layer-by-layer (LBL) stacking strategy. This approach was firstly developed for the synthesis of membranes stacked by graphene and graphene oxide monolayers. Generally, a homogenous suspension of nanosheet dispersions will be obtained firstly by chemical or physical exfoliation of bulk materials in water or organic solvents. Subsequently, the nanosheets will be stacked on the surface of a porous support matrix with the assistance of pressure or vacuum-assisted filtration, or dip coating, thus forming the continuous thin films. The exfoliation of 2D COFs has been well studied in the past years, and various approaches are used to get few- or single-layer COFs.

Dichtel et al. proposed a solvent-assistant method to exfoliate the hydrazone-linked 2D COF by immersing it in specific solvents, such as dioxane, H_2O, and DMF. Soaking COF-43 to mentioned solvents for 2 h under room temperature without sonication, they surprisingly found the crystallinity loss of COF-43 which was confirmed by PXRD measurements [287]. On the contrary, COF-43 after being exposed to THF, $CHCl_3$, MeOH, and toluene retained the crystallinity. The impossibility of the crystallinity loss as the result of the hydrolysis of acyl hydrazone linkages within COF-43 was confirmed by the Fourier transform infrared spectroscopy (FTIR), and no obvious difference was found from the spectra. Selected area electron diffraction (SAED) of these multilayers exhibited a hexagonal diffraction pattern, which was in line with their polycrystalline, hexagonally ordered structure. Those results indicated that the exfoliation of COF-43 could happen in specific solvents. And recently, Ogale and co-workers reported a novel COF with self-exfoliated ability which was synthesized by introducing flexibility into the framework [288]. The asymmetrical triazole-based monomers as the building blocks were used to react with Tp to afford less ordered COF. This COF would grow into self-exfoliated covalent organic nanosheets (CONs) even during synthesis. A chemical stripping strategy was reported to obtain exfoliated few-layered COF nanosheets (E-TFPB-COF) by Wang and co-workers [289]. They used $KMnO_4$ to exfoliate bulk TFPB-COF via a strong oxidant intercalation process, and the exfoliated E-TFPB-COF/MnO_2 composite would be filtered after the reaction was completed. Then HCl aqueous solution was prepared to dissolve and remove the MnO_2 intercalated between monolayers of the COF and afforded E-TFPB-COF. Exfoliated COFs can also be prepared via mechanical exfoliation by using ball milling at room temperature without additional exfoliating agents. Wang and Feng employed this method to exfoliate a series of DAAQ-COFs [290]. The exfoliated DAAQ-ECOF was mounted as the cathode material for lithium-ion batteries exhibiting better rechargeability and faster charge-discharge ability as compared to the pristine COF due to the faster diffusion of lithium ions between few-layered nanochannels of exfoliated COFs. Diverse imine-based 2D COF nanosheets in large scale and high yield are also prepared by Jiang and co-workers [291]. They proposed a scalable bottom-up strategy to generate 2D imine-linked COF nanosheets via an imine-exchange synthesis by the addition of a large excess amount of 2,4,6-trimethylbenzaldehyde (TBA) as the modulator into the reaction system. During the process of COF formation, massive bulky 2,4,6-trimethylphenyl groups would be attached to the edge of the COF nanosheets, thus hindering the axial π-π stacking of the COF nanolayers into bulk COF material and allowing anisotropic growth of the single COF layer along with the planar directions. Finally, the COF nanosheets constructed by a few layers together with large lateral sizes were synthesized *in situ* with a high yield. The crystallinity of imine-linked 2D COF nanosheets was confirmed by the sharp SAED pattern, suggesting the feasibility of TBA-assistant synthesis of COF nanosheets. With this strategy in hand, they successfully synthesized ultrathin nanosheets for COF-366, COF-367, COF-367-Co, TAPB-PDA COF, and TAPB-BPDA COF.

Dichtel et al. proposed the process of casting COF thin films on the porous substrates from exfoliated COF suspension (Fig. 15) [292]. BND-TFB COF synthesized by the condensation of TFB and N-benzidine benzophenone imine was treated by trifluoroacetic acid in the solvent mixture of acetonitrile and tetrahydrofuran. After complete stirring, a suspension on exfoliated BND-TFB COF would be obtained which was ready to deposit onto the surface of the various substrate. The wet surface was exposed to air allowing the evaporation of solvent until the coated COF layer became homogeneous and viscous, followed by the spin program which was initiated to form the continuous COF thin film. The thickness of the resulting films could be controlled by the modification of both the concentration of COF suspensions and the spin speeds during the thin film formation. Additionally, several MMMs are produced by *in situ* growth of COF nanosheets on the porous substrates, such as graphene oxide (GO), under solvothermal conditions. Jiang [293] and Zhang [294] developed the approach to fabricate GO/COF composite membranes from GO/COF nanoheterojunctions via various filtration technologies.

3. Energy-saving applications

Membrane separation involving gas separation and liquid separation is attracting incomparable research interests due to its obvious advantages such as high selectivity with unsuppressed permeability, reduced carbon footprint, small capital investment, and low energy consumption as compared to other separation technologies including chromatography and thermal separation (Scheme 3). Additionally, POP-based membranes exhibit their promising applications in energy storage, sensing, and electro/photo-catalysis, as well [50]. For example, a variety POP-based thin films have been mounted in lithium-ion batteries to provide the reduced ion/electron migration length and improved ion/electronic diffusion; [95,295] and CMP and COF-based membranes are also popular in capacitor and fuel cell design [296,297]. In this section, the significant progress of a typical energy-saving application (molecule

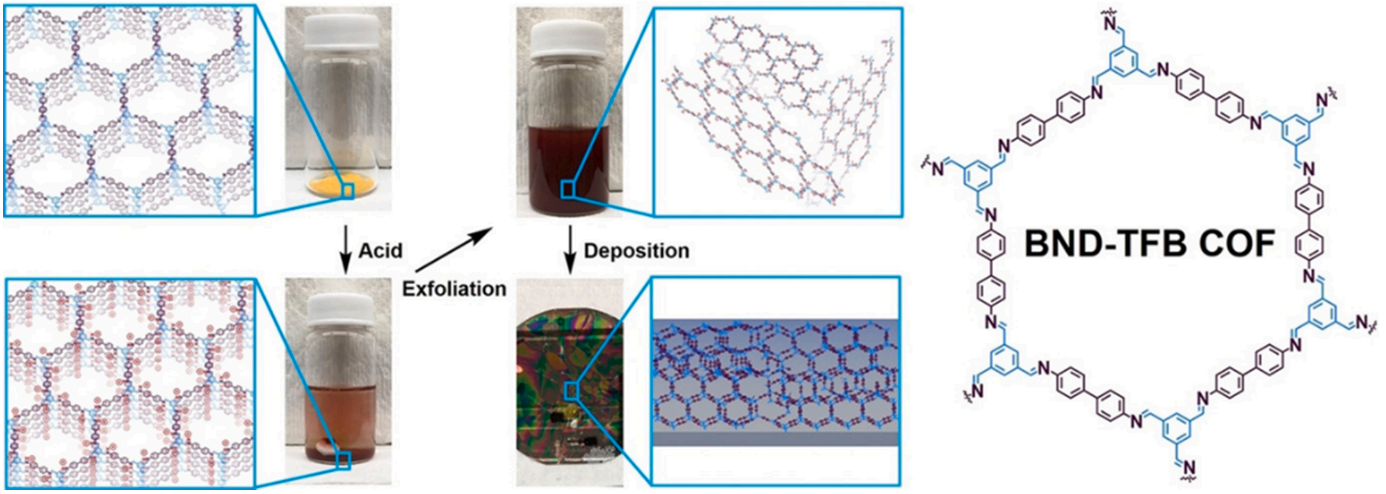

Fig. 15. Schematic illustration of the acid-exfoliation and film-casting procedures for BND-TFB COF. Reproduced with permission [292]. Copyright 2019, John Wiley and Sons.

sieving) of POP-based membranes is highlighted and discussed in detail.

3.1. Gas separation

Membrane-based separation technology used for feedstock gas purification has served as an essential tach in the whole production supply chain. However, conventional polymeric membranes suffer from some inherent flaws, such as disordered pore structure and inconsistent pore size. Besides, the separation performance of old-fashioned membranes is limited by Robeson upper bounds, meaning the trade-off between permeability and selectivity [298]. The emerging porous organic polymers with uniform pore structure and controllable pore size would be preferred for the fabrication of advanced membranes to fine-tune the relationship between permeability and selectivity during molecular sieving (Table 1). The feasibility and accessibility of functionalizing POP-based membranes with diverse chemical or physical properties allow the further manipulation of membrane surfaces for task-specific gas separation. One of the most common gas separations is the purification of H_2 from other gasses based on the fact that H_2 always has a much smaller kinetic diameter than that of other gasses. The membrane separation of hydrocarbon gasses, such as CH_4, from CO_2 or N_2, is also a popular research area to provide cleaner and economic feedstock gasses for industrial applications.

Hydrogen is a class of typical sustainable and clean energy source, which is supposed to replace conventional fuels gradually, thus mitigating environmental concerns. The purification of produced H_2 in industry is necessary due to the unwanted gasses blended during the production process. Microporous membranes fabricated by all types of POPs can be used for H_2 separation from other gasses in theory. But it is also widely accepted that POP-based membranes process lower selectivity as compared to MOF-based membranes whose aperture sizes can be precisely tuned according to the kinetic diameter of H_2 molecular (0.289 nm), which is far smaller than the typical pore size of COFs (0.8–5 nm). In a pioneer study reported in 2015, Gao et al. generated a COF/Al_2O_3 composite membrane by growing the COF-320 on the NH_2-mofided α- Al_2O_3 porous support *in situ* [299]. The fabricated novel 3D COF-320 membranes were tested for H_2 separation from CH_4 and N_2, representing a lower separation factor of 2.83 for H_2/CH_4 and 3.74 for H_2/N_2. Later, a comprehensive computational study was carried out in 2016 to discuss the feasibility of COF-based membranes for gas separation based on the electron density overlaps between gas molecules and skeleton [300]. The report demonstrated that monolayer CTF-0 based membrane possessed an exceptionally high selective permeation of H_2 from the gas mixtures such as H_2/CO_2, H_2/N_2, H_2/CO, and H_2/CH_4 with the separation factor up to 9×10^{13}, 4×10^{24}, 1×10^{22}, and 2×10^{36}, respectively. The experimental data, however, showed a much lower separation factor than the theoretical value for separation of H_2/CO_2, H_2/CH_4, and H_2/N_2, which was 31.4 [279], 140 [301], and 84 [252], respectively. This difference might be the result of experimental COF-based membranes bearing increased thickness than monolayer COF membranes.

Ben and co-workers creatively synthesized a COF-MOF composite membrane for gas separation with enhanced separation selectivity of H_2/CO_2 gas mixtures [302]. The polyaniline (PANI) coated SiO_2 disk was used to support the first fabrication of COF-300 membrane through solvothermal method. Then one side of the SiO_2 disk grown COF-300 was further treated in the DMF solution of zinc nitrate hexahydrate, terephthalic acid, and 1,4-diazabicyclo[2.2.2]octane under heating to grow MOF layer on covering the pre-synthesized COF layer. The resulting composite membrane exhibited higher selectivity of the H_2/CO_2 gas mixture as compared to the individual COF and MOF membranes, giving a higher separation factor of 12.6. Subsequently, they fabricated a 2D COF layer on the as-synthesized MOF layer to generate a COF-MOF composite membrane [303]. A similar synthetic strategy with slight modifications as compared to the above method was employed in this recent report. The UiO-66 was synthesized on the PANI coated SiO_2 disk at first, and then H_2P-DHPh COF which was obtained from the polycondensation of 5,10,15,20-tetrakis(4-aminophenyl) porphyrin and 2,5-dihydroxyterephthalaldehyde was grown on the MOF layer. The selectivity of the H_2/CO_2 gas mixture with this COF/-MOF composites membrane surpassed the previous work reported by them with a separation factor up to 32.9, which also outperformed the present Robeson upper bound. Caro and Meng developed another composite membrane with excellent separation of hydrogen with high selectivity via taking advantage of both COFs and MOFs (Fig. 16) [253]. They introduced ZIF-67 structures to the synthesized TpPa-1 membrane by the confined growth inside COF pores. The separation performance of ZIF-67-in-TpPa-1 membrane supported by α-Al_2O_3 processing uniform, compact, and the defect-free surface was envaulted for the H_2 separation from equimolar various gasses, demonstrating better separation selectivity as compared to that of the single TpPa-1 membrane without the introduction of ZIF-67 with a separation fact as high as 34.9, 33.3, 110.5, and 192.7 for H_2/CO_2, H_2/CH_4, H_2/C_3H_6, and C_3H_8, respectively. Caro's group also proposed a strategy to grow COF films layer by layer with the composition of two types of COFs with different pore sizes to generate interlaced pore networks, thus improving separation selectivity for H_2 [252]. COF-LZU-1 was firstly fabricated on the NH_2-modified Al_2O_3 substrate and ACOF-1 with a smaller pore size was covered on the

Table 1
Summary of gas separation performance of representative POP-based membranes.

Membrane	Name	Thickness (μm)	Separation	Selectivity	Permeability
COF	COF-320 [299]	~4	H_2/CH_4	2.83	5.67×10^{-7} mol (m^2 s Pa)$^{-1}$
			H_2/N_2	3.74	
COF	COF-300-Zn$_2$(bdc)$_2$(dabco)[302]	~97	H_2/CO_2	12.6	1.3×10^5 Barrer
COF	COF-300-ZIF-8 [302]	~100	H_2/CO_2	13.5	1.1×10^5 Barrer
COF	H$_2$P-DHPh COF-UiO-66 [303]	120	H_2/CO_2	32.9	108,341 Barre
COF	ZIF-67-in-TpPa-1 [253]	0.9	H_2/CO_2	34.9	~3800 GPU
			H_2/CH_4	33.3	
COF	COF-LZU1–ACOF-1 [252]	0.5−1	H_2/CH_4	100	2.4×10^{-7} mol (m^2 s Pa)$^{-1}$
COF	TpTG$_{Cl}$@TpPa-SO$_3$H/COF-LZU1 [304]	0.155	H_2/CO_2	26	2163 GPU
COF	TpEBr@TpPa-SO$_3$Na Icon [305]	0.41	H_2/CO_2	22.6	2566 GPU
COF	ACOF [280]	30−50	CO_2/CH_4	32	5.01×10^{-13} mol (m^2 s Pa)$^{-1}$
COF	ACOF-1 [306]	8	CO_2/CH_4	86.3	9.9×10^{-9} mol (m^2 s Pa)$^{-1}$
COF	TpPa-1@SBR TFC [307]	~2	C_3H_8/N_2	15	311 GPU
			C_3H_6/N_2	20	463 GPU
COF	Ag-IL@TpPa–SO$_3$H [308]	0.24	C_2H_4/C_2H_6	120	135 GPU
COF	20 wt%NUS-2@PBI [279]	50–100	H_2/CO_2	31.4	4.08 ± 0.01 Barrer
COF	TpBD(50)@PBI-BuI [301]	47–80	CO_2/CH_4	48.7	14.8 Barrer
PIM	PIM-6FDA-OH[309]		H_2S/CH_4	29.9	~35 Barre
PIM	AO-PIM-1 [310]	50−60	H_2S/CH_4	75	4000 Barrer
PIM	PIM-TMN-Trip [311]	161 ± 13	SO_2/N_2	29	28,300−29,900 Barrer
PIM	CANAL-Me-Me$_2$F [312]	50	H_2/N_2	134	2380 ± 90 Barrer
			H_2/CH_4	185	
			O_2/N_2	7.8	139 ± 6 Barrer
			CO_2/CH_4	46	590 ± 20 Barrer
PIM	SBF-PIM [210]	180	CO_2/N_2	12	10,400 Barrer
			CH_4/N_2	4.3	754 Barrer
			H_2/N_2	0.15	5240 Barrer
			O_2/N_2	1.0	1950 Barrer
PIM	PIM-EA-TB [211]	181	CO_2/N_2	12	7140 Barrer
			CH_4/N_2	4.3	699 Barrer
			H_2/N_2	<0.06	7760 Barrer
			O_2/N_2	1.1	2150 Barrer
PIM	PIM-SBI-TB [211]	157	CO_2/N_2	13	2900 Barrer
			CH_4/N_2	4.6	450 Barrer
			H_2/N_2	<0.20	2200 Barrer
			O_2/N_2	1.35	720 Barrer
PIM	PIM-1 [218]	53–70	CO_2/N_2	18.0 ± 0.5	7200 ± 600 Barrer
PIM	PIM-NH$_2$ [218]	51–82	H_2/N_2	10.8 ± 0.6	1450 ± 70 Barrer
PIM	PIM-tBOC [218]	67–75	H_2/N_2	36 ± 3	130 ± 10 Barrer
PIM	PIM-deBOC(thermal) [218]	54–82	CO_2/N_2	20 ± 3	2300 ± 500 Barrer
PIM	PIM-deBOC(acid) [218]	65–95	H_2/N_2	10 ± 1	1700 ± 300 Barrer
CMP	CMP film [313]	0.008	H_2/N_2	36	~4 Barrer
CMP	CMT [314]	1	H_2/CO_2	~6.3	28,280 Barrer
			H_2/N_2	~11.3	
			H_2/CH_4	~10.9	
			H_2/C_3H_6	~12.1	
			H_2/C_3H_8	~12.5	
PAF	iPAF-5 [241]	0.12	H_2/N_2	72.7	51,844 GPU
			CO_2/N_2	60.0	23,058 GPU
PAF	iPAF-8IL [315]		CO_2/CH_4	223	1002 Barrer
PAF	PAF-97 [255]	30	CO_2/CH_4	22.48	2.90×10^{-7} mol (m^2 s Pa)$^{-1}$
HCP	porous polymeric membranes [230]	97	CO_2/N_2	29.6 ± 0.4	222.2 ± 5.9 Barrer
HCP	PTMSP/*p*-DCX [316]		CO_2/N_2	12	44,000 Barrer
HCP	PI/HCPs-NH$_2$ MMMs [317]		CO_2/CH_4	22.44	5.16 Barrer
			O_2/N_2	4.01	17.91 Barrer
POC	CC3 [245]	0.05	H_2/N_2	30	1.53×10^{-6} mol (m^2 s Pa)$^{-1}$
POC	CC3 [318]	2.5	He/Xe	13	2114 GPU
			CH_4/Xe	12	1962 GPU
			CO_2/Xe	10.5	1705 GPU
			Kr/Xe	4.8	773 GPU
POC	CC3 MMM [319]	82	C_3H_6/C_3H_8	12.1	390 Barrer
POC	10 wt% CC1135/Matrimid [320]	~50	CO_2/N_2	27.1	29.5 Barrer
			CO_2/CH_4	29.3	
			N_2/SF_6	69.0	1.09 Barrer

surface of COF-LZU-1 as followed. The sequential formation of the COF-LZU1 layer and the ACOF-1 layer was confirmed by SEM with detectable morphological changes. The gas separation tests were conducted in H_2/CO_2, H_2/N_2, and H_2/CH_4 gas mixtures, and the corresponding separation factor for the bilayer membrane reached 24.2, 83.9, and 100.2, respectively.

Zhao et al. went a step further to fabricate the COF/COF/COF composite membrane with narrowed apertures at the COF-COF interfaces via a multi-interfacial engineering strategy (Fig. 17) [304]. The COF-LZU1 membrane bearing a larger pore size was synthesized via interfacial polymerization and then transformed to the support. Subsequently, various COF layers including TpPa-SO$_3$H and TpTG$_{Cl}$ were formed on the COF-LZU1 surface via the liquid-solid-liquid interface polymerization in sequence. The apertures at the COF-COF interfaces could also be further narrowed by overlaying more TpPa-SO$_3$H/TpTG$_{Cl}$ layers. The separation selectivity of this novel composite membrane was

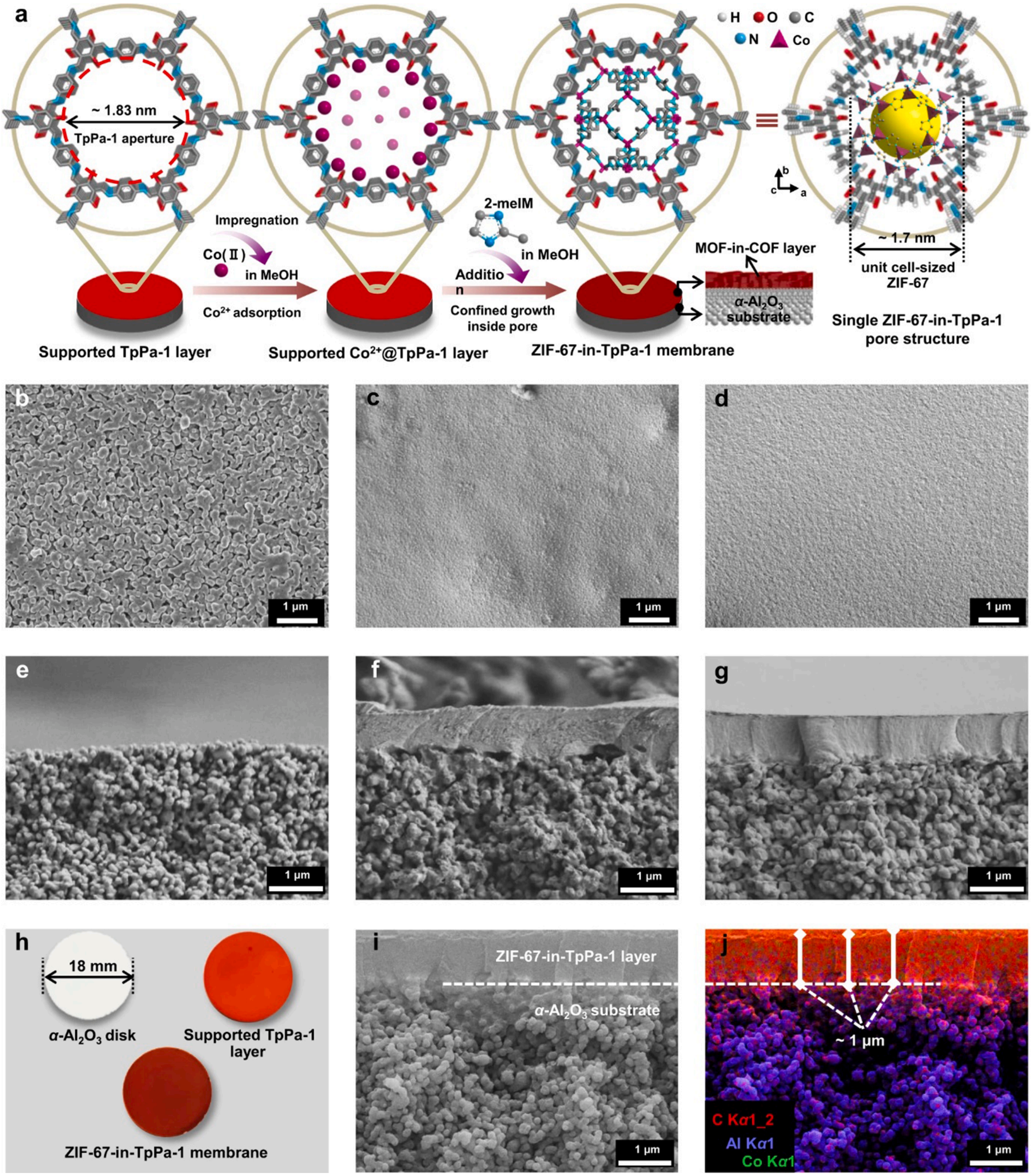

Fig. 16. (a) Scheme depicting ZIF-67-in-TpPa-1 membrane synthesis and schematic of single pore structure. Top-view (b–d) and cross-sectional (e–g, i) SEM images of porous α-Al_2O_3 substrate (b, e), supported TpPa-1 layer (c, f) and ZIF-67-in-TpPa-1 membrane (d, g, i). (h) Optical photograph of membranes. (j) EDXS mapping and elemental distributions corresponding to (i). Reproduced with permission [253]. Copyright 2021, Springer Nature.

measured for H_2 purification from H_2/CO_2 gas mixture, and the best separation factor of 26 was obtained from the optimal membrane. The charge of the membrane for H_2 separation was also studied by Zhao et al. [305]. They select two COFs with different ionic frameworks to fabricate the COF/COF composite membrane via the LBL assembly. The cationic CONs constructed by Tp and EB and anionic CONs built up from Tp and Pa-SO_3Na were synthesized aforehand via the air-water interface polymerization. The resulting CONs then were transformed on porous α-Al_2O_3 support by LBL assembly using the LS method, and the composite membrane with narrowed apertures was successfully generated.

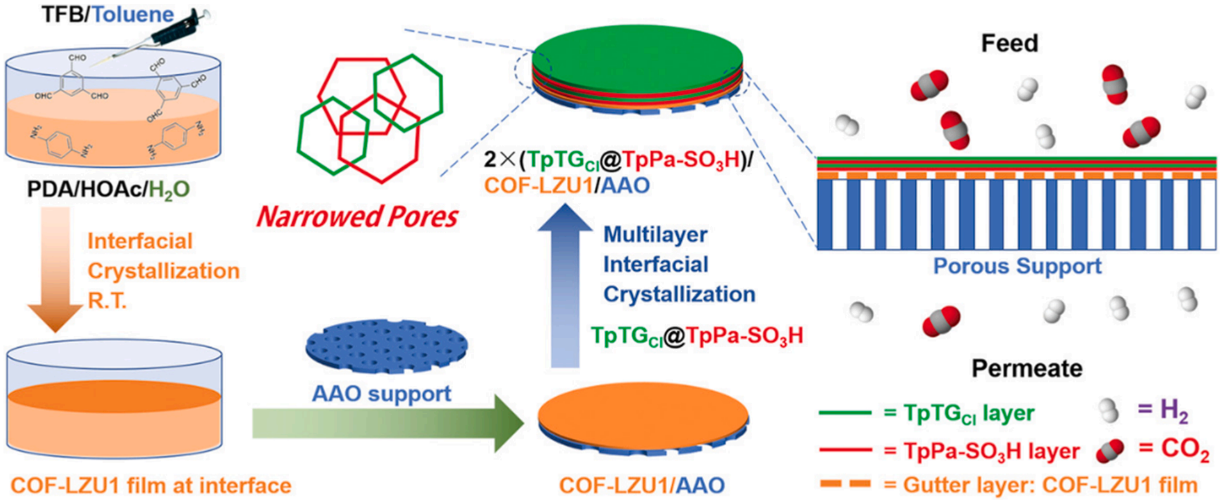

Fig. 17. Schematic illustration of the fabrication and gas separation application of the ultrathin COF membranes with narrowed apertures using a multi-interfacial engineering strategy. Reproduced with permission [304]. Copyright 2021, John Wiley and Sons.

The electrostatic interactions between layered iCONs were conducted by surface zeta potentials. The cationic TpEBr nanosheet membrane displayed a positive surface zeta potential of +36 mV at pH 8.0 while anionic TpPa-SO_3Na processed a negative value of −58.9 mV. After the assembling of two iCONs, however, the surface zeta potential of the hybrid membrane of two iCONs was almost neutralized at pH 8.0 with a value of −7.1 mV, suggesting the strong electrostatic interactions between these TpEBr and TpPa-SO_3Na nanosheets, which might contribute to the formation of the compact dense membrane structure. The H_2/CO_2 separation experiment of this iCONs-based membrane was conducted at 423 K, and a separation factor of 22.6 was reached.

A few COF-based membranes have been used for CO_2/CH_4 separation. Gascon and co-workers reported the application of azine-linked COFs MMMs in CO_2/CH_4 separation in 2016 [280]. The synthesized A-COF-1 particles were dispersed into THF first to obtain homogenous suspension following the addition of Matrimid®, and the MMM was fabricated by knife casting later. The resulting MMM containing 16 wt% of ACOF-1 had an increased CO_2 permeability (5.01×10^{-13} mol m^{-2} s^{-1} Pa^{-1}) with a mild increase of selectivity of 32 as compared to the pure Matrimid® membrane. Caro et al. also tried to separate CO_2 from CH_4 by ACOF-1-based membrane [306]. In their report, an optimal MMM was generated by directly growing ACOF-1 on the NH_2-modified surface of Al_2O_3 support with a thickness of 8 μm. This MMM exhibited a high selectivity of 86.3 in CO_2/CH_4 separation combined with favorable permeance of about 9.9×10^{-9} mol m^{-2} s^{-1} Pa^{-1} for CO_2.

The separation of various hydrocarbons is also a crucial industrial process but is full of challenges due to the similar physicochemical properties and close kinetic diameters between unsaturated hydrocarbons and the corresponding saturated hydrocarbons. Kharul and co-workers blended TpPa-1 with a styrene-butadiene rubber (SBR) polymer to fabricate COF MMMs with various ratios of TpPa-1 and SBR via the dip-coating method [307]. The resulting MMM with loading 50 wt% TpPa-1 demonstrated an appreciable reverse selectivity for C_3H_8/N_2 and C_3H_6/N_2, which was 15 and 20, respectively. More recently, Jiang et al. introduced ionic liquids containing Ag^+ into the COF membrane inventively to enhance the capacity of ethylene/ethane separation [308]. In this report, the prepared solution mixture from ionic liquid solution and silver nitrate aqueous solution was spun onto the synthesized TpPa-SO_3H membrane, the final membrane was vacuum-dried for the following test. The gas permeation experiments were conducted in the gas mixture feed using ethylene/ethane (50 : 50 %vol) and propylene/propane (50 : 50 %vol), respectively. During the gas separation, the confinement layer rooted in the introduction of silver ion-containing ionic liquid played a vital role in the reduction of the nanochannel size in the membrane, thus allowing high ethylene permeance by the primary confinement effect. The channel size via the modification of Ag^+-IL rationally could be sharply reduced to 0.87 nm, and an excellent separation performance was achieved with a high ethylene/ethane selectivity of 120 together with the ethylene permeance of 135 gas permeation unit (GPU).

PIM-based membranes are also employed in the gas separation, such as O_2/N_2, H_2/N_2, CO_2/N_2, and CO_2 /CH_4. Besides, functional PIMs can be synthesized with a wide range of conventional polymer monomers and fabricated to membranes by many methods, allowing the great potential in more industrial processes, such as toxic gas separation and gas emission purification. Koros et al. modified PIM-6FDA with hydroxy groups to afford PIM-6FDA-OH, and the corresponding membrane was cast from the PIM-6FDA-OH solution [309]. Gas permeation experiments were conducted in the gas mixture with 15/15/70% $H_2S/CO_2/CH_4$ as the feed, and a high separation factor up to 29.9 for H_2S/CH_4 was recorded during the measurement, which was higher than that of many commercial polyimide membranes. Koros and co-workers functionalized PIM-1 with the amidoxime groups by converting −CN to −AO in the building unit of PIM-1 (Fig. 18) [310]. The introduction of the basic group might be preferred by the "sour" gas such as H_2S. The permeation experiments were carried out in a ternary gas mixture with 20/20/60% $H_2S/CO_2/CH_4$ under a feed pressure of 77 bar. The results showed that AO-PIM-1 membrane had remarkable H_2S/CH_4 selectivity up to 75 together with an ultrahigh H_2S permeability which was higher than 4000 Barrers. SO_2 separation from other gasses was also studied, and Izak et al. selected PIM-TMN-Trip membrane to realize effective removal of SO_2 from the binary gas mixed with N_2 [311]. PIM-TMN-Trip membrane was prepared from the solution casting method with a compact and continuous surface. A high selectivity was obtained from the permeation test by using SO_2/N_2 as the gas feed, which was up to 29. Additionally, a low selectivity of around 1.8 was observed when the gas feed was changed to SO_2/CO_2. The gas separation performance of PIM-based membranes can also be enhanced via physical aging. Xia and Smith reported a library of microporous ladder polymers constructed by repeat norbornyl enzocyclobutene units [312]. Upon aging, the resulting PIM-based membrane, CANAL-Me-Me_2F, exhibited better gas separation performance due to the more ordered and compact pore structure as compared to the fresh PIM-based membranes with excess free volume. Such transformation is commonly observed for PIMs after the certain contortion of polymer chains in PIMs as time passed. The separation selectivity for several industrially relevant gas pairs including H_2/CH_4, CO_2/CH_4, H_2/N_2, H_2/CO_2, and O_2/N_2 was improved greatly in comparison with fresh PIM-based membranes.

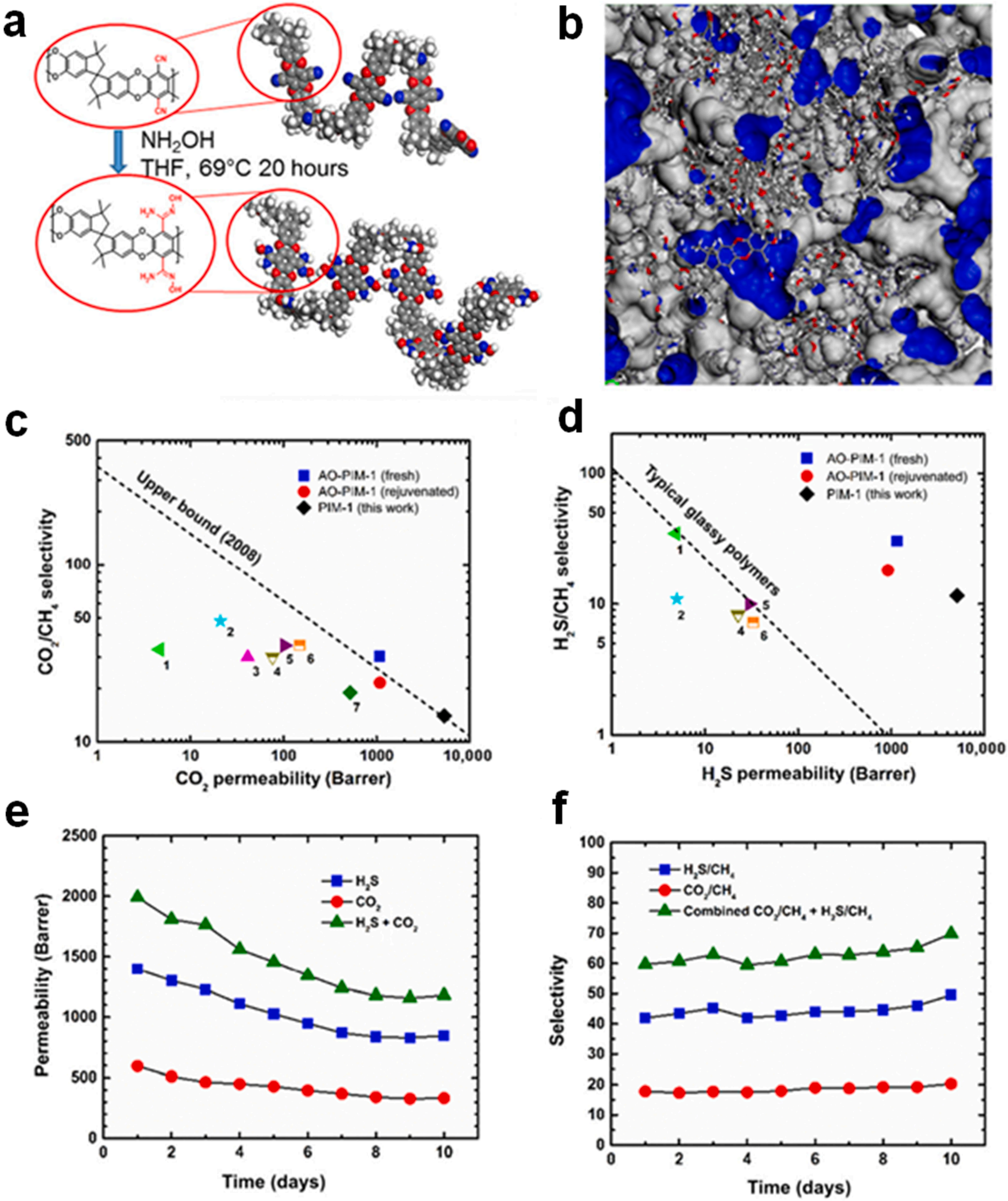

Fig. 18. (a) Structures of PIM-1 and amidoxime-functionalized PIM-1 (AO-PIM-1). (b) Void morphology in AO-PIM-1. (c) Pure-gas permeability/selectivity (CO_2/CH_4) trade-off curve comparison of PIM-1 and AO-PIM-1 to other polymeric materials. (d) Pure-gas permeability/selectivity (H_2S/CH_4) trade-off curve comparison of PIM-1 and AO-PIM-1 to other polymeric materials. (e) CO_2/CH_4 performance of AO-PIM-1 for long-term continuous active feed of 20 mol% H_2S/20 mol% CO_2 and 60 mol% CH_4 at feed pressure of 8.6 bar at 35 °C. (f) H_2S/CH_4 performance of AO-PIM-1 for long-term continuous active feed of 20 mol% H_2S/20 mol% CO_2 and 60 mol % CH_4 at feed pressure of 8.6 bar at 35 °C. Reproduced with permission [310]. Copyright 2019, American Association for the Advancement of Science.

3.2. Liquid separation

The vast majority of POPs reported so far have higher chemical and water stability than that of MOFs which always tend to decompose when being treated in aqueous for a long time. Thus, POP-based membranes are regarded as the rising candidates for liquid separation. The feasibility of functionalizing POPs further allows the employ of POP-based membranes in task-specific applications in liquid. In the following section, recent progress for some relevant applications, such as water treatment, nanofiltration, and electrodialysis, will be summarized and discussed.

Water pollution is a serious problem along with the rapid development of the society and sharp increase of the population. Apart from keeping water resources away from pollution emissions, cleaning reclaimed water for daily use is another sustainable approach to solve the problem of global water shortages. Comparing with conventional water treatment technologies including distillation and evaporation, membrane separation is more effective and cost-saving due to its low energy consumption and durability. The trade-off effect during separation, however, is still existing in the traditional polymeric membrane when being applied in the water treatment because of the irregular apertures. Advanced POPs usually processing much ordered pore structure and pore size are regarded as the perfect candidate at present to avoid the effect caused by the trade-off between permeation and selectivity. Especially COF-based membranes, which have the most uniform pore structures and most diverse functions, are widely used for molecular sieving.

Banerjee and co-workers firstly reported a series of Tp-based COF membranes via the solid-state casting method with PTSA as the catalyst [250,251]. The free-standing membranes had high water and organic solvent permeability and were used for dye removal from the aqueous solution. It demonstrated that the complete rejection of dyes could be easily achieved in these COF-based membranes. Since then, a great number of COF-based membranes have been applied for the removal of various dyes. A facile molecularly soldered strategy was proposed by Shao et al. to fabricate the defect-free ultrathin COF membranes with strong interlamellar interaction *in situ* (Fig. 19) [321]. Dopamine (DA) was added into the solution with excess Pa to obtain a homogenous solution, following the mixing with the pre-prepared Tp solution. The polyimide substrate was placed into the mixed solution before the initiation of polymerization. In the process of membrane production, a novel free radical reaction happened to start the oxidation polymerization of DA, and the reactive oxygen species (ROS) that occurred during the formation of pDA polymer would promote the synthesis of TpPa. Meanwhile, the hydroxy groups in pDA would react with one of the amines groups of PA to connect TpPa units, thus molecularly soldering pDA polymer to TpPa COF and forming the continuous pDA/TpPa (W/E)-COF membrane with narrowed apertures. The resulting membrane exhibited outstanding separation performance for organic solvent nanofiltration with permeances that were higher than 86 L m^{-2} h^{-1}

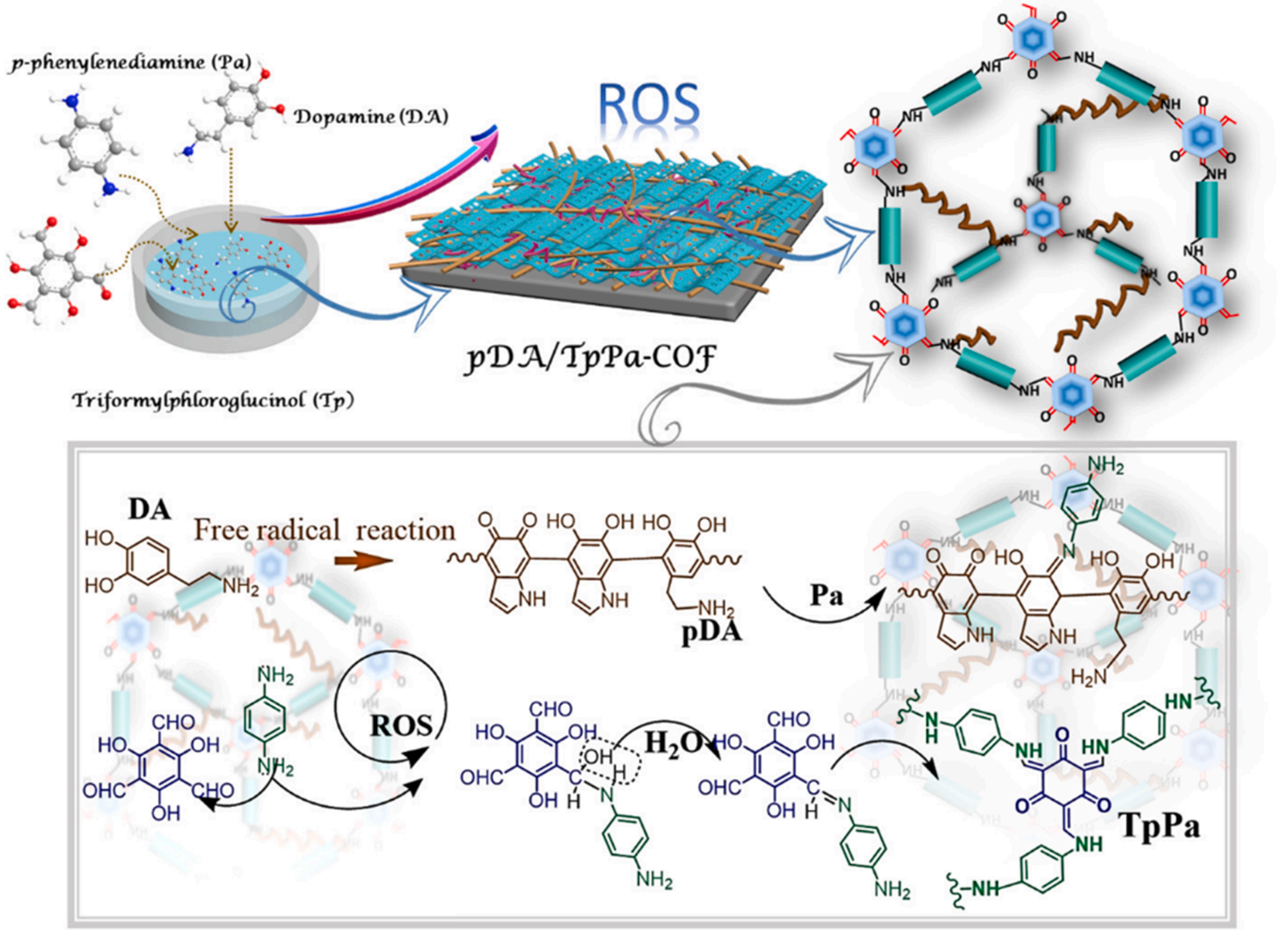

Fig. 19. Schematic illustration of *in situ* molecular soldering engineering to fabricate COF membranes. Reproduced with permission [321]. Copyright 2021, American Association for the Advancement of Science.

bar^{-1} combined with more than 95% rejections for various dyes. Additionally, pDA/TpPa(W/E)-COF membrane also demonstrated high rejection for ions, that is, 99.5% Na_2SO_4 retention could be obtained, surpassing most of the state-of-the-art membranes. Jiang and co-workers recently developed a COF membrane that had high rejection of salts via the adhesion of TpPa-SO_3H nanosheets and TpTTPA nanoribbons [322]. In the resulting membrane, TpTTPA nanoribbons were served as the "adhesive tape" to hold TpPa-SO_3H nanosheets together via electrostatic and π–π interactions. They mixed TpPa-SO_3H colloidal solution with TpTTPA colloidal solution with sonication first, and the COF dispersion would be deposited on the polytetrafluoroethylene (PTFE) substrate under vacuum-assisted self-assembly to form a defect-free and ordered COF membrane. In comparison, TpPa-SO_3H membrane prepared without the addition of TpTTPA was defective and fragmentary, which would degrade the membrane performance for rejecting ions. The optimal COF membrane was used for the seawater desalination, and an ultrafast water flux of 267 kg m^{-2} h^{-1} combined with excellent rejection of NaCl (99.91%) was recorded, suggesting the scalability of using such COF composite membranes for water purification.

COF-LZU1 is a popular selection for the fabrication of high-performance COF-based membranes. Caro and Meng prepared an ultrathin COF-LZU1 membrane on alumina tubes by *in situ* solvothermal syntheses [323]. The compact COF-LZU1 membrane demonstrated excellent stability with more than 90% rejection for most of the dyes. Bruggen and Jia proposed a COF-LZU1/PAN composite membrane by stoichiometric spraying layer-by-layer self-assembly [324]. The staggered pores in the thin COF-LZU1 membrane could reject more than 90% of dyes with a high permeance of 400 L m^{-2} h^{-1} MPa^{-1}. Additionally, GO/COF composite membranes are also favored for dye or salt separation. Zhang and Wang cooperated and successfully intercalated COF-1 nanosheets on the interlayers of graphene nanosheets to form GO/COF-1 thin films which were coated on the porous polymeric substrate via a dead-end filtration device [298]. The intercalation of COF-1 between GO layers produced an extra passageway for water penetration, thus improving the water permeability as compared to the pristine GO membrane which has narrowed interlayer space. In the separation experiments, the GO/COF-1 composite membrane showed a high rejection for water-soluble dyes up to 99% together with a rapid water permeability over 310 L m^{-2} h^{-1} MPa^{-1}. Sun et al. also selected GO to blend with COFs to obtain a composite membrane assembled by GO and COF nanosheets layer by layer via hot pressing. Being different from intercalating COF nanosheets into the GO layers, Sun and co-workers mixed GO and COF-TpPa first, then fabricated the membrane through vacuum filtration onto a polymeric support after well sonication and dispersion [325]. The heating process was conducted to mitigate the interface voids between GO and COF-TpPa to produce a compact membrane. The thin composite film supported on nylon substrate had a high dye rejection rate for various dyes, for example, 97.05% methylene blue dissolved in water could be rejected after water permeability. Additionally, a water permeance of 166.8 L m^{-2} h^{-1} bar^{-1} was recorded in the test. The self-standing and flexible COF membrane was generated for dye removal as well. Chung et al. fabricated the transparent ultrathin COF films via the interfacial reaction between tris(4-aminophenyl)amine (TAPA) and Tp or TFB [326]. The thicknesses of resulting COF membranes could be adjusted precisely from as low as 5 nm to as high as 300 nm in accordance with the interfacial reaction time from 1 min to 24 hours. Before applying these membranes in permeation experiments, the thin film would be transformed onto the anodized aluminum oxide (AAO) substrate. The high-polar channel environment of TAPA-TFP allowed effective superhighways for polar molecules, thus polar solvents such as methanol, could penetrate the membrane with a high permeance of 241.9 L m^{-2} hour^{-1} bar^{-1}, which was nearly four times higher than the reported polyamide-based nanofiltration membrane. However, when the membrane was used for water permeance, various dyes could be completely rejected by TAPA-TFP thin film except for rose Bengal, which has a smaller kinetic diameter (11.2 to 12.4 Å) than the pore size of TAPA-TFP (11.7 to 12.5 Å).

The POP-based membrane can also be used as an adsorbent during the water treatment rather than rejecting barrier. Dichtel et al. proposed the thick and polycrystalline COF membranes as an adsorption layer to reserve dye molecules during the water penetration, rather than rejecting dye molecules outside the channels via size-sieving [327]. The thick TAPB-PDA COF membrane showed high rejection for most dyes when the flow rate of the aqueous solution is low, over 99% of dyes would be adsorbed by the pellet-like TAPB-PDA COF membrane. While the rejection would keep decreasing when the flow rate is increased, which was in accord with the adsorption mechanism. PIM-based membranes can also be used as an extraction media for metal ions adsorption. Wen et al. proposed the fabrication of a bioinspired hierarchical porous membrane from PIM-1 through non-solvent-induced phase separation (NIPS), generating interconnected multiscale channels with three different scales in the synthesized membrane by taking advantage of the unordered packing of the polymer chains in PIMs (Fig. 20) [328]. Then PIM-1 can be converted to AO-PIM-1 with the uranium-specific binding sites. During the sorption of uranium in AO-PIM-1 membrane, two-step adsorption of uranyl occurred, allowing more efficient and sufficient sorption for uranium from the seawater. In natural seawater, AO-PIM-1 membrane can extract measurable uranium with a capacity of 9.03 mg g^{-1} after four weeks. Significantly, an uptake capacity of 6.63 mg g^{-1} could be obtained after only one week, suggesting the high efficiency of AO-PIM-1 membrane in seawater uranium extraction. The PAF-based membrane can also be functionalized as an adsorptive membrane to capture ions from an aqueous solution. Long et al. reported a family of PAF-1-based MMMs with diverse functional groups and their applications in various ions adsorption [329]. PAF-1 was first converted to PAF-1-CH_2Cl via chloromethylation, then diverse moieties including −SH, −SMe, −ET, and −NMDG, were functionalized to PAF-1-CH_2Cl to form corresponding functional PAF-1. The functional PAF-1-based MMMs were fabricated by blending with sulfonated polysulfone (sPSF) via a solvent evaporation approach. Then the resulting MMM would be clamped between two half-cells to serve as an adsorptive barrier. While the voltage was applied on two sides of the membrane, target ions could be attracted by the electric field and swim to the elaborate membrane. During the electrodialysis, the target ions would be selectively captured. In this electricity-assistant way which they called IC-DC, a variety of ions, such as Hg^{2+}, Cu^{2+}, Fe^{3+}, and $B(OH)_3$, were selectively extracted from the water feed containing various competing ions.

COFs bearing uniform pore size and tunable pore environment are preferential for nanofluidic membranes fabrication. The resulting membranes usually demonstrate good ion permselectivity, which allows them to be assembled in nanofluidic devices and make more aggressive moves at the cutting-edge research, such as valuable metal ion separation and osmotic energy production. Sun and our groups reported a series of charged Tp-COF membranes with various ratios of EB and BD as amine monomers (Fig. 21) [266]. The thin COF film was grown on the surface of PAN via the interfacial synthesis method to prepare nanofiltration membranes. The highest Li^+/Mg^{2+} selectivity via electrodialysis of 385 was achieved by COF-EB_1BD_1/PAN from the simulated Yiliping brine with Mg^{2+} and Li^+ concentrations of 0.83 and 0.031 mol L^{-1}, respectively. By contrast, a selectivity of only 0.0377 could be observed without applying the current. Sun et al. also proposed another effective method to narrow down the pore aperture size via the introduction of lithiophilic chains with different lengths into the pore space [268]. With the longer chain existing in the pore, the flux for Li^+ and Mg^{2+} were both decreased due to the size-exclusion effect, however, the selectivity for Li^+ and Mg^{2+} would be increased sharply from 6 for COF-OMe/PAN and 3 for COF-OHep/PAN to 64 because of the stronger binding between lithiophilic oligoether moiety and Li^+ existing in COF-4EO/PAN.

More recently, Lai et al. reported the construction of the pH-gating nanofluidic transport based on the well-designed COF [330]. The

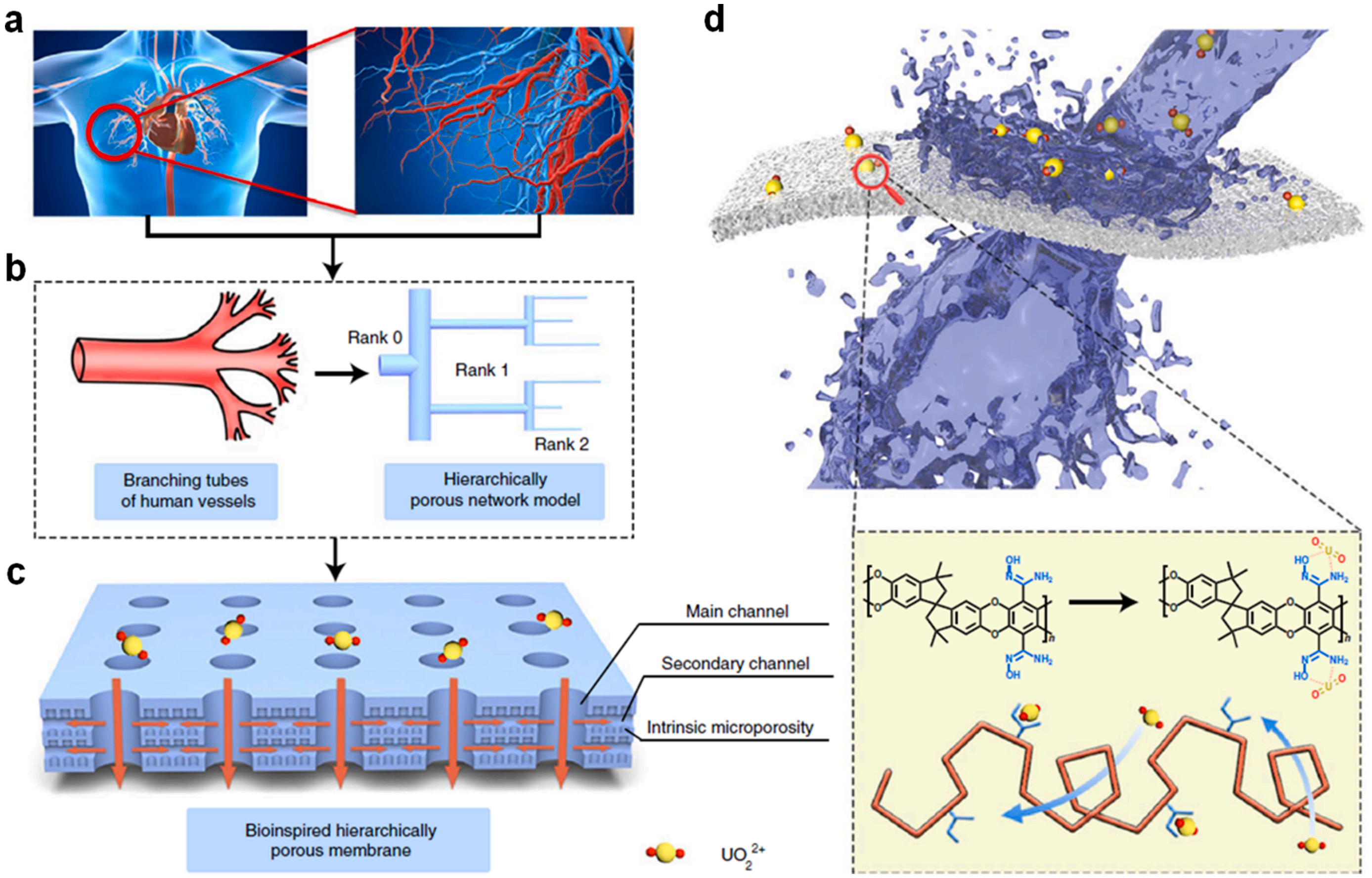

Fig. 20. Biological inspiration and schematic of the bioinspired hierarchical porous membrane. (a) Hierarchical networks of blood vessels in living organisms. (b) Branched tube-based model inspired by the mammalian circulatory system. Increasing the number of branch points while reducing the branch diameter allows for efficient substance transfer at low energy consumption. (c) Schematic illustration of the bioinspired hierarchical porous membrane. It contains pores with sizes on three different scales, including intrinsic micropores. (d) Working principle of the hierarchical porous membrane for uranium adsorption. Amidoxime functionalization provides specific binding sites. Reproduced with permission [328]. Copyright 2022, Springer Nature.

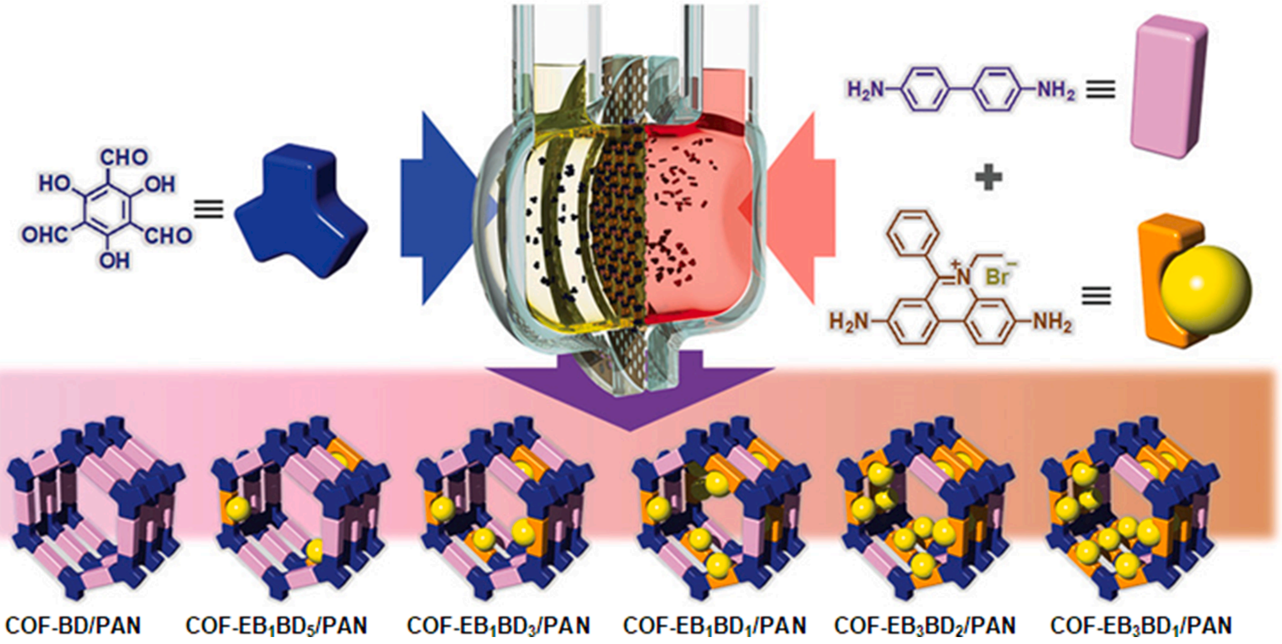

Fig. 21. Synthetic scheme illustration of COF-based membranes with varied charge densities via interface polymerization. Reproduced with permission [266]. Copyright 2021, John Wiley and Sons.

precursor solution comprising (2,5-dihydroxy-1,4-benzenedicarboxaldehyde (DHTA) and TAPB was prepared first, followed by the growth of COF-DT membrane on a SiO_2/Si wafer via slow nucleation and oriented growth. Subsequently, the free-standing thin film would be transferred to a track-etched polyethylene terephthalate support to prepare for the electrical measurements. The drift-diffusion I-V curves of COF-DT membranes were conducted in the homemade electrochemical cell with the mounting of the COF-DT membrane in the middle of two separated cell chambers. The representative I-V curves were measured by introducing a KCl concentration gradient of 10 on two sides of the membrane. Then, the diffusion potential (E_{diff}) generated by the selective transport of ions through the COF-DT membrane could be recorded by the electrochemical station. The ultrahigh transmembrane ion flux was found from the drift-diffusion I-V curves, more significantly, the COF-DT nanofluidic membrane was ion-selective under different pH ranges, which allowed anion penetrating in the low pH range while cation was preferred in the high pH range. Jiang et al. prepared the COF membranes with ultrafast anion transport via the introduction of various quaternary ammonium (QA) groups that had different organic spacers (Fig. 22) [331]. A series of hydrazide building units containing QA groups with different chain lengths were reacted with TFB to form colloidal COFs via phase-transfer polymerization. The self-standing COF-QAs membranes bearing densely packed structures were produced in the COF colloidal suspension, and the transparent COF membranes could be assembled during solvent evaporation. The resulting membranes were named as COF-QA-2, COF-QA-4, COF-QA-6, and COF-QA-EO according to the organic spacers (ethyl, butyl, hexyl, and diethyl ether spacers) attached to the hydrazide monomers. They found that COF-QA-2 membranes with shorter and more hydrophilic moiety are favorable for improving the anion conductivity among four COF-QA-based membranes.

The diffusion potential generated by the ion-selective permeation through nanofluidic membranes can be used for harvesting salinity gradient (blue) energy, which is a popular topic of osmotic energy production. Sun and co-worker presented a strategy to confine cationic and anionic dyes in the same 3D COF skeletons, respectively, to prepare a pair of the cation- and anion-selective membranes (Fig. 23) [180]. COF-300 was selected in the report to immobilize ionic dyes. The $HB_{67.7}$@COF/PAN charged by an anionic dye (hydroxynaphthol blue) and $JG_{80.1}$@COF/PAN encapsulated by Janus green B (cationic dye) were used as the pair for the salinity gradient energy generation. The membranes were mounted in a three-compartment conductive cell to investigate their osmotic energy conversion efficiency. The salinity gradient was established by a standard simulated seawater (0.5 M NaCl) and river water (0.01 M NaCl) solution, and a power density of up to 51.4 W m^{-2} was recorded in the measurement. The previous study by Sun et al. has proven that the charge density of the nanofluidic membranes would affect the ion permselectivity, thus causing a difference in salinity gradient energy production [266]. Accordingly, Sun and our group contributed a strategy for the manipulation of charge population in the COF membranes to obtain the highest harvesting of osmotic energy [270]. 2,2′-((2,5-di(hydrazinecarbonyl)-1,4-phenylene) bis(oxy)) bis(N,N,N-trimethylethan-1-aminium) iodide (BTA) and 2,5-bis(2-(dimethylamino)ethoxy)terephthalohydrazide (BTH) were used to adjust the charge property in the resulting membranes via the multivariate strategy to fabricate a family of COF membranes, and the content of ionic sites can be precisely tuned from 0 to 0.18 C m^{-2} in terms of this method. An optimal power density of up to 54.0 W m^{-2} was obtained in COF-BTA_3BTH_2/PAN when being tested at a 50-fold salinity gradient. More recently, Tang and Li proposed a novel strategy to homogeneously distribute atomic charges across the COF-based membranes via the bottom-up method to enhance the output power density [332]. The

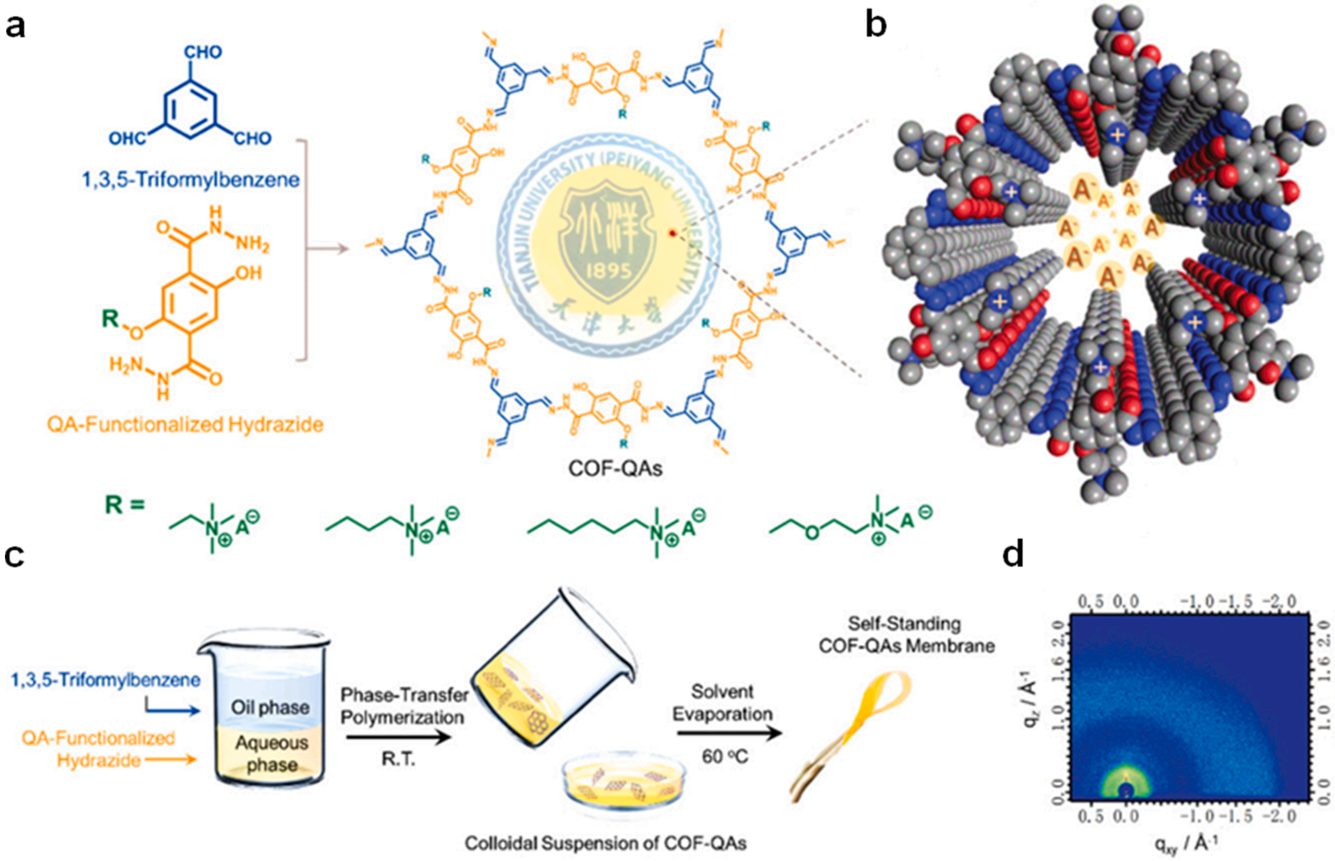

Fig. 22. (a) Schematic illustration of the *de novo* synthesis of COF-QAs. (b) Schematic of anion transport through the 1D channel of COF-QAs. (c) Schematic of COF-QAs membrane fabrication process. (d) GIWAXS data of the COF-QA-2 membrane. Reproduced with permission [331]. Copyright 2020, John Wiley and Sons.

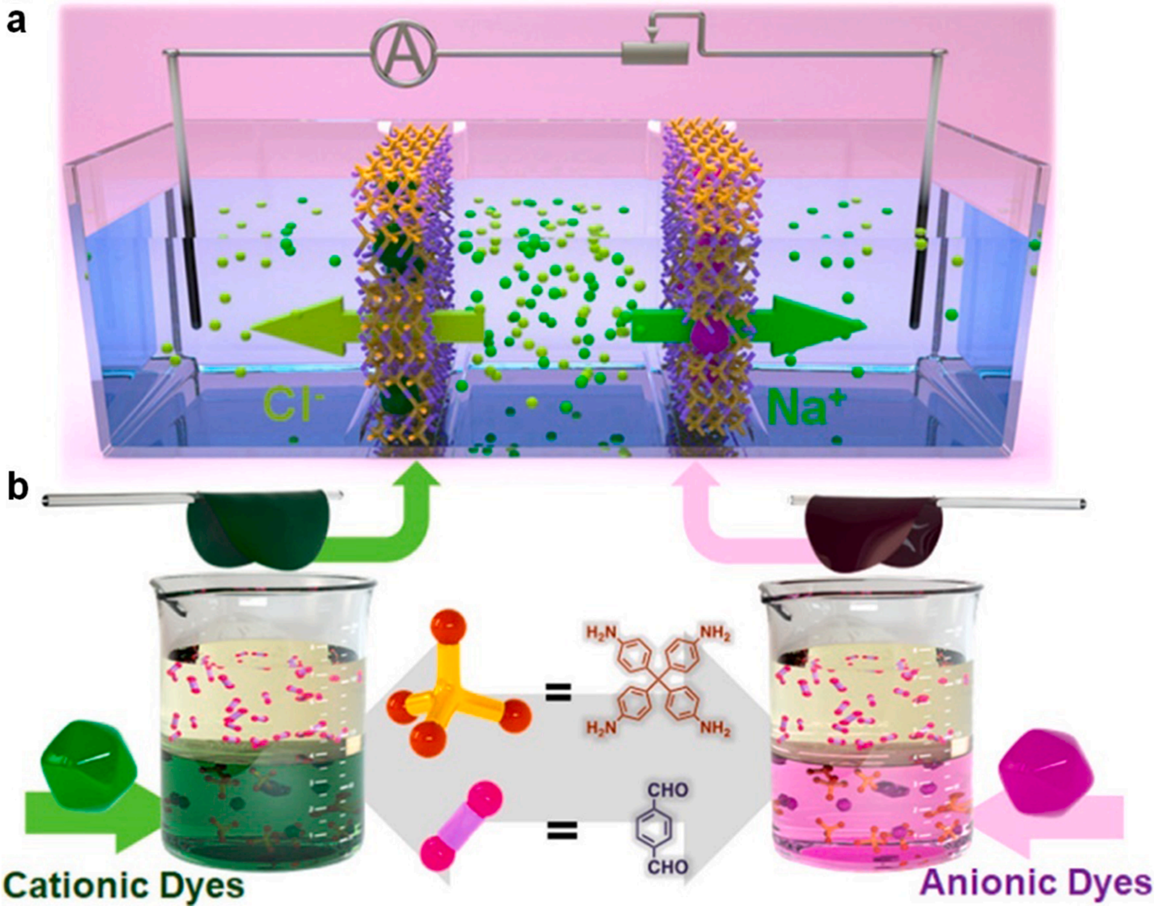

Fig. 23. (a) Diagrammatic sketch of a pair of the cation- and anion-selective membranes mounted in a three-compartment conductive cell to harvest osmotic energy. (b) Bottom-up assembly of ionic dye modified COF-based nanofluidic membranes. Reproduced with permission [180]. Copyright 2021, American Chemical Society.

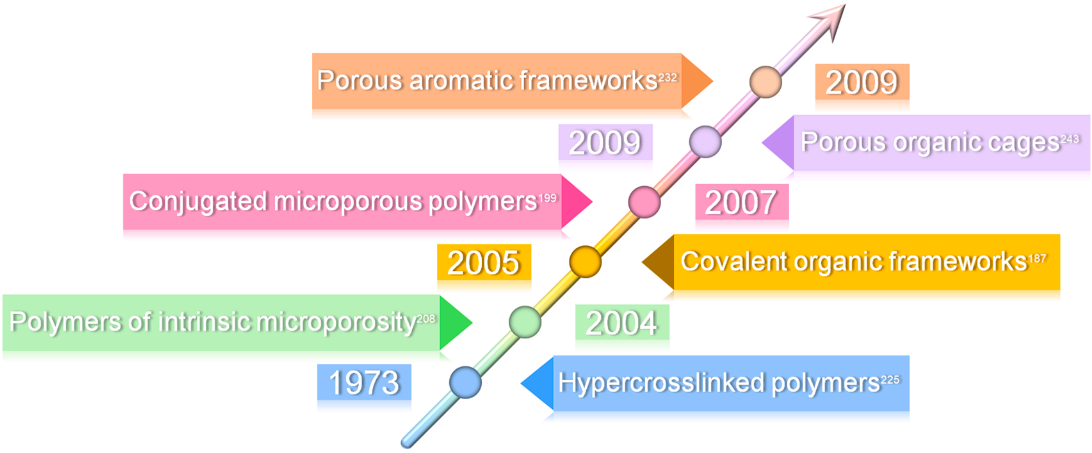

Scheme 1. Timeline of the development of advanced porous organic polymers.

recorded power density herein is higher than any reported value of porous monolayer membrane, which was over 200 W m^{-2} at the salinity gradient between artificial seawater and river water. To immobilize the positive metal ions with a homogenous distribution, amine-ended zinc tetraphenylporphyrin (ZnTPP) monomers was screened as the building blocks to anchor Zn^{2+} in the resulting ZnTPP-COF membrane. Furthermore, the positive charge intensity in COF-based membrane could also be manipulated by coordinating various metal centers, such as Cu^{2+} and Ni^{2+}. The decreased selectivity of NiTPP-COF (2.9 mC m^{-2}) and CuTPP-COF (1.7 mC m^{-2}) as compared to ZnTPP-COF (4.1 mC m^{-2}) was observed due to their relatively low surface charge density.

The diffusion potential variation can be observed along with the disturbance of temperature [269], thus, the osmotic power density can also be influenced by the temperature difference. Sun and co-workers developed a series of iCOF-based membranes with varied charge density and then applied these membranes in the thermo-osmotic energy conversion to study the feasibility of the direct conversion of the low-grade heat (<100 °C) and the Gibbs free energy from salinity

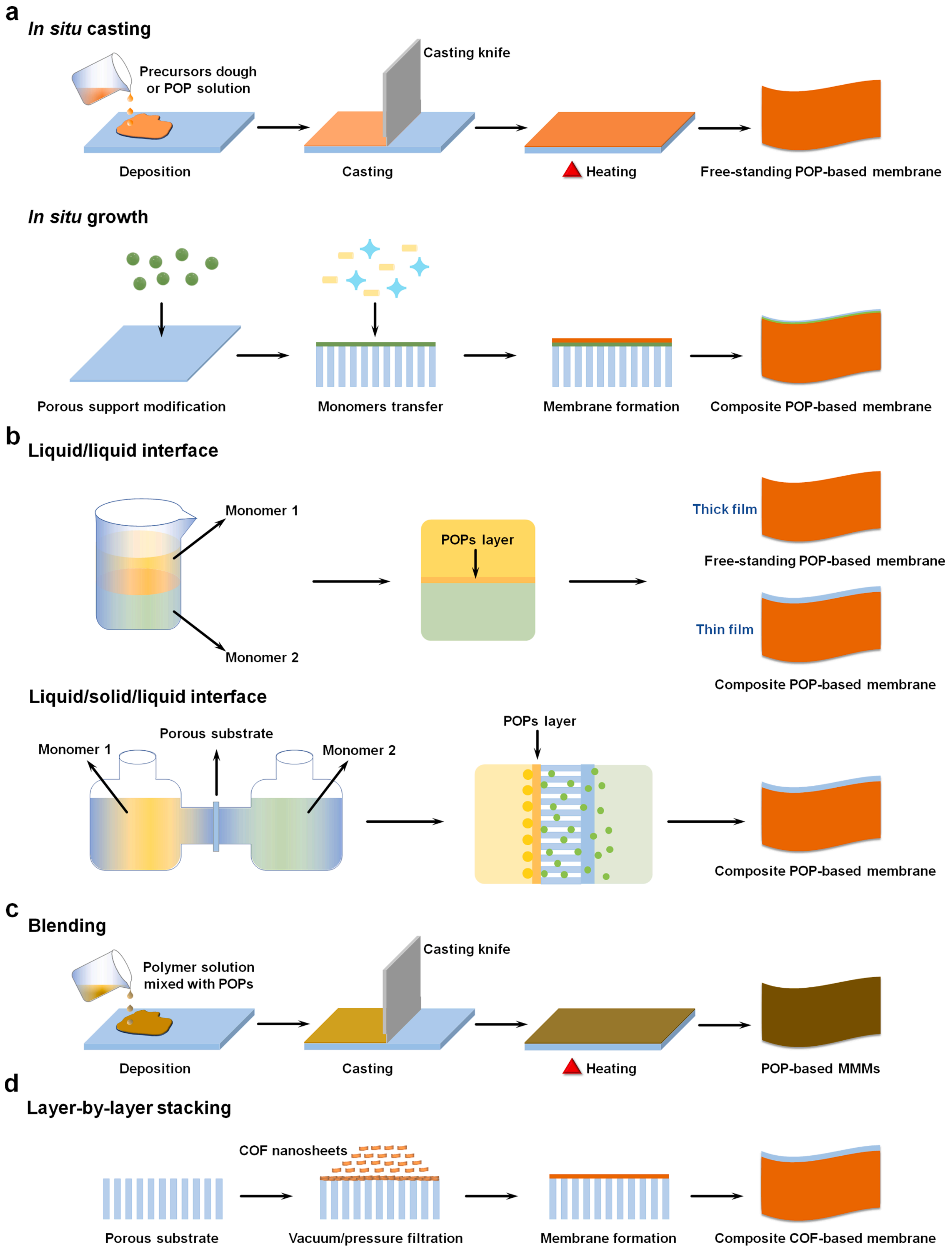

Scheme 2. Schematic illustration of four well-known strategies for POP-based membrane fabrication.

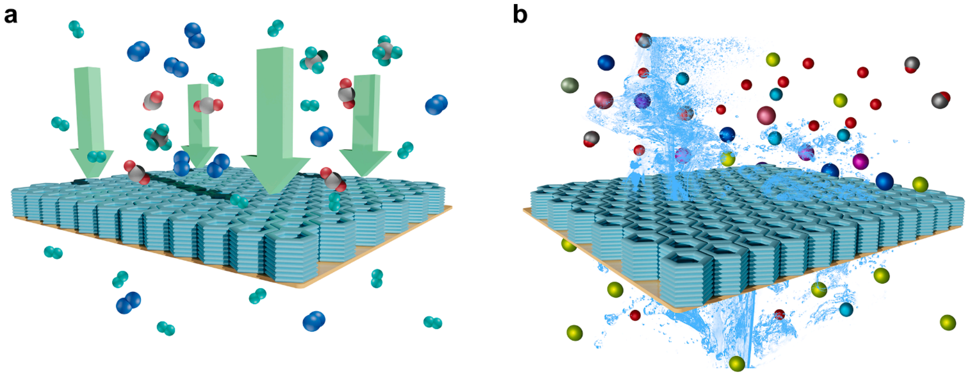

Scheme 3. Schematic diagrams of gas separation (a) and liquid separation (b) using POP-based membranes.

gradients into electricity [271]. COF-$(SO_3Na)_x$/PAN was directly grown on the PAN support by the interfacial polymerization of Tp and the mixed amine monomers of sodium 2,5-diaminobenzenesulfonate and benzene-1,4-diamine with various ration. The results demonstrated that the highest power density of about 231 W m^{-2} could be achieved while the measurement was conducted under simulated estuary conditions which processed a temperature difference of 60 K. Additionally, Sun and our group also found that the evolution between open-circuit voltage (V_{oc}) and the temperature change in solutions could be fitted with the linear model with correlation coefficients over 0.99 [267]. A high thermosensation sensitivity of 1.27 mV K^{-1} was observed due to the superior permselectivity in the resulting nanofluidic membranes, which surpassed any known natural system.

4. Conclusion and outlook

The prosperity and the welfare of people cannot be divorced from the progress of technology and industrial process. Advanced membrane technology for industrial separations is playing a significant role in the whole production supply chain. The development of commercial membranes with high performance is flourishing over the past few years, and tremendous porous membranes fabricated from advanced POPs have been designed and utilized in real-world separation applications. A large amount of artificial porous powders has been used in the gas separation, especially MOFs, which have diverse pore structures and smaller pore sizes than other porous materials and been well studied for challenged gas separation on the bench-scale, showing unparalleled performance for the selective capture of gasses. However, the long-time regeneration of column fillers, costly synthesis, and poor durability impeded their large-scale applications in the real world [107–110]. Unlike the applications of porous polymer solids used for separation technology, the future of using porous membranes for molecular sieving in industry is more promising and realistic. Whereas the fabrication of POP-based membranes is much more technically challenging. A qualified membrane should own two basic properties, such as defect-free and continuous surface, and then, more considerations are required to meet the specific demand before the fabrication of the membrane. Herein, a compressive overview of the recent development of POP-based membranes has been given, from the key properties of advanced porous membranes to the fabrication methods.

Challenges remain for the employ of POP-based membranes in practical applications. In comparison with conventional polymeric membranes with pores, the novel POP-based membranes are more fragile and expensive. Therefore, the modification of traditional polymeric membranes to enhance their performance is also favorable. Recently, Sandru and Spontak proposed a hybrid-integrated membrane strategy to graft the membrane surface with CO_2-philic chains [333]. The commercialized polymer for CO_2 separation, polydimethylsiloxane (PDMS), was selected to coated with a layer of benzophenone followed by the polymerization of glycidyl methacrylate (GMA), the modified membrane surface was further reacted with ethylene diamine (EDA) in aqueous solution to introduce CO_2-philic groups. All the materials used are commercially available and cheap. Besides, another commercialized polymer, polytetrafluoroethylene (PTFE AF), was also used for the modification of CO_2-philic chains on the surface. The CO_2 separation tests were conducted in a mixed 10/90 CO_2/N_2 gas feed (at 100% relative humidity) to create the most common conditions for CO_2 separation. Both modified membranes exhibited enhanced CO_2 selectivity by more than ~150-fold as compared to that of the pristine membranes, and much of their high CO_2 permeability could be retained after the modification. Commercial polyamide membranes were also modified for improved water purification. Zhang et al. reported a strategy to construct nanoscale Turing structures on the surface of the membrane interfacial polymerization to enhance the water-salt separation performance [334]. The resulting membrane with unique Turing structures on the surface was evaluated in saltwater desalination, demonstrating an excellent water permeability of 125 L m^{-2} h^{-1} with high rejection of various salts, which was superior to the upper-bound line of traditional desalination membranes. Therefore, to advance POP-based membranes as industrial-scale products and surpass conventional polyimide membranes in performance, the following concerns must be addressed: (1) reducing the cost of synthesizing POP-based membranes; (2) developing a scalable method for the preparation of larger-area POP-based membranes; (3) improving the durability and prolonging the life cycle of POP-based membranes.

The rapid development of crystalline POPs like COFs has pushed forward the study of high-performance membrane design and their cutting-edge applications since the generated membranes formed by COFs usually have ordered nanochannels, controllable pore structures, sizes, and tailorable chemical or physical membrane surface. With a huge stock of monomers to choose from to synthesize COFs, the pore aperture and functional pore environment can be precisely customized according to the specific requirements of the membrane-based applications, by either predesigning organic precursors or introducing required functionality via post-synthetic modifications. Beyond that, the huge effort made by researchers for the evolution of COF synthesis also facilitate the manufacturing improvement of monomers, allowing the fabrication of advanced COF-based membranes with more convenient synthesis and lower cost. In addition, the fabrication of COF-based membrane to obtain better morphology and performance is also at the center of such a research area, which is discussed in detail in this review with our perspective. The modification of membrane preparation is also crucial for its practical application. As we known, COF-based freestanding membranes are usually fragile, and it turns out that growing such membranes on the liquid-solid-liquid interface would be a more promising method to produce more robust and larger membranes than the membrane grown between the interface of two liquids without support. This strategy could also be applied to other POP-based membrane fabrication to realize the goal of producing large-scale and tough membranes. Apart from the discussion of COF-based membranes, some other POP-based membranes are introduced with our own evaluations, as well. For example, PIM is a type of atypical POPs with intrinsic microporosity and rigid polymer structure but can be dissolved in an organic solvent to form a homogenous polymer solution. After the evaporation of the solvent, the porosity of PIMs will be reproduced. It is worth mentioning that the porous structure of PIMs could be controlled by the non-solvent-induced phase separation (NIPS). Wen et al. took advantage of this feature of PIMs to fabricate an AO-PIM-1 membrane with multiscale nanochannels, thus greatly increasing the flow path in the membrane and enhancing the adsorption capacity [317]. PAFs which are synthesized by the direct connection of aromatic groups usually have the highest stability among POPs, therefore, PAF-based membranes are competent for the tough tasks in complex working conditions [321]. Looking forward, the potential and opportunity of those novel POP-based membranes are enormous, and we strongly believe that the day of large-scale application of such materials is approaching.

CRediT authorship contribution statement

Yanpei Song: Writing – original draft, Writing – review & editing. **Changjia Zhu:** Writing – original draft. **Shengqian Ma:** Conceptualization, Supervision, Writing – review & editing.

Declaration of Competing Interest

The authors declare no conflict of interest.

Acknowledgement

The authors acknowledge the Robert A. Welch Foundation (B-0027) for financial support of this work.

References

[1] D.S. Sholl, R.P. Lively, Seven chemical separations to change the world, Nature 532 (2016) 435–437.
[2] E.K. Bekedam, H.A. Schols, M.A.J.S. van Boekel, G. Smit, High molecular weight melanoidins from coffee brew, J. Agric. Food Chem. 54 (2006) 7658–7666.
[3] J. Ruan, Z. Xu, Constructing environment-friendly return road of metals from e-waste: combination of physical separation technologies, Renew. Sust. Energ. Rev. 54 (2016) 745–760.
[4] T.J. Oli-Estes, M.R. Palermo, Recovery of dreged material for beneficial use: the future role of physical separation processes, J. Hazard. Mater. 85 (2001) 39–51.
[5] G. Dermont, M. Bergeron, G. Mercier, M. Richer-Lafleche, Soil washing for metal removal: a review of physical/chemical technologies and field applications, J. Hazard. Mater. 152 (2008) 1–31.
[6] T. Kraemer, H.H. Maurer, Determination of amphetamine, methamphetamine and amphetamine-derived designer drugs or medicaments in blood and urine, J. Chromatogr. B 713 (1998) 163–187.
[7] P. Elliott, T.C. Peakman, U.K Biobank, The UK Biobank sample handling and storage protocol for the collection, processing and archiving of human blood and urine, Int. J. Epidemiol. 37 (2008) 234–244.
[8] B.C. Reed, Centrifugation during the Manhattan project, Phys. Perspect. 11 (2009) 426–441.
[9] M. Elimelech, W.A. Phillip, The future of seawater desalination: energy, technology, and the environment, Science 333 (2011) 712–717.
[10] A.G. Fane, R. Wang, M.X. Hu, Synthetic membranes for water purification: status and future, Angew. Chem. Int. Ed. 54 (2015) 3368–3386.
[11] C.A. Scholes, G.W. Stevens, S.E. Kentish, Membrane gas separation applications in natural gas processing, Fuel 96 (2012) 15–28.
[12] D.F. Sanders, Z.P. Smith, R. Guo, L.M. Robeson, J.E. McGrath, D.R. Paul, B. D. Freeman, Energy-efficient polymeric gas separation membranes for a sustainable future: a review, Polymer 54 (2013) 4729–4761.
[13] P.M. Budd, N.B. McKeown, Highly permeable polymers for gas separation membranes, Polym. Chem. 1 (2010) 63–68.
[14] R. Zhang, Y. Liu, M. He, Y. Su, X. Zhao, M. Elimelech, Z. Jiang, Antifouling membranes for sustainable water purification: strategies and mechanisms, Chem. Soc. Rev. 45 (2016) 5888–5924.
[15] A. Roy, S.R. Venna, G. Rogers, L. Tang, T.C. Fitzgibbons, J. Liu, H. McCurry, D. J. Vickery, D. Flick, B. Fish, Membranes for olefin-paraffin separation: an industrial perspective, Proc. Natl. Acad. Sci 118 (37) (2021), e2022194118.
[16] J.Y.S Lin, Molecular sieves for gas separation, Science 353 (2016) 121–122.
[17] X. Cui, K. Chen, H. Xing, Q. Yang, R. Krishna, Z. Bao, H. Wu, W. Zhou, X. Dong, Y. Han, et al., Pore chemistry and size control in hybrid porous materials for acetylene capture from ethylene, Science 353 (2016) 141–144.
[18] A. Cadiau, K. Adil, P.M. Bhatt, Y. Belmabkhout, M. Eddaoudi, A metal-organic framework-based splitter for separating propylene from propane, Science 353 (2016) 137–140.
[19] R.-B. Lin, S. Xiang, H. Xing, W. Zhou, B. Chen, Exploration of porous metal–organic frameworks for gas separation and purification, Coord. Chem. Rev. 378 (2019) 87–103.
[20] H. Li, L. Li, R.-B. Lin, W. Zhou, Z. Zhang, S. Xiang, B. Chen, Porous metal-organic frameworks for gas storage and separation: status and challenges, EnergyChem 1 (2019), 100006.
[21] P. Nugent, Y. Belmabkhout, S.D. Burd, A.J. Cairns, R. Luebke, K. Forrest, T. Pham, S. Ma, B. Space, L. Wojtas, et al., Porous materials with optimal adsorption thermodynamics and kinetics for CO_2 separation, Nature 495 (2013) 80–84.
[22] Z. Wang, S. Zhang, Y. Chen, Z. Zhang, S. Ma, Covalent organic frameworks for separation applications, Chem. Soc. Rev. 49 (2020) 708–735.
[23] L. Li, R.-B. Lin, R. Krishna, H. Li, S. Xiang, H. Wu, J. Li, W. Zhou, B. Chen, Ethane/ethylene separation in a metal-organic framework with iron-peroxo sites, Science 362 (2018) 443–446.
[24] K.-J. Chen, D.G. Madden, S. Mukherjee, T. Pham, K.A. Forrest, A. Kumar, B. Space, J. Kong, Q.-Y. Zhang, M.J. Zaworotko, Synergistic sorbent separation for one-step ethylene purification from a four-component mixture, Science 366 (2019) 241–246.
[25] Y. Chai, X. Han, W. Li, S. Liu, S. Yao, C. Wang, W. Shi, I. da-Silva, P. Manuel, Y. Cheng, et al., Control of zeolite pore interior for chemoselective alkyne/olefin separations, Science 368 (2020) 1002–1006.
[26] X. Zhao, Y. Wang, D.S. Li, X. Bu, P. Feng, Metal-organic frameworks for separation, Adv. Mater. 30 (2018), 1705189.
[27] S. Qiu, M. Xue, G. Zhu, Metal-organic framework membranes: from synthesis to separation application, Chem. Soc. Rev. 43 (2014) 6116–6140.
[28] X. Li, Y. Liu, J. Wang, J. Gascon, J. Li, Van der Bruggen, B. Metal-organic frameworks based membranes for liquid separation, Chem. Soc. Rev. 46 (2017) 7124–7144.
[29] E. Ploetz, H. Engelke, U. Lächelt, S. Wuttke, The chemistry of reticular framework nanoparticles: MOF, ZIF, and COF materials, Adv. Funct. Mater. 30 (2020), 1909062.
[30] Y. Lu, H. Zhang, Y. Zhu, P.J. Marriott, H. Wang, Emerging homochiral porous materials for enantiomer separation, Adv. Funct. Mater. 31 (2021), 2101335.
[31] T.A. Adams, A. Pascall, Semicontinuous thermal separation systems, Chem. Eng. Technol. 35 (2012) 1153–1170.
[32] K.P. Lee, T.C. Arnot, D. Mattia, A review of reverse osmosis membrane materials for desalination—development to date and future potential, J. Membr. Sci. 370 (2011) 1–22.
[33] R.W. Baker, B.T. Low, Gas separation membrane materials: a perspective, Macromolecules 47 (2014) 6999–7013.
[34] M.M. Pendergast, E.M.V Hoek, A review of water treatment membrane nanotechnologies, Energy Environ. Sci. 4 (2011) 1946–1971.
[35] N.K. Khanzada, M.U. Farid, J.A. Kharraz, J. Choi, C.Y. Tang, L.D. Nghiem, A. Jang, A.K. An, Removal of organic micropollutants using advanced membrane-based water and wastewater treatment: a review, J. Membr. Sci. 598 (2020), 117672.
[36] M. Ulbricht, Advanced functional polymer membranes, Polymer 47 (2006) 2217–2262.
[37] H. Dai, Z. Dong, L. Jiang, Directional liquid dynamics of interfaces with superwettability, Sci. Adv. 6 (2020) eabb5528.
[38] Z. Sheng, J. Zhang, J. Liu, Y. Zhang, X. Chen, X. Hou, Liquid-based porous membranes, Chem. Soc. Rev. 49 (2020) 7907–7928.
[39] S. Wang, L. Yang, G. He, B. Shi, Y. Li, H. Wu, R. Zhang, S. Nunes, Z. Jiang, Two-dimensional nanochannel membranes for molecular and ionic separations, Chem. Soc. Rev. 49 (2020) 1071–1089.
[40] Y. Yampolskii, N. Belov, A. Alentiev, Perfluorinated polymers as materials of membranes for gas and vapor separation, J. Membr. Sci. 598 (2020), 117779.
[41] B.H. Monjezi, K. Kutonova, M. Tsotsalas, S. Henke, A. Knebel, Current trends in metal-organic and covalent organic framework membrane materials, Angew. Chem. Int. Ed. 60 (2021) 15153–15164.
[42] H.E. Karahan, K. Goh, C.J. Zhang, E. Yang, C. Yildirim, C.Y. Chuah, M. G. Ahunbay, J. Lee, S.B. Tantekin-Ersolmaz, Y. Chen, et al., MXene materials for designing advanced separation membranes, Adv. Mater. 32 (2020), e1906697.
[43] Y. Shi, B. Liang, R.-B. Lin, C. Zhang, B. Chen, Gas separation via hybrid metal–organic framework/polymer membranes, Trends Chem 2 (2020) 254–269.
[44] Y. Liu, Y. Ban, W. Yang, Microstructural engineering and architectural design of metal-organic framework membranes, Adv. Mater. 29 (2017), 1606949.
[45] J. Li, H. Wang, X. Yuan, J. Zhang, J.W. Chew, Metal-organic framework membranes for wastewater treatment and water regeneration, Coord. Chem. Rev. 404 (2020), 213116.
[46] B.-M. Jun, Y.A.J. Al-Hamadani, A. Son, C.M. Park, M. Jang, A. Jang, N.C. Kim, Y. Yoon, Applications of metal-organic framework based membranes in water purification: a review, *Sep. Purif. Technol* 247 (2020), 116947.
[47] M.S. Denny, J.C. Moreton, L. Benz, S.M. Cohen, Metal-organic frameworks for membrane-based separations, Nat. Rev. Mater. 1 (2016) 16078.
[48] S. Yuan, X. Li, J. Zhu, G. Zhang, P. Van Puyvelde, Van der Bruggen, B. Covalent organic frameworks for membrane separation, Chem. Soc. Rev. 48 (2019) 2665–2681.

[49] H. Wang, M. Wang, X. Liang, J. Yuan, H. Yang, S. Wang, Y. Ren, H. Wu, F. Pan, Z. Jiang, Organic molecular sieve membranes for chemical separations, Chem. Soc. Rev. 50 (2021) 5468–5516.
[50] H. Wang, Z. Zeng, P. Xu, L. Li, G. Zeng, R. Xiao, Z. Tang, D. Huang, L. Tang, C. Lai, et al., Recent progress in covalent organic framework thin films: fabrications, applications and perspectives, Chem. Soc. Rev. 48 (2019) 488–516.
[51] R. Wang, J. Guo, J. Xue, H. Wang, Covalent organic framework membranes for efficient chemicals separation, Small Struct 2 (2021), 2100061.
[52] J. Zhu, S. Yuan, J. Wang, Y. Zhang, M. Tian, Van der Bruggen, B. Microporous organic polymer-based membranes for ultrafast molecular separations, Prog. Polym. Sci. 110 (2020), 101308.
[53] H. Dou, M. Xu, B. Wang, Z. Zhang, G. Wen, Y. Zheng, D. Luo, L. Zhao, A. Yu, L. Zhang, et al., Microporous framework membranes for precise molecule/ion separations, Chem. Soc. Rev. 50 (2021) 986–1029.
[54] J. Zhang, J.A. Schott, S.M. Mahurin, S. Dai, Porous structure design of polymeric membranes for gas separation, Small Methods 1 (2017), 1600051.
[55] M.I.G.S. Almeida, R.W. Cattrall, S.D. Kolev, Recent trends in extraction and transport of metal ions using polymer inclusion membranes (PIMs), J. Membr. Sci. 415-416 (2012) 9–23.
[56] N. Du, H.B. Park, M.M. Dal-Cin, M.D. Guiver, Advances in high permeability polymeric membrane materials for CO_2 separations, Energy Environ. Sci. 5 (2012) 7306–7322.
[57] Q. Li, S. Razzaque, S. Jin, B. Tan, Morphology design of microporous organic polymers and their potential applications: an overview, Sci. China Chem. 60 (2017) 1056–1066.
[58] S. Noh, J.Y. Jeon, S. Adhikari, Y.S. Kim, C. Bae, Molecular engineering of hydroxide conducting polymers for anion exchange membranes in electrochemical energy conversion technology, Acc. Chem. Res. 52 (2019) 2745–2755.
[59] H. Zhou, W. Jin, Membranes with intrinsic micro-porosity: structure, solubility, and applications, Membranes 9 (2019) 3.
[60] A.A. Shamsabadi, M. Rezakazemi, F. Seidi, H. Riazi, T. Aminabhavi, M. Soroush, Next generation polymers of intrinsic microporosity with tunable moieties for ultrahigh permeation and precise molecular CO_2 separation, Prog. Energy Combust. Sci. 84 (2021), 100903.
[61] J. Wang, S. Zhuang, Covalent organic frameworks (COFs) for environmental applications, Coord. Chem. Rev. 400 (2019), 213046.
[62] Y. Liu, W. Zhou, W.L. Teo, K. Wang, L. Zhang, Y. Zeng, Y. Zhao, Covalent-organic-framework-based composite materials, Chem 6 (2020) 3172–3202.
[63] F. Zhang, J.-B. Fan, S. Wang, Interfacial polymerization: from chemistry to functional materials, Angew. Chem. Int. Ed. 59 (2020) 21840–21856.
[64] J. Hou, H. Zhang, G.P. Simon, H. Wang, Polycrystalline advanced microporous framework membranes for efficient separation of small molecules and ions, Adv. Mater. 32 (2020), 1902009.
[65] J. Li, X. Zhou, J. Wang, X. Li, Two-dimensional covalent organic frameworks (COFs) for membrane separation: a mini review, Ind. Eng. Chem. Res. 58 (2019) 15394–15406.
[66] C. Zhang, B.-H. Wu, M.-Q. Ma, Z. Wang, Z.-K. Xu, Ultrathin metal/covalent–organic framework membranes towards ultimate separation, Chem. Soc. Rev. 48 (2019) 3811–3841.
[67] M.-X. Wu, Y. Wang, G. Zhou, X. Liu, Sparks from different worlds: collaboration of MOFs and COFs, Coord. Chem. Rev. 430 (2021), 213735.
[68] R. Freund, O. Zaremba, G. Arnauts, R. Ameloot, G. Skorupskii, M. Dinca, A. Bavykina, J. Gascon, A. Ejsmont, J. Goscianska, et al., The current status of MOF and COF applications, Angew. Chem. Int. Ed. 60 (2021) 23975–24001.
[69] X. Ren, G. Liao, Z. Li, H. Qiao, Y. Zhang, X. Yu, B. Wang, H. Tan, L. Shi, X. Qi, et al., Two-dimensional MOF and COF nanosheets for next-generation optoelectronic applications, Coord. Chem. Rev. 435 (2021), 213781.
[70] J. Wang, N. Li, Y. Xu, H. Pang, Two-dimensional MOF and COF nanosheets: synthesis and applications in electrochemistry, Chem. Eur. J. 26 (2020) 6402–6422.
[71] Z. Li, X. Feng, Y. Zou, Y. Zhang, H. Xia, X. Liu, Y. Mu, A 2D azine-linked covalent organic framework for gas storage applications, Chem. Commun. 50 (2014) 13825–13828.
[72] T. Ben, C. Pei, D. Zhang, J. Xu, F. Deng, X. Jing, S. Qiu, Gas storage in porous aromatic frameworks (PAFs), Energy Environ. Sci. 4 (2011) 3991–3999.
[73] Z. Chang, D.-S. Zhang, Q. Chen, X.-H. Bu, Microporous organic polymers for gas storage and separation applications, Phys. Chem. Chem. Phys. 15 (2013) 5430–5442.
[74] W. Lu, D. Yuan, D. Zhao, C.I. Schilling, O. Plietzsch, T. Muller, S. Brase, J. Guenther, J. Blumel, R. Krishna, et al., Porous polymer networks: synthesis, porosity, and applications in gas storage/separation, Chem. Mater. 22 (2010) 5964–5972.
[75] P. Zhang, S. Wang, S. Ma, F.-S. Xiao, Q. Sun, Exploration of advanced porous organic polymers as a platform for biomimetic catalysis and molecular recognition, Chem. Commun. 56 (2020) 10631–10641.
[76] Y. Zhang, B. Li, S. Ma, Dual functionalization of porous aromatic frameworks as a new platform for heterogeneous cascade catalysis, Chem. Commun. 50 (2014) 8507–8510.
[77] S.Y. Ding, J. Gao, Q. Wang, Y. Zhang, W.G. Song, C.Y. Su, W. Wang, Construction of covalent organic framework for catalysis: Pd/COF-LZU1 in Suzuki-Miyaura coupling reaction, J. Am. Chem. Soc. 133 (2011) 19816–19822.
[78] Y. Yusran, H. Li, X. Guan, Q. Fang, S. Qiu, Covalent organic frameworks for catalysis, EnergyChem 2 (2020), 100035.
[79] Y.-B. Zhou, Z.-P. Zhan, Conjugated microporous polymers for heterogeneous catalysis, Chem. Asian J. 13 (2018) 9–19.
[80] Y. Zhang, S.N. Riduan, Functional porous organic polymers for heterogeneous catalysis, Chem. Soc. Rev. 41 (2012) 1083–1094.
[81] P. Kaur, J.T. Hupp, S.T. Nguyen, Porous organic polymers in catalysis: opportunities and challenges, ACS Catal 1 (2011) 819–835.
[82] R. Tao, X. Ma, X. Wei, Y. Jin, L. Qiu, W Zhang, Porous organic polymer material supported palladium nanoparticles, J. Mater. Chem. A 8 (2020) 17360–17391.
[83] S. Lu, Y. Jin, H. Gu, W. Zhang, Recent development of efficient electrocatalysts derived from porous organic polymers for oxygen reduction reaction, Sci. China Chem. 60 (2017) 999–1006.
[84] X. Liu, D. Huang, C. Lai, G. Zeng, L. Qin, H. Wang, H. Yi, B. Li, S. Liu, M. Zhang, et al., Recent advances in covalent organic frameworks (COFs) as a smart sensing material, Chem. Soc. Rev. 48 (2019) 5266–5302.
[85] W. Li, C.-X. Yang, X.-P. Yan, A versatile covalent organic framework-based platform for sensing biomolecules, Chem. Commun. 53 (2017) 11469–11471.
[86] W.K. Haug, E.M. Moscarello, E.R. Wolfson, P.L. McGrier, The luminescent and photophysical properties of covalent organic frameworks, Chem. Soc. Rev. 49 (2020) 839–864.
[87] J.L. Novotney, W.R. Dichtel, Conjugated porous polymers for TNT vapor detection, ACS Macro Lett 2 (2013) 423–426.
[88] J. Liu, K.-K. Yee, K.K.-W. Lo, K.Y. Zhang, W.-P. To, C.-M. Che, Z. Xu, Selective Ag(I) binding, H_2S sensing, and white-light emission from an easy-to-make porous conjugated polymer, J. Am. Chem. Soc. 136 (2014) 2818–2824.
[89] Q. Gao, X. Li, G.-H. Ning, K. Leng, B. Tian, C. Liu, W. Tang, H-S. Xu, K.P. Loh, Highly photoluminescent two-dimensional imine-based covalent organic frameworks for chemical sensing, Chem. Commun. 54 (2018) 2349–2352.
[90] C.R. DeBlase, K.E. Silberstein, T.-T. Truong, H.D. Abruna, W.R. Dichtel, βKetoenamine-linked covalent organic frameworks capable of pseudocapacitive energy storage, J. Am. Chem. Soc. 135 (2013) 16821–16824.
[91] D.-G. Wang, T. Qiu, W. Guo, Z. Liang, H. Tabassum, D. Xia, R. Zou, Covalent organic framework-based materials for energy applications, Energy Environ. Sci. 14 (2021) 688–728.
[92] C.-Y. Lin, D. Zhang, Z. Zhao, Z. Xia, Covalent organic framework electrocatalysts for clean energy conversion, Adv. Mater. 30 (2018), 1703646.
[93] M. Barawi, L. Collado, M. Gomez-Mendoza, F.E. Oropeza, M. Liras, V.A. de la Peña O'Shea, Conjugated porous polymers: ground-breaking materials for solar energy conversion, Adv. Energy Mater. 11 (2021), 2101530.
[94] F. Vilela, K. Zhang, M. Antonietti, Conjugated porous polymers for energy applications, Energy. Environ. Sci. 5 (2012) 7819–7832.
[95] Y. Hu, L.J. Wayment, C. Haslam, X. Yang, S.-h. Lee, Y. Jin, W Zhang, Covalent organic framework based lithium-ion battery: fundamental, design and characterization, EnergyChem 3 (2021), 100048.
[96] B. Li, X. Yang, L. Xia, M.I. Majeed, B. Tan, Hollow microporous organic capsules, Sci. Rep. 3 (2013) 2128.
[97] Q. Li, S. Jin, B. Tan, Template-mediated synthesis of hollow microporous organic nanorods with tunable aspect ratio, Sci. Rep. 6 (2016) 31359.
[98] X. Feng, F. Lv, L. Liu, H. Tang, C. Xing, Q. Yang, S. Wang, Conjugated polymer nanoparticles for drug delivery and imaging, ACS Appl. Mater. Interfaces 2 (2010) 2429–2435.
[99] Q. Fang, J. Wang, S. Gu, R.B. Kaspar, Z. Zhuang, J. Zheng, H. Guo, S. Qiu, Y. Yan, 3D porous crystalline polyimide covalent organic frameworks for drug delivery, J. Am. Chem. Soc. 137 (2015) 8352–8355.
[100] G. Zhang, X. Li, Q. Liao, Y. Liu, K. Xi, W. Huang, X. Jia, Water-dispersible PEG-curcumin/amine-functionalized covalent organic framework nanocomposites as smart carriers for *in vivo* drug delivery, Nat. Commun. 9 (2018) 2785.
[101] Q. Sun, B. Aguila, L.D. Earl, C.W. Abney, L. Wojtas, P.K. Thallapally, S. Ma, Covalent organic frameworks as a decorating platform for utilization and affinity enhancement of chelating sites for radionuclide sequestration, Adv. Mater. 30 (2018), 1705479.
[102] Q. Sun, B. Aguila, Y. Song, S. Ma, Tailored porous organic polymers for task-specific water purification, Acc. Chem. Res. 53 (2020) 812–821.
[103] Q. Sun, L. Zhu, B. Aguila, P.K. Thallapally, C. Xu, J. Chen, S. Wang, D. Rogers, S. Ma, Optimizing radionuclide sequestration in anion nanotraps with record pertechnetate sorption, Nat. Commun. 10 (2019) 1646.
[104] Q. Sun, B. Aguila, J. Perman, A.S. Ivanov, V.S. Bryantsev, L.D. Earl, C.W. Abney, L. Wojtas, S. Ma, Bio-inspired nano-traps for uranium extraction from seawater and recovery from nuclear waste, Nat. Commun. 9 (2018) 1644.
[105] Q. Sun, B. Aguila, S. Ma, Opportunities of porous organic polymers for radionuclide sequestration, Trends Chem 1 (2019) 292–303.
[106] Y. Song, C. Zhu, Q. Sun, B. Aguila, C.W. Abney, L. Wojtas, S. Ma, Nanospace decoration with uranyl-specific "hooks" for selective uranium extraction from seawater with ultrahigh enrichment index, ACS Cent. Sci. 7 (2021) 1650–1656.
[107] M. Shah, M.C. McCarthy, S. Sachdeva, A.K. Lee, H.-K. Jeong, Current status of metal-organic framework membranes for gas separations: promises and challenges, Ind. Eng. Chem. Res. 51 (2012) 2179–2199.
[108] Z. Kang, L. Fan, D Sun, Recent advances and challenges of metal–organic framework membranes for gas separation, J. Mater. Chem. A 5 (2017) 10073–10091.
[109] Y. Zhang, X. Feng, S. Yuan, J. Zhou, B. Wang, Challenges and recent advances in MOF–polymer composite membranes for gas separation, Inorg. Chem. Front. 3 (2016) 896–909.
[110] E. Adatoz, A.K. Avci, S. Keskin, Opportunities and challenges of MOF-based membranes in gas separations, Sep. Purif. Technol. 152 (2015) 207–237.
[111] Y. Song, P.C. Lan, K. Martin, S. Ma, Rational design of bifunctional conjugated microporous polymers, Nanoscale Adv 3 (2021) 4891–4906.
[112] A.I. Cooper, Conjugated microporous polymers, Adv. Mater. 21 (2009) 1291–1295.

[113] Y. Xu, S. Jin, H. Xu, A. Nagai, D. Jiang, Conjugated microporous polymers: design, synthesis and application, Chem. Soc. Rev. 42 (2013) 8012–8031.

[114] J.-S. Lee, A.I. Cooper, Advances in conjugated microporous polymers, Chem. Rev. 120 (2020) 2171–2214.

[115] N. Fontanals, R.M. Marcé, F. Borrull, P.A.G Cormack, Hypercrosslinked materials: preparation, characterisation and applications, Polym. Chem. 6 (2015) 7231–7244.

[116] V. Davankov, M. Tsyurupa, M. Ilyin, L Pavlova, Hypercross-linked polystyrene and its potentials for liquid chromatography: a mini-review, J. Chromatogr. A 965 (2002) 65–73.

[117] M.P. Tsyurupa, V.A. Davankov, Porous structure of hypercrosslinked polystyrene: state-of-the-art mini-review, React. Funct. Polym. 66 (2006) 768–779.

[118] J. Huang, S.R. Turner, Hypercrosslinked polymers: a review, Polym. Rev. 58 (2018) 1–41.

[119] H. Masoumi, A. Ghaemi, H.G. Gilani, Evaluation of hyper-cross-linked polymers performances in the removal of hazardous heavy metal ions: a review, Sep. Purif. Technol. 260 (2021), 118221.

[120] N.B. McKeown, P.M. Budd, K.J. Msayib, B.S. Ghanem, H.J. Kingston, C. E. Tattershall, S. Makhseed, K.J. Reynolds, D. Fritsch, Polymers of intrinsic microporosity (PIMs): bridging the void between microporous and polymeric materials, Chem. Eur. J. 11 (2005) 2610–2620.

[121] D. Ramimoghadam, E.M. Gray, C.J. Webb, Review of polymers of intrinsic microporosity for hydrogen storage applications, Int. J. Hydrog. Energy 41 (2016) 16944–16965.

[122] N.B. McKeown, P.M. Budd, Polymers of intrinsic microporosity (PIMs): organic materials for membrane separations, heterogeneous catalysis and hydrogen storage, Chem. Soc. Rev. 35 (2006) 675–683.

[123] N.B. McKeown, The synthesis of polymers of intrinsic microporosity (PIMs), Sci. China Chem. 60 (2017) 1023–1032.

[124] Y. Yuan, Y. Yang, G. Zhu, Multifunctional porous aromatic frameworks: state of the art and opportunities, EnergyChem 2 (2020), 100037.

[125] Y. Tian, G. Zhu, Porous aromatic frameworks (PAFs), Chem. Rev. 120 (2020) 8934–8986.

[126] Y. Yuan, G. Zhu, Porous aromatic frameworks as a platform for multifunctional applications, ACS Cent. Sci. 5 (2019) 409–418.

[127] T. Hasell, A.I. Cooper, Porous organic cages: soluble, modular and molecular pores, Nat. Rev. Mater. 1 (2016) 16053.

[128] H. Wang, Y. Jin, N. Sun, W. Zhang, J. Jiang, Post-synthetic modification of porous organic cages, Chem. Soc. Rev. 50 (2021) 8874–8886.

[129] J.D. Evans, C.J. Sumby, C.J. Doonan, Synthesis and applications of porous organic cages, Chem. Lett. 44 (2015) 582–588.

[130] M.A. Little, A.I. Cooper, The chemistry of porous organic molecular materials, Adv. Funct. Mater. 30 (2020), 1909842.

[131] M.E. Briggs, A.I. Cooper, A perspective on the synthesis, purification, and characterization of porous organic cages, Chem. Mater. 29 (2017) 149–157.

[132] S. Huang, Z. Lei, Y. Jin, W. Zhang, By-design molecular architectures via alkyne metathesis, Chem. Sci. 12 (2021) 9591–9606.

[133] C. Liu, Y. Jiang, A. Nalaparaju, J. Jiang, A Huang, Post-synthesis of a covalent organic framework nanofiltration membrane for highly efficient water treatment, J. Mater. Chem. A 7 (2019) 24205–24210.

[134] R. Zhao, H. Wu, L. Yang, Y. Ren, Y. Liu, Z. Qu, Y. Wu, L. Cao, Z. Chen, Z. Jiang, Modification of covalent organic frameworks with dual functions ionic liquids for membrane-based biogas upgrading, J. Membr. Sci. 600 (2020), 117841.

[135] T. Arumugham, N.J. Kaleekkal, S. Gopal, J. Nambikkattu, R. K, A.M. Aboulella, S. R. Wickramasinghe, F Banat, Recent developments in porous ceramic membranes for wastewater treatment and desalination: a review, J. Environ. Manage. 293 (2021), 112925.

[136] A. Lee, J.W. Elam, S.B. Darling, Membrane materials for water purification: design, development, and application, Environ. Sci.: Water Res. Technol. 2 (2016) 17–42.

[137] P. Shao, R.Y.M Huang, Polymeric membrane pervaporation, J. Membr. Sci. 287 (2007) 162–179.

[138] A. Pagidi, R. Saranya, G. Arthanareeswaran, A.F. Ismail, T. Matsuura, Enhanced oil–water separation using polysulfone membranes modified with polymeric additives, Desalination 344 (2014) 280–288.

[139] J. Zhou, Y. Wang, Selective swelling of block copolymers: an upscalable greener process to ultrafiltration membranes? Macromolecules 53 (2020) 5–17.

[140] C. Bellona, J.E. Drewes, The role of membrane surface charge and solute physico-chemical properties in the rejection of organic acids by NF membranes, J. Membr. Sci. 249 (2005) 227–234.

[141] Q. Sun, B. Aguila, J. Perman, N. Nguyen, S. Ma, Flexibility matters: cooperative active sites in covalent organic framework and threaded ionic polymer, J. Am. Chem. Soc. 138 (2016) 15790–15796.

[142] H.B. Aiyappa, J. Thote, D.B. Shinde, R. Banerjee, S. Kurungot, Cobalt-modified covalent organic framework as a robust water oxidation electrocatalyst, Chem. Mater. 28 (2016) 4375–4379.

[143] T. Ma, J. Li, J. Niu, L. Zhang, A.S. Etman, C. Lin, D. Shi, P. Chen, L.H. Li, X. Du, et al., Observation of interpenetration isomerism in covalent organic frameworks, J. Am. Chem. Soc. 140 (2018) 6763–6766.

[144] S.Y. Ding, M. Dong, Y.W. Wang, Y.T. Chen, H.Z. Wang, C.Y. Su, W. Wang, Thioether-based fluorescent covalent organic framework for selective detection and facile removal of mercury(II), J. Am. Chem. Soc. 138 (2016) 3031–3037.

[145] F.J. Uribe-Riomo, C.J. Doonan, H. Furukawa, K. Oisaki, O.M. Yaghi, Crystalline covalent organic frameworks with hydrazone linkages, J. Am. Chem. Soc. 133 (2011) 11478–11481.

[146] Q. Sun, B. Aguila, J. Perman, L.D. Earl, C.W. Abney, Y. Cheng, H. Wei, N. Nguyen, L. Wojtas, S. Ma, Postsynthetically modified covalent organic frameworks for efficient and effective mercury removal, J. Am. Chem. Soc. 139 (2017) 2786–2793.

[147] H. Ding, A. Mal, C. Wang, Tailored covalent organic frameworks by post-synthetic modification, Mater. Chem. Front. 4 (2020) 113–127.

[148] J.L. Segura, S. Royuela, M.M. Ramos, Post-synthetic modification of covalent organic frameworks, Chem. Soc. Rev. 48 (2019) 3903–3945.

[149] P. Shao, J. Li, F. Chen, L. Ma, Q. Li, M. Zhang, J. Zhou, A. Yin, X. Feng, B. Wang, Flexible films of covalent organic frameworks with ultralow dielectric constants under high humidity, Angew. Chem. Int. Ed. 57 (2018) 16501–16505.

[150] B.F. Hoskins, R. Robson, Design and construction of a new class of Scaffolding-like materials comprising infinite polymeric frameworks of 3D-linked molecular rods. A reappraisal of the $Zn(CN)_2$ and $Cd(CN)_2$ structures and the synthesis and structure of the diamond-related frameworks $[N(CH_3)_4][Cu^{I}Zn^{II}(CN)_4]$ and $Cu^{I}[4,4^{\prime},4^{\prime\prime},4^{\prime\prime\prime}$-tetracyanotetraphenylmethane]$BF_4{\bullet}xC_6H_5NO_2$, J. Am. Chem. Soc. 112 (1990) 1546–1554.

[151] Z. Wang, S.M. Cohen, Postsynthetic covalent modification of a neutral metal-organic framework, J. Am. Chem. Soc. 129 (2007) 12368–12369.

[152] T. Ratvijitvech, R. Dawson, A. Laybourn, Y.Z. Khimyak, D.J. Adams, A.I. Cooper, Post-synthetic modification of conjugated microporous polymers, Polymer 55 (2014) 321–325.

[153] R. Dawson, A. Laybourn, R. Clowes, Y.Z. Khimyak, D.J. Adams, A.I. Cooper, Functionalized conjugated microporous polymers, Macromolecules 42 (2009) 8809–8816.

[154] Y. Zhang, B. Li, K. Williams, W.-Y. Gao, S. Ma, A new microporous carbon material synthesized via thermolysis of a porous aromatic framework embedded with an extra carbon source for low-pressure CO_2 uptake, Chem. Commun. 49 (2013) 10269–10271.

[155] M.S. Lohse, T. Stassin, G. Naudin, S. Wuttke, R. Ameloot, D.D. Vos, D.D. Medina, T. Bein, Sequential pore wall modification in a covalent organic framework for application in lactic acid adsorption, Chem. Mater. 28 (2016) 626–631.

[156] M. Liu, Y.-J. Chen, X. Huang, L.-Z. Dong, M. Lu, C. Guo, D. Yuan, Y. Chen, G. Xu, S.-L. Li, et al., Porphyrin-based COF 2D materials: variable modification of sensing performances by post-metallization, Angew. Chem. Int. Ed. 61 (2022), e202115308.

[157] Y. Yusran, Q. Fang, S. Qiu, Postsynthetic covalent modification in covalent organic frameworks, Isr. J. Chem. 58 (2018) 971–984.

[158] A. Nagai, Z. Guo, X. Feng, S. Jin, X. Chen, X. Ding, D. Jiang, Pore surface engineering in covalent organic frameworks, Nat. Commun. 2 (2011) 536.

[159] H. Xu, J. Gao, D. Jiang, Stable, crystalline, porous, covalent organic frameworks as a platform for chiral organocatalysts, Nat. Chem. 7 (2015) 905–912.

[160] A.K. Mohammed, A.A. Al Khoori, M.A. Addicoat, S. Varghese, I. Othman, M. A. Jaoude, K. Polychronopoulou, M. Baias, M.A. Haija, D Shetty, Solvent-influenced fragmentations in free-standing three-dimensional covalent organic framework membranes for hydrophobicity switching, Angew. Chem. Int. Ed. 61 (2022), 202200905.

[161] B.M. Ganesh, A.M. Isloor, A.F. Ismail, Enhanced hydrophilicity and salt rejection study of graphene oxide-polysulfone mixed matrix membrane, Desalination 313 (2013) 199–207.

[162] K. Zhang, Z. He, K.M. Gupta, J. Jiang, Computational design of 2D functional covalent– organic framework membranes for water desalination, Environ. Sci.: Water Res. Technol. 3 (2017) 735–743.

[163] A. Zirehpour, A. Rahimpour, S. Khoshhal, M.D. Firouzjaei, A.A. Ghoreyshi, The impact of MOF feasibility to improve the desalination performance and antifouling properties of FO membranes, RSC Adv 6 (2016) 70174–70185.

[164] T. Imae, Fluorinated polymers, Curr. Opin. Colloid Interface Sci. 8 (2003) 307–314.

[165] N.A. Ahmad, C.P. Leo, A.L. Ahmad, W.K.W. Ramli, Membranes with great hydrophobicity: a review on preparation and characterization, Sep. Purif. Rev. 44 (2015) 109–134.

[166] Q. Sun, B. Aguila, J.A. Perman, T. Butts, F.-S. Xiao, S. Ma, Integrating superwettability within covalent organic frameworks for functional coating, Chem 4 (2018) 1726–1739.

[167] Q. Sun, B. Aguila, G. Verma, X. Liu, Z. Dai, F. Deng, X. Meng, F.-S. Xiao, S. Ma, Superhydrophobicity: constructing homogeneous catalysts into superhydrophobic porous frameworks to protect them from hydrolytic degradation, Chem 1 (2016) 628–639.

[168] H. Ma, B. Liu, B. Li, L. Zhang, Y.-G. Li, H.-Q. Tan, H.-Y. Zhang, G. Zhu, Cationic covalent organic frameworks: a simple platform of anionic exchange for porosity tuning and proton conduction, J. Am. Chem. Soc. 138 (2016) 5897–5903.

[169] H. Yang, L. Yang, H. Wang, Z. Xu, Y. Zhao, Y. Luo, N. Nasir, Y. Song, H. Wu, F. Pan, et al., Covalent organic framework membranes through a mixed-dimensional assembly for molecular separations, Nat. Commun. 10 (2019) 2101.

[170] Z. Zhang, X. Shi, R. Wang, A. Xiao, Y. Wang, Ultra-permeable polyamide membranes harvested by covalent organic framework nanofiber scaffolds: a two-in-one strategy, Chem. Sci. 10 (2019) 9077–9083.

[171] Y. Peng, G. Xu, Z. Hu, Y. Cheng, C. Chi, D. Yuan, H. Cheng, D. Zhao, Mechanoassisted synthesis of sulfonated covalent organic frameworks with high intrinsic proton conductivity, ACS Appl. Mater. Interfaces 8 (2016) 18505–18512.

[172] L. Gao, H. Wu, Y. Cao, C. Fan, R. Zhao, X. He, P. Yang, B. Shi, X. You, Z. Jiang, Weakly humidity-dependent proton-conducting COF membranes, Adv. Mater. 32 (2020), 2005565.

[173] N. Huang, P. Wang, M.A. Addicoat, T. Heine, D. Jiang, Ionic covalent organic frameworks: design of a charged interface aligned on 1D channel walls and its unusual electrostatic functions, Angew. Chem. Int. Ed. 56 (2017) 4982–4986.

[174] A. Mal, S. Vijayakumar, R.K. Mishra, J. Jacob, R.S. Pillai, B.S.D. Kumar, A. Ajayaghosh, Supramolecular surface charge regulation in ionic covalent organic nanosheets: reversible exfoliation and controlled bacterial growth, Angew. Chem. Int. Ed. 59 (2020) 8713–8719.

[175] L. Liu, L. Yin, D. Cheng, S. Zhao, H.-Y. Zang, N. Zhang, G. Zhu, Surface-mediated construction of an ultrathin free-standing covalent organic framework membrane for efficient proton conduction, Angew. Chem. Int. Ed. 60 (2021) 14875–14880.

[176] W. Zhang, L. Zhang, H. Zhao, B. Li, H Ma, A two-dimensional cationic covalent organic framework membrane for selective molecular sieving, J. Mater. Chem. A 6 (2018) 13331–13339.

[177] P.H.H. Duong, V.A. Kuehl, B. Mastorovich, J.O. Hoberg, B.A. Parkinson, K.D. Li-Oakey, Carboxyl-functionalized covalent organic framework as a two-dimensional nanofiller for mixed-matrix ultrafiltration membranes, J. Membr. Sci. 574 (2019) 338–348.

[178] Y. Yuan, F. Sun, F. Zhang, H. Ren, M. Guo, K. Cai, X. Jing, X. Gao, G. Zhu, Targeted synthesis of porous aromatic frameworks and their composites for versatile, facile, efficacious, and durable antibacterial polymer coatings, Adv. Mater 25 (2013) 6619–6624.

[179] Z. Zhou, D.B. Shinde, D. Guo, l. Cao, R.A. Nuaimi, Y. Zhang, L.R. Enakonda, Z Lai, Flexible ionic conjugated microporous polymer membranes for fast and selective ion transport, Adv. Funct. Mater. 32 (2022), 2108672.

[180] S. Chen, C. Zhu, W. Xian, X. Liu, X. Liu, Q. Zhang, S. Ma, Q. Sun, Imparting ion selectivity to covalent organic framework membranes using *de novo* assembly for blue energy harvesting, J. Am. Chem. Soc. 143 (2021) 9415–9422.

[181] N. Zhang, Y. Liu, R. Liu, Z. She, M. Tan, D. Mao, R. Fu, Y. Zhang, Polymer inclusion membrane (PIM) containing ionic liquid as a proton blocker to improve waste acid recovery efficiency in electrodialysis process, J. Membr. Sci. 581 (2019) 18–27.

[182] T. He, K. Geng, D. Jiang, All sp^2 carbon covalent organic frameworks, Trends Chem 3 (2021) 431–444.

[183] E. Jin, M. Asada, Q. Xu, S. Dalapati, M.A. Addicoat, M.A. Brady, H. Xu, T. Nakamura, T. Heine, Q. Chen, et al., Two-dimensional sp^2 carbon-conjugated covalent organic frameworks, Science 357 (2017) 673–676.

[184] J. Feng, Y.-J. Zhang, S.-H. Ma, C. Yang, Z.-P. Wang, S.-Y. Ding, Y. Li, W. Wang, Fused-ring-linked covalent organic frameworks, J. Am. Chem. Soc. 144 (2022) 6594–6603.

[185] P.-F. Wei, M.-Z. Qi, Z.-P. Wang, S.-Y. Ding, W. Yu, Q. Liu, L.-K. Wang, H.-Z. Wang, W.-K. An, W. Wang, Benzoxazole-linked ultrastable covalent organic frameworks for photocatalysis, J. Am. Chem. Soc. 140 (2018) 4623–4631.

[186] X. Li, C. Zhang, S. Cai, X. Lei, V. Altoe, F. Hong, J.J. Urban, J. Ciston, E.M. Chan, Y. Liu, Facile transformation of imine covalent organic frameworks into ultrastable crystalline porous aromatic frameworks, Nat. Commun. 9 (2018) 2998.

[187] A.P. Cote, A.I. Benin, N.W. Ockwig, M. O'Keeffe, A.J. Matzger, O.M. Yaghi, Porous, crystalline, covalent organic frameworks, Science 310 (2005) 1166–1170.

[188] K. Geng, T. He, R. Liu, S. Dalapati, K.T. Tan, Z. Li, S. Tao, Y. Gong, Q. Jiang, D. Jiang, Covalent organic frameworks: design, synthesis, and functions, Chem. Rev. 120 (2020) 8814–8933.

[189] S.-Y. Ding, W. Wang, Covalent organic frameworks (COFs): from design to applications, Chem. Soc. Rev. 42 (2013) 548–568.

[190] Y. Song, Q. Sun, B. Aguila, S. Ma, Opportunities of covalent organic frameworks for advanced applications, Adv. Sci. 6 (2019), 1801410.

[191] F.J. Uribe-Romo, J.R. Hunt, H. Furukawa, C. Klock, M. O'Keeffe, O.M. Yaghi, A crystalline imine-linked 3-D porous covalent organic framework, J. Am. Chem. Soc. 131 (2009) 4570–4571.

[192] Y. Li, W. Chen, G. Xing, D. Jiang, L. Chen, New synthetic strategies toward covalent organic frameworks, Chem. Soc. Rev. 49 (2020) 2852–2868.

[193] Y.-B. Zhang, J. Su, H. Furukawa, Y. Yun, F. Gandara, A. Duong, X. Zou, O. M. Yaghi, Single-crystal structure of a covalent organic framework, J. Am. Chem. Soc. 135 (2013) 16336–16339.

[194] T. Ma, E.A. Kapustin, S.X. Yin, L. Liang, Z. Zhou, J. Niu, L.-H. Li, Y. Wang, J. Su, J. Li, et al., Single-crystal x-ray diffraction structures of covalent organic frameworks, Science 361 (2018) 48–52.

[195] L. Peng, Q. Guo, C. Song, S. Ghosh, H. Xu, L. Wang, D. Hu, L. Shi, L. Zhao, Q. Li, et al., Ultra-fast single-crystal polymerization of large-sized covalent organic frameworks, Nat. Commun. 12 (2021) 5077.

[196] C. Kang, K. Yang, Z. Zhang, A.K. Usadi, D.C. Calabro, L.S. Baugh, Y. Wang, J. Jiang, X. Zou, Z. Huang, et al., Growing single crystals of two-dimensional covalent organic frameworks enabled by intermediate tracing study, Nat. Commun. 13 (2022) 1370.

[197] H.M. El-Kaderi, J.R. Hunt, J.L. Mendoza-Cortes, A.P. Cote, R.E. Taylor, M. O'Keeffe, O.M. Yaghi, Designed synthesis of 3D covalent organic frameworks, Science 316 (2007) 268–272.

[198] P. Kuhn, M. Antonietti, A. Thomas, Porous, covalent triazine-based frameworks prepared by ionothermal synthesis, Angew. Chem. Int. Ed. 47 (2008) 3450–3453.

[199] J.-X. Jiang, F. Su, A. Trewin, C.D. Wood, N.L. Campbell, H. Niu, C. Dickinson, A. Y. Ganin, M.J. Rosseinsky, Y.Z. Khimyak, et al., Conjugated microporous poly (aryleneethynylene) networks, Angew. Chem. Int. Ed. 46 (2007) 8574–8578.

[200] S. Luo, Z. Zeng, G. Zeng, Z. Liu, R. Xiao, P. Xu, H. Wang, D. Huang, Y. Liu, B. Shao, et al., Recent advances in conjugated microporous polymers for photocatalysis: designs, applications, and prospects, J. Mater. Chem. A 8 (2020) 6434–6470.

[201] G. Cheng, T. Hasell, A. Trewin, D.J. Adams, A.I. Cooper, Soluble conjugated microporous polymers, Angew. Chem. Int. Ed. 51 (2012) 12727–12731. **This work reported the first example of soluble CMP networks and corresponding CMP-based membrane via the solution casting method**.

[202] P. Pallavi, S. Bandyopadhyay, J. Louis, A. Deshmukh, A. Patra, A soluble conjugated porous organic polymer: efficient white light emission in solution, nanoparticles, gel and transparent thin film, Chem. Commun. 53 (2017) 1257–1260.

[203] B. Huang, P. Zhao, Y. Dai, S. Deng, A. Hu, Size-controlled synthesis of soluble-conjugated microporous polymer nanoparticles through sonogashira polycondensation in confined nanoreactors, J. Polym. Sci. A: Polym. Chem. 54 (2016) 2285–2290.

[204] S. Luo, Z. Zeng, H. Wang, W. Xiong, B. Song, C. Zhou, A. Duan, X. Tan, Q. He, G. Zeng, et al., Recent progress in conjugated microporous polymers for clean energy: synthesis, modification, computer simulations, and applications, Prog. Polym. Sci. 115 (2021), 101374.

[205] Y. Wang, X. Ma, B.S. Ghanem, F. Alghunaimi, I. Pinnau, Y. Han, Polymers of intrinsic microporosity for energy-intensive membrane-based gas separations, Mater. Today Nano 3 (2018) 69–95.

[206] W.H. Lee, J.G. Seong, X. Hu, Y.M. Lee, Recent progress in microporous polymers from thermally rearranged polymers and polymers of intrinsic microporosity for membrane gas separation: pushing performance limits and revisiting trade-off lines, J. Polym. Sci. 58 (2020) 2450–2466.

[207] P. Bernardo, V. Scorzafave, G. Clarizia, E. Tocci, J.C. Jansen, A. Borgogno, R. Malpass-Evans, N.B. McKeown, M. Carta, F. Tasselli, Thin film composite membranes based on a polymer of intrinsic microporosity derived from Tröger's base: a combined experimental and computational investigation of the role of residual casting solvent, J. Membr. Sci. 569 (2019) 17–31.

[208] P.M. Budd, B.S. Ghanem, S. Makhseed, N.B. McKeown, K.J. Msayib, C. E. Tattershall, Polymers of intrinsic microporosity (PIMs): 2, Chem. Commun. (2004) 230–231.

[209] P.M. Budd, E.S. Elabas, B.S. Ghanem, S. Makhseed, N.B. McKeown, K.J. Msayib, C.E. Tattershall, D. Wang, Solution-processed, organophilic membrane derived from a polymer of intrinsic microporosity, Adv. Mater. 16 (2004) 456–459. **This work pioneered the fabrication of self-supported PIM-based membrane (PIM-1)**.

[210] C.G. Bezzu, M. Carta, A. Tonkins, J.C. Jansen, P. Bernardo, F. Bazzarelli, N. B. McKeown, A spirobifluorene-based polymer of intrinsic microporosity with improved performance for gas separation, Adv. Mater. 24 (2012) 5930–5933.

[211] M. Carta, R. Malpass-Evans, M. Croad, Y. Rogan, J.C. Jansen, P. Bernardo, F. Bazzarelli, N.B. McKeown, An efficient polymer molecular sieve for membrane gas separations, Science 339 (2013) 303–307.

[212] P. Gorgojo, S. Karan, H.C. Wong, M.F. Jimenez-Solomon, J.T. Cabral, A. G. Livingston, Ultrathin polymer films with intrinsic microporosity: anomalous solvent permeation and high flux membranes, Adv. Funct. Mater. 24 (2014) 4729–4737.

[213] C.R. Mason, L. Maynard-Atem, K.W.J. Heard, B. Satilmis, P.M. Budd, K. Firess, M. Lanc, P. Bernardo, G. Clarizia, J.C. Jansen, Enhancement of CO$_2$ affinity in a polymer of intrinsic microporosity by amine modification, Macromolecules 47 (2014) 1021–1029.

[214] N. Du, H.B. Park, G.P. Robertson, M.M. Dal-Cin, T. Visser, L. Scoles, M.D. Guiver, Polymer nanosieve membranes for CO$_2$-capture applications, Nat. Mater. 10 (2011) 372–375.

[215] X. Weng, J.E. Baez, M. Khiterer, M.Y. Hoe, Z. Bao, K.J. Shea, Chiral polymers of intrinsic microporosity: selective membrane permeation of enantiomers, Angew. Chem. Int. Ed. 54 (2015) 11214–11218.

[216] C.R. Mason, L. Maynard-Atem, N.M. Al-Harbi, P.M. Budd, P. Bernardo, F. Bazzarelli, G. Clarizia, J.C. Jansen, Polymer of intrinsic microporosity incorporating thioamide functionality: preparation and gas transport properties, Macromolecules 44 (2011) 6471–6479.

[217] H.A. Patel, C.T. Yavuz, Noninvasive functionalization of polymers of intrinsic microporosity for enhanced CO$_2$ capture, Chem. Commun. 48 (2012) 9989–9991.

[218] K.M. Rodriguez, S. Lin, A.X. Wu, G. Han, J.J. Teesdale, C.M. Doherty, Z.P. Smith, Leveraging free volume manipulation to improve the membrane separation performance of amine-functionalized PIM-1, Angew. Chem. Int. Ed. 60 (2021) 6593–6599.

[219] B.S. Ghanem, N.B. McKeown, P.M. Budd, J.D. Selbie, D. Fritsch, High-performance membranes from polyimides with intrinsic microporosity, Adv. Mater. 20 (2008) 2766–2771.

[220] Z. Yang, R. Guo, R. Malpass-Evans, M. Carta, N.B. McKeown, M.D. Guiver, L. Wu, T. Xu, Highly conductive anion-exchange membranes from microporous Tröger's base polymers, Angew. Chem. Int. Ed. 55 (2016) 11499–11502.

[221] B.S. Ghanem, R. Swaidan, X. Ma, E. Litwiller, I. Pinnau, Energy-efficient hydrogen separation by AB-type ladder-polymer molecular sieves, Adv. Mater. 26 (2014) 6696–6700.

[222] I. Rose, C.G. Bezzu, M. Carta, B. Comesaña-Gándara, E. Lasseuguette, M. C. Ferrari, P. Bernardo, G. Clarizia, A. Fuoco, J.C. Jansen, et al., Polymer ultrapermeability from the inefficient packing of 2D chains, Nat. Mater. 16 (2017) 932–937.

[223] X. Guan, H. Li, Y. Ma, M. Xue, Q. Fang, Y. Yan, V. Valtchev, S. Qiu, Chemically stable polyarylether-based covalent organic frameworks, Nat. Chem. 11 (2019) 587–594.

[224] B. Zhang, M. Wei, H. Mao, X. Pei, S.A. Alshmimri, J.A. Reimer, O.M. Yaghi, Crystalline dioxin-linked covalent organic frameworks from irreversible reactions, J. Am. Chem. Soc. 140 (2018) 12715–12719.

[225] V. Davankov, S. Rogozhin, M. Tsyurupa, New approach to preparation of uniformly crosslinked macroreticular polystyrene structures, Mezhdunarodnaya Kniga 15 (1973) 463–465.

[226] S. Xu, Y. Luo, B. Tan, Recent development of hypercrosslinked microporous organic polymers, Macromol. Rapid Commun. 34 (2013) 471–484.

[227] C.D. Wood, B. Tan, A. Trewin, H. Niu, D. Bradshaw, M.J. Rosseinsky, Y. Z. Khimyak, N.L. Campbell, R. Kirk, E. Stockel, et al., Hydrogen storage in microporous hypercrosslinked organic polymer networks, Chem. Mater. 19 (2007) 2034–2048.

[228] Y. Gu, S.U. Son, T. Li, B. Tan, Low-cost hypercrosslinked polymers by direct knitting strategy for catalytic applications, Adv. Funct. Mater. 31 (2021), 2008265.

[229] S. Wang, C. Zhang, Y. Shu, S. Jiang, Q. Xia, L. Chen, S. Jin, I. Hussain, A.I. Cooper, B. Tan, Layered microporous polymers by solvent knitting method, Sci. Adv. 3 (2017), e1602610.

[230] Z.-A. Qiao, S.-H. Chai, K. Nelson, Z. Bi, J. Chen, S.M. Mahurin, X. Zhu, S Dai, Polymeric molecular sieve membranes via in situ cross-linking of non-porous polymer membrane templates, Nat. Commun. 5 (2014) 3705.

[231] T. Wang, Y. Yang, J. Zheng, Q. Zhang, S. Zhang, A novel highly permeable positively charged nanofiltration membrane based on a nanoporous hyper-crosslinked polyamide barrier layer, J. Mater. Sci. 448 (2013) 180–189.

[232] T. Ben, H. Ren, S. Ma, D. Cao, J. Lan, X. Jing, W. Wang, J. Xu, F. Deng, J. M. Simmons, et al., Targeted synthesis of a porous aromatic framework with high stability and exceptionally high surface area, Angew. Chem. Int. Ed. 48 (2009) 9457–9460.

[233] H. Ren, T. Ben, E. Wang, X. Jing, M. Xue, B. Liu, Y. Cui, S. Qiu, G. Zhu, Targeted synthesis of a 3D porous aromatic framework for selective sorption of benzene, Chem. Commun. 46 (2010) 291–293.

[234] B. Li, Y. Zhang, R. Krishna, K. Yao, Y. Han, Z. Wu, D. Ma, Z. Shi, T. Pham, B. Space, et al., Introduction of πcomplexation into porous aromatic framework for highly selective adsorption of ethylene over ethane, J. Am. Chem. Soc. 136 (2014) 8654–8660.

[235] B. Li, Y. Zhang, D. Ma, Z. Shi, S. Ma, Mercury nano-trap for effective and efficient removal of mercury(II) from aqueous solution, Nat. Commun. 5 (2014) 5537.

[236] B. Li, Y. Zhang, D. Ma, Z. Xing, T. Ma, Z. Shi, X. Ji, S. Ma, Creation of a new type of ion exchange material for rapid, high-capacity, reversible and selective ion exchange without swelling and entrainment, Chem. Sci. 7 (2016) 2138–2144.

[237] D. Banerjee, S.K. Elsaidi, B. Aguila, B. Li, D. Kim, M.J. Schweiger, A.A. Kruger, C. J. Doonan, S. Ma, P.K. Thallapally, Removal of pertechnetate-related oxyanions from solution using functionalized hierarchical porous frameworks, Chem. Eur. J. 22 (2016) 17581–17584.

[238] B. Li, Q. Sun, Y. Zhang, C.W. Abney, B. Aguila, W. Lin, S. Ma, Functionalized porous aromatic framework for efficient uranium adsorption from aqueous solutions, ACS Appl. Mater. Interfaces 9 (2017) 12511–12517.

[239] B. Aguila, Q. Sun, H. Cassady, C.W. Abney, B. Li, S. Ma, Design strategies to enhance amidoxime chelators for uranium recovery, ACS Appl. Mater. Interfaces 11 (2019) 30919–30926.

[240] L. Meng, X. Zou, S. Guo, H. Ma, Y. Zhao, G. Zhu, Self-supported fibrous porous aromatic membranes for efficient CO_2/N_2 separations, ACS Appl. Mater. Interfaces 7 (2015) 15561–15569.

[241] Y. Ma, F. Cui, H. Rong, J. Song, X. Jing, Y. Tian, G Zhu, Continuous porous aromatic framework membranes with modifiable sites for optimized gas separation, Angew. Chem. Int. Ed. 61 (2022), 202113682.

[242] Z. Zhai, C. Jiang, N. Zhao, W. Dong, P. Li, H. Sun, Q.J. Niu, Polyarylate membrane constructed from porous organic cage for high-performance organic solvent nanofiltration, J. Membr. Sci. 595 (2020), 117505.

[243] T. Tozawa, J.T.A. Jones, S.I. Swamy, S. Jiang, D.J. Adams, S. Shakespeare, R. Clowes, D. Bradshaw, T. Hasell, S.Y. Chong, et al., Porous organic cages, Nat. Mater. 8 (2009) 973–978.

[244] M. Mastalerz, Porous shape-persistent organic cage compounds of different size, geometry, and function, Acc. Chem. Res. 51 (2018) 2411–2422.

[245] Q. Song, S. Jiang, T. Hasell, M. Liu, S. Sun, A.K. Cheetham, E. Sivaniah, A. I. Cooper, Porous organic cage thin films and molecular-sieving membranes, Adv. Mater. 28 (2016) 2629–2637. **This work firstly reported the casting of continuous and defect-free POC-based thin films via a solution-processing method without the addition of other polymeric support**.

[246] J. Liu, D. Hua, Y. Zhang, S. Japip, T.-S. Chung, Precise molecular sieving architectures with janus pathways for both polar and nonpolar molecules, Adv. Mater. 30 (2018), 1705933.

[247] M.J.T. Raaijmakers, M. Wessling, A. Nijmeijer, N.E. Benes, Hybrid polyhedral oligomeric silsesquioxanes−imides with tailored intercage spacing for sieving of hot gases, Chem. Mater. 26 (2014) 3660–3664.

[248] A.F. Bushell, P.M. Budd, M.P. Attfield, J.T.A. Jones, T. Hasell, A.I. Cooper, P. Bernardo, F. Bazzarelli, G. Clarizia, J.C. Jansen, Nanoporous organic polymer/cage composite membranes, Angew. Chem. Int. Ed. 52 (2013) 1253–1256.

[249] D. Hao, J. Zhang, H. Lu, W. Leng, R. Ge, X. Dai, Y. Gao, Fabrication of a COF-5 membrane on a functionalized α-Al_2O_3 ceramic support using a microwave irradiation method, Chem. Commun. 50 (2014) 1462–1464.

[250] S. Kandambeth, B.P. Biswal, H.D. Chaudhari, K.C. Rout, H., S. Kunjattu, S. Mitra, S. Karak, A. Das, R. Mukherjee, U.K. Kharul, et al., Selective molecular sieving in self-standing porous covalent-organic-framework membranes, Adv. Mater. 29 (2017), 1603945. **This work firstly proposed the fesible method to generate self-standing COF-based membrnaes and their capacity for organic solvent nanofiltration**.

[251] H.S. Sasmal, H.B. Aiyappa, S.N. Bhange, S. Karak, A. Halder, S. Kurungot, R. Benerjee, Superprotonic conductivity in flexible porous covalent organic framework membranes, Angew. Chem. Int. Ed. 57 (2018) 10894–10898.

[252] H. Fan, A. Mundstock, A. Feldhoff, A. Knebel, J. Gu, H. Meng, J. Caro, Covalent organic framework−covalent organic framework bilayer membranes for highly selective gas separation, J. Am. Chem. Soc. 140 (2018) 10094–10098.

[253] H. Fan, M. Peng, I. Strauss, A. Mundstock, H. Meng, J. Caro, MOF-in-COF molecular sieving membrane for selective hydrogen separation, Nat. Commun. 12 (2021) 38.

[254] J. Shen, R. Zhang, Y. Su, B. Shi, X. You, W. Guo, Y. Ma, J. Yuan, F. Wang, Z Jiang, Polydopamine-modulated covalent organic framework membranes for molecular separation, J. Mater. Chem. A 7 (2019) 18063–18071.

[255] L. Wang, J. Jia, M. Faheem, Y. Tian, G. Zhu, Fabrication of triazine-based porous aromatic framework (PAF) membrane with structural flexibility for gas mixtures separation, J. Ind. Eng. Chem. 67 (2018) 373–379.

[256] X. Zhu, C. Tian, S.M. Mahurin, S.-H. Chai, C. Wang, S. Brown, G.M. Veith, H. Luo, H. Liu, S. Dai, A superacid-catalyzed synthesis of porous membranes based on triazine frameworks for CO_2 separation, J. Am. Chem. Soc. 134 (2012) 10478–10484.

[257] B. Liang, H. Wang, X. Shi, B. Shen, X. He, Z.A. Ghazi, N.A. Khan, H. Sin, A. M. Khattak, L. Li, et al., Microporous membranes comprising conjugated polymers with rigid backbones enable ultrafast organic-solvent nanofiltration, Nat. Chem. 10 (2018) 961–967.

[258] Y. Jin, Y. Hu, M. Ortiz, S. Huang, Y. Ge, W. Zhang, Confined growth of ordered organic frameworks at an interface, Chem. Soc. Rev. 49 (2020) 4637–4666.

[259] K. Dey, M. Pal, K.C. Rout, H.S. Kunjattu, A. Das, R. Mukherjee, U.K. Kharul, R Banerjee, Selective molecular separation by interfacially crystallized covalent organic framework thin films, J. Am. Chem. Soc. 139 (2017) 13083–13091. **This work pioneered the fabrication of COF thin films via interfacial polymerization**.

[260] H.S. Sasmal, A. Halder, H.S. Kunjattu, K. Dey, A. Nadol, T.G. Ajithkumar, P. R. Bedadur, R Benerjee, Covalent self-assembly in two dimensions: connecting covalent organic framework nanospheres into crystalline and porous thin films, J. Am. Chem. Soc. 141 (2019) 20371–20379.

[261] C. Fam, H. Geng, H. Wu, Q. Peng, X. Wang, B. Shi, Y. Kong, Z. Yin, Y. Liu, Z Jiang, Three-dimensional covalent organic framework membrane for efficient proton conduction, J. Mater. Chem. A 9 (2021) 17720–17723.

[262] M. Matsumoto, R.R. Dasari, W. Ji, C.H. Feriante, T.C. Parker, S.R. Marder, W. R. Dichtel, Rapid, low temperature formation of imine-linked covalent organic frameworks catalyzed by metal triflates, J. Am. Chem. Soc. 139 (2017) 4999–5002.

[263] M. Matsumoto, L. Valentino, G.M. Stiehl, H.B. Balch, A.R. Corcos, F. Wang, D. C. Ralph, B.J. Marinas, W.R. Dichtel, Lewis-acid-catalyzed interfacial polymerization of covalent organic framework films, Chem 4 (2018) 308–317.

[264] D.B. Shinde, G. Sheng, X. Li, M. Ostwal, A.-H. Emwas, K.-W. Huang, Z. Lai, Crystalline 2D covalent organic framework membranes for high-flux organic solvent nanofiltration, J. Am. Chem. Soc. 140 (2018) 14342–14349.

[265] D.B. Shinde, L. Cao, A.D.D. Wonanke, X. Li, S. Kumar, X. Liu, M.N. Hedhili, A.-H. Emwas, M. Addicoat, K.-W. Huang, et al., Pore engineering of ultrathin covalent organic framework membranes for organic solvent nanofiltration and molecular sieving, Chem. Sci. 11 (2020) 5434–5440.

[266] L. Hou, W. Xian, S. Bing, Y. Song, Q. Sun, L. Zhang, S. Ma, Understanding the ion transport behavior across nanofluidic membranes in response to the charge variations, Adv. Funct. Mater. 31 (2021), 2009970.

[267] P. Zhang, S. Chen, C. Zhu, L. Hou, W. Xian, X. Zuo, Q. Zhang, L. Zhang, S. Ma, Q. Sun, Covalent organic framework nanofluidic membrane as a platform for highly sensitive bionic thermosensation, Nat. Commun. 12 (2021) 1844.

[268] S. Bing, W. Xian, S. Chen, Y. Song, L. Hou, X. Liu, S. Ma, Q. Sun, L. Zhang, Bio-inspired construction of ion conductive pathway in covalent organic framework membranes for efficient lithium extraction, Matter 4 (2021) 2027–2038.

[269] W. Xian, P. Zhang, C. Zhu, X. Zuo, S. Ma, Q. Sun, Bionic thermosensation inspired temperature gradient sensor based on covalent organic framework nanofluidic membrane with ultrahigh sensitivity, CCS Chem 3 (2021) 2464–2472.

[270] C. Zhu, W. Xian, Y. Song, X. Zuo, Y. Wang, S. Ma, Q. Sun, Manipulating charge density in nanofluidic membranes for optimal osmotic energy production density, Adv. Funct. Mater. 32 (2022), 2109210.

[271] X. Zuo, C. Zhu, W. Xian, Q.-W. Meng, Q. Guo, X. Zhu, S. Wang, Y. Wang, S. Ma, Q. Sun, Thermo-osmotic energy conversion enabled by covalent-organic-framework membranes with record output power density, Angew. Chem. Int. Ed. 61 (2022), e202116910. **This work pioneered the empoly of COF-base membrnaes for thermo-osmotic energy conversion**.

[272] R. Wang, X. Shi, A. Xiao, W. Zhou, Y. Wang, Interfacial polymerization of covalent organic frameworks (COFs) on polymeric substrates for molecular separations, J. Membr. Sci. 566 (2018) 197–204.

[273] R. Wang, X. Shi, Z. Zhang, A. Xiao, S.-P. Sun, Z. Cui, Y. Wang, Unidirectional diffusion synthesis of covalent organic frameworks (COFs) on polymeric substrates for dye separation, J. Membr. Sci. 586 (2019) 274–280.

[274] R. Wang, M. Wei, Y. Wang, Secondary growth of covalent organic frameworks (COFs) on porous substrates for fast desalination, J. Membr. Sci. 604 (2020), 118090.

[275] C. Yin, S. Fang, X. Shi, Z. Zhang, Y. Wang, Pressure-modulated synthesis of self-repairing covalent organic frameworks (COFs) for high-flux nanofiltration, J. Membr. Sci. 618 (2021), 118727.

[276] X. Wu, Z. Tian, S. Wang, D. Peng, L. Yang, Y. Wu, Q. Xin, H. Wu, Z. Jiang, Mixed matrix membranes comprising polymers of intrinsic microporosity and covalent organic framework for gas separation, J. Membr. Sci. 528 (2017) 273–283.

[277] X. Cao, H. Xu, S. Dong, J. Xu, Z. Qiao, S. Zhao, J. Wang, Z. Wang, Preparation of high-performance and pressure-resistant mixed matrix membranes for CO_2/H_2 separation by modifying COF surfaces with the groups or segments of the polymer matrix, J. Membr. Sci. 601 (2020), 117882.

[278] X. Cao, Z. Qiao, Z. Wang, S. Zhao, P. Li, J. Wang, S. Wang, Enhanced performance of mixed matrix membrane by incorporating a highly compatible covalent organic

framework into poly(vinylamine) for hydrogen purification, Int. J. Hydrog. Energy 41 (2016) 9167–9174.

[279] Z. Kang, Y. Peng, Y. Qian, D. Yuan, M.A. Addicoat, T. Heine, Z. Hu, L. Tee, Z. Guo, D. Zhao, Mixed matrix membranes (MMMs) comprising exfoliated 2D covalent organic frameworks (COFs) for efficient CO_2 separation, Chem. Mater. 28 (2016) 1277–1285.

[280] M. Shan, B. Seoane, E. Rozhko, A. Dikhtiarenko, G. Clet, F. Kapteijn, J. Gascon, Azine-linked covalent organic framework (COF)-based mixed-matrix membranes for CO_2 /CH_4 separation, Chem. Eur. J. 22 (2016) 14467–14470.

[281] C. Zou, Q. Li, Y. Hua, B. Zhou, J. Duan, W. Jin, Mechanical synthesis of COF nanosheet cluster and its mixed matrix membrane for efficient CO_2 removal, ACS Appl. Mater. Interfaces 9 (2017) 29093–29100.

[282] L. Xu, B. Shan, C. Gao, J. Xu, Multifunctional thin-film nanocomposite membranes comprising covalent organic nanosheets with high crystallinity for efficient reverse osmosis desalination, J. Membr. Sci. 593 (2020), 117398.

[283] R. Hou, S.J.D. Smith, K. Konstas, C.M. Doherty, C.D. Easton, J. Park, H. Yoon, H. Wang, B.D. Freeman, M.R. Hill, Synergistically improved PIM-1 membrane gas separation performance by PAF-1 incorporation and UV irradiation, J. Mater. Chem. A. (2022), https://doi.org/10.1039/D2TA00138A.

[284] T. Mitra, R.S. Bhavsar, D.J. Adams, P.M. Budd, A.I. Cooper, PIM-1 mixed matrix membranes for gas separations using cost-effective hypercrosslinked nanoparticle fillers, Chem. Commun. 52 (2016) 5581–5584.

[285] Z. Zhao, J. Jiang, POC/PIM-1 mixed-matrix membranes for water desalination: A molecular simulation study, J. Membr. Sci. 608 (2020), 118173.

[286] X. Kong, J Liu, An atomistic simulation study on POC/PIM mixed-matrix membranes for gas separation, J. Phys. Chem. C 123 (2019) 15113–15121.

[287] Z. Cheng, H. Pan, H. Zhong, Z. Xiao, X. Li, R. Wang, Porous organic polymers for polysulfide trapping in lithium–sulfur batteries, Adv. Funct. Mater. 28 (2018), 1707597.

[288] V. Singh, H.R. Byon, Advances in electrochemical energy storage with covalent organic frameworks, Mater. Adv. 2 (2021) 3188–3212.

[289] Y. Liao, H. Wang, M. Zhu, A. Thomas, Efficient supercapacitor energy storage using conjugated microporous polymer networks synthesized from Buchwald–Hartwig coupling, Adv. Mater 30 (2018), 1705710.

[290] D.N. Bunck, W.R. Dichtel, Bulk synthesis of exfoliated two-dimensional polymers using hydrazone-linked covalent organic frameworks, J. Am. Chem. Soc. 135 (2013) 14952–14955.

[291] S. Haldar, K. Roy, S. Nandi, D. Chakraborty, D. Puthusseri, Y. Gawli, S. Ogale, R. Vaidhyanathan, High and reversible lithium ion storage in self-exfoliated triazole-triformyl phloroglucinol-based covalent organic nanosheets, Adv. Energy Mater. 8 (2018), 1702170.

[292] X. Chen, Y. Li, L. Wang, Y. Xu, A. Nie, Q. Li, F. Wu, W. Sun, X. Zhang, R. Vajtai, et al., High-lithium-affinity chemically exfoliated 2D covalent organic frameworks, Adv. Mater. 31 (2019), 1901640.

[293] S. Wang, Q. Wang, P. Shao, Y. Han, X. Gao, L. Ma, S. Yuan, X. Ma, J. Zhou, X. Feng, et al., Exfoliation of covalent organic frameworks into few-layer redox-active nanosheets as cathode materials for lithium-ion batteries, J. Am. Chem. Soc. 139 (2017) 4258–4261.

[294] W. Liu, X. Li, C. Wang, H. Pan, W. Liu, K. Wang, Q. Zeng, R. Wang, J. Jiang, A scalable general synthetic approach toward ultrathin imine-linked two-dimensional covalent organic framework nanosheets for photocatalytic CO_2 reduction, J. Am. Chem. Soc. 141 (2019) 17431–17440.

[295] D.W. Burke, C. Sun, I. Castano, N.C. Flanders, A.M. Evans, E. Vitaku, D. C. McLeod, R.H. Lambeth, L.X. Chen, N.C. Gianneschi, et al., Acid exfoliation of imine-linked covalent organic frameworks enables solution processing into crystalline thin films, Angew. Chem. Int. Ed. 59 (2020) 5165–5171.

[296] Y. Liu, J. Guan, Y. Su, R. Zhang, J. Cao, M. He, J. Yuan, F. Wang, X. You, Z Jiang, Graphene oxide membranes with an ultra-large interlayer distance through vertically grown covalent organic framework nanosheets, J. Mater. Chem. A 7 (2019) 25458–25466.

[297] X. Zhang, H. Li, J. Wang, D. Peng, J. Liu, Y. Zhang, In-situ grown covalent organic framework nanosheets on graphene for membrane-based dye/salt separation, J. Membr. Sci. 581 (2019) 321–330.

[298] L.M. Robeson, The upper bound revisited, J. Membr. Sci. 320 (2008) 390–400.

[299] H. Lu, C. Wang, J. Chen, R. Ge, W. Leng, B. Dong, J. Huang, Y. Gao, A novel 3D covalent organic framework membrane grown on a porous α-Al_2O_3 substrate under solvothermal conditions, Chem. Commun. 51 (2015) 15562–15565.

[300] Y. Wang, J. Li, Q. Yang, C. Zhong, Two-dimensional covalent triazine framework membrane for helium separation and hydrogen purification, ACS Appl. Mater. Interfaces 8 (2016) 8694–8701.

[301] B.P. Biswal, H.D. Chaudhari, R. Banerjee, U.K. Kharul, Chemically stable covalent organic framework (COF)- polybenzimidazole hybrid membranes: enhanced gas separation through pore modulation, Chem. Eur. J. 22 (2016) 4695–4699.

[302] J. Fu, S. Das, G. Xing, T. Ben, V. Valtchev, S. Qiu, Fabrication of COF-MOF composite membranes and their highly selective separation of H_2/CO_2, J. Am. Chem. Soc. 138 (2016) 7673–7680. **This work firstly reported the fabrication of COF-MOF composite membranes for gas separation**.

[303] S. Das, T. Ben, S. Qiu, V. Valtchev, Two-dimensional COF−three-dimensional MOF dual-layer membranes with unprecedentedly high H_2/CO_2 selectivity and ultrahigh gas permeabilities, ACS Appl. Mater. Interfaces 12 (2020) 52899–52907.

[304] Y. Ying, S.B. Peh, H. Yang, Z. Yang, D. Zhao, Ultrathin covalent organic framework membranes via a multi-interfacial engineering strategy for gas separation, Adv. Mater. (2021), 2104946.

[305] Y. Ying, M. Tong, S. Ning, S.K. Ravi, S.B. Peh, S.C. Tan, S.J. Pennycook, D. Zhao, Ultrathin two-dimensional membranes assembled by ionic covalent organic nanosheets with reduced apertures for gas separation, J. Am. Chem. Soc. 142 (2020) 4472–4480.

[306] H. Fan, A. Mundstock, J. Gu, H. Meng, J. Caro, An azine-linked covalent organic framework ACOF-1 membrane for highly selective CO_2/CH_4 separation, J. Mater. Chem. A 6 (2018) 16849–16853.

[307] B.P. Biswal, S.H. Kunjattu, T. Kaur, R. Banerjee, U.K. Kharul, Transforming covalent organic framework into thin-film composite membranes for hydrocarbon recovery, Sep. Sci. Technol. 53 (2018) 1752–1759.

[308] X. Liang, H. Wu, H. Huang, X. Wang, M. Wang, H. Dou, G. He, Y. Ren, Y. Liu, Y. Wu, et al., Efficient ethylene/ethane separation through ionic liquid-confined covalent organic framework membranes, J. Mater. Chem. A 10 (2022) 5420–5429.

[309] S. Yi, X. Ma, I. Pinnau, W.J Koros, A high-performance hydroxyl-functionalized polymer of intrinsic microporosity for an environmentally attractive membrane-based approach to decontamination of sour natural gas, J. Mater. Chem. A 3 (2015) 22794–22806.

[310] S. Yi, B. Ghanem, Y. Liu, I. Pinnau, W.J. Koros, Ultraselective glassy polymer membranes with unprecedented performance for energy-efficient sour gas separation, Sci. Adv. 5 (2019) eaaw5459.

[311] P. Stanovsky, A. Zitkova, M. Karaszova, M. Šyc, J.C. Jansen, B.C. Gándara, N. McKeown, P. Izak, Flue gas purification with membranes based on the polymer of intrinsic microporosity PIM-TMN-Trip, Sep. Purif. Technol. 242 (2020), 116814.

[312] H.W.H. Lai, F.M. Benedetti, J.M. Ahn, A.M. Robinson, Y. Wang, I. Pinnau, Z. P. Smith, Y. Xia, Hydrocarbon ladder polymers with ultrahigh permselectivity for membrane gas separations, Science 375 (2022) 1390–1392. **This work reported the great progress of aged PIM-based membranes for enhanced performance of gas separations**.

[313] P. Lindemann, M. Tsotsalas, S. Shishatskiy, V. Abetz, P. Krolla-Sidenstein, C. Azucena, L. Monnereau, A. Beyer, A. Gölzhäuser, V. Mugnaini, et al., Preparation of freestanding conjugated microporous polymer nanomembranes for gas separation, Chem. Mater. 26 (2014) 7189–7193.

[314] W. Liu, S.-D. Jiang, Y. Yan, W. Wang, J. Li, K. Leng, S. Japip, J. Liu, H. Xu, Y. Liu, et al., A solution-processable and ultra-permeable conjugated microporous thermoset for selective hydrogen separation, Nat. Commun. 11 (2020) 1633.

[315] Z. Tian, S. Dai, D.-e. Jiang, Confined ionic liquid in an ionic porous aromatic framework for gas separation, ACS Appl. Polym. Mater. 1 (2019) 95–102.

[316] C.H. Lau, X. Mulet, K. Konstas, C.M. Donherty, M.-A. Sani, F. Separovic, M.R. Hill, C.D. Wood, Hypercrosslinked additives for ageless gas-separation membranes, Angew. Chem. Int. Ed. 55 (2016), 1998-2001.

[317] W. Li, L. Peng, Y. Li, Z. Chen, C. Duan, S. Yan, B. Yuan, Hyper cross-linked polymers containing amino group functionalized polyimide mixed matrix membranes for gas separation, J. Appl. Polym. Sci 139 (2022) e52171.

[318] J.M. Lucero, M.A. Carreon, Separation of light gases from xenon over porous organic cage membranes, ACS Appl. Mater. Interfaces 12 (2020) 32182–32188.

[319] Q. Zhang, H. Li, S. Chen, J. Duan, W. Jin, Mixed-matrix membranes with soluble porous organic molecular cage for highly efficient C_3H_6/C_3H_8 separation, J. Membr. Sci. 611 (2012), 118288.

[320] G. Zhu, F. Zhang, M.P. Rivera, X. Hu, G. Zhang, C.W. Jones, R.P. Lively, Molecularly mixed composite membranes for advanced separation processes, Angew. Chem. Int. Ed. 58 (2019) 2638–2643.

[321] Y. Zhang, J. Guo, G. Han, Y. Bai, Q. Ge, J. Ma, C.H. Lau, L. Shao, Molecularly soldered covalent organic frameworks for ultrafast precision sieving, Sci. Adv. 7 (2021) eabe8706.

[322] M. Wang, P. Zhang, X. Liang, J. Zhao, Y. Liu, Y. Cao, H. Wang, Y. Chen, Z. Zhang, F. Pan, et al., Ultrafast seawater desalination with covalent organic framework membranes, Nat. Sustain. (2022), https://doi.org/10.1038/s41893-022-00870-3.

[323] H. Fan, J. Gu, H. Meng, A. Knebel, J. Caro, High-flux membranes based on the covalent organic framework COF-LZU1 for selective dye separation by nanofiltration, Angew. Chem. Int. Ed. 57 (2018) 4083–4087.

[324] S. Hao, L. Jiang, Y. Li, Z. Jia, B.V. der Bruggen, Facile preparation of COF composite membranes for nanofiltration by stoichiometric spraying layer-by-layer self-assembly, Chem. Commun. 56 (2020) 419–422.

[325] G. Kong, J. Pang, Y. Tang, L. Fan, H. Sun, R. Wang, S. Feng, Y. Feng, W. Fan, W. Kang, et al., Efficient dye nanofiltration of a graphene oxide membrane via combination with a covalent organic framework by hot pressing, J. Mater. Chem. A 7 (2019) 24301–24310.

[326] J. Liu, G. Han, D. Zhao, K. Lu, J. Gao, T.-S. Chung, Self-standing and flexible covalent organic framework (COF) membranes for molecular separation, Sci. Adv. 6 (2020) eabb1110.

[327] J.L. Fenton, D.W. Burke, D. Qian, M.O. de la Cruz, W.R. Dichtel, Polycrystalline covalent organic framework films act as adsorbents, not membranes, J. Am. Chem. Soc. 143 (2021) 1466–1473. **This work pioneered the application of COF-based membrane as adsorbents rather than the rejecting barrier**.

[328] L. Yang, H. Xiao, Y. Qian, X. Zhao, X.-Y. Kong, P. Liu, W. Xin, L. Fu, L. Jiang, L. Wen, Bioinspired hierarchical porous membrane for efficient uranium extraction from seawater, Nat. Sustain. 5 (2022) 71–80.

[329] A.A. Uliana, N.T. Bui, J. Kamcev, M.K. Taylor, J.J. Urban, J.R. Long, Ion-capture electrodialysis using multifunctional adsorptive membranes, Science 372 (2021) 296–299. **This work firstly reported the employ of PAF-based membranes as adsorptive membranes for ion-capture electrodialysis**.

[330] L. Cao, X. Liu, D.B. Shinde, C. Chen, I.-C. Chen, Z. Li, Z. Zhou, Z. Yang, Y. Han, Z. Lai, Oriented two-dimensional covalent organic framework membranes with high ion flux and smart gating nanofluidic transport, Angew. Chem. Int. Ed. 61 (2022), e202113141.

[331] X. He, Y. Yang, H. Wu, G. He, Z. Xu, Y. Kong, L. Cao, B. Shi, Z. Zhang, C. Tongsh, et al., *De novo* design of covalent organic framework membranes toward ultrafast anion transport, Adv. Mater. 32 (2020), 2001284.

[332] J. Yang, B. Tu, G. Zhang, P. Liu, K. Hu, J. Wang, Z. Yan, Z. Huang, M. Fang, J. Hou, et al., Advancing osmotic power generation by covalent organic framework monolayer, Nat. Nanotechnol. (2022), https://doi.org/10.1038/s41565-022-01110-7.

[333] M. Sandru, E.M. Sandru, W.F. Ingram, J. Deng, P.M. Stenstad, L. Deng, R. J. Spontak, An integrated materials approach to ultrapermeable and ultraselective CO_2 polymer membranes, Science 376 (2022) 90–94.

[334] Z. Tan, S. Chen, X. Peng, L. Zhang, C. Gao, Polyamide membranes with nanoscale Turing structures for water purification, Science 360 (2018) 518–521.

Yanpei Song received his B.S. degree from Beijing University of Chemical Technology in 2017. He is currently a Ph.D. candidate under the supervision of Prof. Shengqian Ma in the Department of Chemistry, University of North Texas. His-current research interests lie primarily in the development of functional porous organic polymers for environmental remediation and precious metal recovery.

Changjia Zhu received his B.S. degree from University of Science and Technology of China in 2020. He then worked for one year as an research assistant at Zhejiang University before starting his Ph.D. career with Prof. Shengqian Ma at the University of North Texas. His-research focuses on the development of covalent organic frameworks membranes for environmental remediation and precious metal recovery.

Shengqian Ma obtained his BS degree from Jilin University, China in 2003, and graduated from Miami University (Ohio) with a PhD degree in 2008. After finishing a two-year Director's Postdoctoral Fellowship at Argonne National Laboratory, he joined the Department of Chemistry at University of South Florida as an Assistant Professor in 2010; he was promoted to an Associate Professor with early tenure in 2015 and to a Full Professor in 2018. In August 2020, he joined University of North Texas as the Robert A. Welch Chair in Chemistry. His-current research interest focuses on the task-specific design and functionalization of advanced porous materials for energy, biological, and environmental-related applications.